

**DIRECT SYNTHESIS OF HYDROGEN PEROXIDE FROM OXYGEN AND
HYDROGEN USING CARBON DIOXIDE AS AN ENVIRONMENTALLY BENIGN
SOLVENT AND ITS APPLICATION IN GREEN OXIDATION**

by

Qunlai Chen

B.S. in Chemical Engineering, Zhengzhou University, 1986

M.S. in Chemical Engineering, Beijing University of Chemical Technology, 1989

Submitted to the Graduate Faculty of
School of Engineering in partial fulfillment
of the requirements for the degree of
Doctor of Philosophy

University of Pittsburgh

2007

UNIVERSITY OF PITTSBURGH

SCHOOL OF ENGINEERING

This dissertation was presented

by

Qunlai Chen

It was defended on

September 24, 2007

and approved by

Dr. Robert M. Enick, Professor, Department of Chemical and Petroleum Engineering

Dr. Götz Vesper, Associate professor, Department of Chemical and Petroleum Engineering

Dr. Terrence J. Collins, Professor, Department of Chemistry, Carnegie Mellon University

Dissertation Advisor: Dr. Eric J. Beckman, Professor, Department of Chemical and Petroleum
Engineering

Copyright © by Qunlai Chen

2007

**DIRECT SYNTHESIS OF HYDROGEN PEROXIDE FROM OXYGEN AND
HYDROGEN USING CARBON DIOXIDE AS AN ENVIRONMENTALLY BENIGN
SOLVENT AND ITS APPLICATION IN GREEN OXIDATION**

Qunlai Chen, PhD

University of Pittsburgh, 2007

Based on the concept of green chemistry, a new green chemistry metric was developed with the consideration of both quantity and quality (hazard) of chemicals involved in the synthesis of a chemical product. This new metric was used to evaluate the greenness of various synthetic methods in this study.

Hydrogen peroxide (H_2O_2), a widely used green oxidant, is currently produced by an anthraquinone auto-oxidation (AO) process. This AO process is not environmentally benign because it generates wastes, uses large volumes of organic solvents, and has low efficiency and high energy consumption. Direct synthesis of H_2O_2 from O_2 and H_2 is a green technology to replace the AO process since it is the most atomic-efficient method by which H_2O_2 can be synthesized. Compressed CO_2 has the potential to replace the conventional solvents used in this direct synthesis process. In this study, a method was developed to measure the amount of directly synthesized H_2O_2 in compressed CO_2 over precious metal loaded titanium silicalite (TS-1) molecular sieve by using a selected indicator to react immediately with the *in situ* generated H_2O_2 . The experimental results proved, for the first time, that H_2O_2 could be effectively generated from O_2 and H_2 using CO_2 as the solvent.

This *in situ* generated H_2O_2 in CO_2 was then used in the epoxidation of propylene to propylene oxide (PO). A PO yield over 20% with vital selectivity was achieved, for the first

time, using compressed CO₂ as the solvent and small amounts of polar co-solvents. The addition of a selected weak base inhibitor effectively suppressed a number of common side-reactions, including the hydrogenation of propylene, the hydrolysis of PO and the reaction between PO and methanol.

The oxidation of cyclohexene by *in situ* generated H₂O₂ in compressed CO₂—an alternative and green approach to the synthesis of adipic acid was also explored using precious metal loaded TS-1 and W-MCM-41 (a silicate mesoporous molecular sieve). Experimental results showed that the oxidation of cyclohexene by *in situ* generated H₂O₂ in CO₂ was limited by the small pore size of TS-1, while W-MCM-41 was an effective catalyst in carrying out this reaction.

TABLE OF CONTENTS

PREFACE.....	XIV
1.0 INTRODUCTION.....	1
2.0 LITERATURE REVIEW AND BACKGROUND.....	9
2.1 PRODUCTION OF H₂O₂ VIA ANTHRAQUINONE (AO) PROCESS.....	9
2.2 DIRECT SYNTHESIS OF H₂O₂ FROM O₂ AND H₂	19
2.3 APPLICATION OF <i>IN SITU</i> GENERATED H₂O₂ IN GREEN OXIDATION.....	30
2.3.1 Green synthesis of propylene oxide	30
2.3.2 Green synthesis of adipic acid using H₂O₂.....	38
3.0 RESEARCH OBJECTIVES	46
4.0 DEVELOPMENT OF A GREEN CHEMISTRY METRIC.....	48
4.1 DEFINITION OF GREENNESS INDEX FOR A CHEMICAL (GIC)	53
4.2 DEFINITIONS OF GIF, GIO, GIR AND GIP	59
4.3 APPLICATION OF THE NEW GREEN CHEMISTRY METRIC	62
4.4 SUMMARY	67
5.0 DIRECT SYNTHESIS OF H₂O₂ FROM O₂ AND H₂ IN CO₂.....	70
5.1 EXPERIMENTAL.....	71
5.1.1 Chemicals and Catalysts.....	71
5.1.2 General procedures for direct synthesis of H₂O₂ in CO₂	72
5.1.3 General procedures for the decomposition of H₂O₂	74

5.2	CATALYST CHARACTERIZATION	75
5.2.1	FT-IR spectra	75
5.2.2	Powder X-ray diffraction (XRD) spectra	78
5.3	SELECTION OF AN “INDICATOR” COMPOUND	82
5.4	RESULTS AND DISCUSSION FOR THE DIRECT OF SYNTHESIS OF H ₂ O ₂ IN CO ₂	85
5.5	INTERACTION BETWEEN H ₂ O ₂ AND TS-1.....	95
5.6	SUMMARY	98
6.0	ONE-POT GREEN SYNTHESIS OF PROPYLENE OXIDE USING <i>IN SITU</i> GENERATED H ₂ O ₂ IN CO ₂	100
6.1	EXPERIMENTAL.....	102
6.1.1	Chemicals and catalysts.....	102
6.1.2	General procedures for the direct synthesis of PO in CO ₂	103
6.2	RESULTS AND DISCUSSION FOR THE GREEN SYNTHESIS OF PROPYLENE OXIDE	105
6.3	SUMMARY	115
7.0	GREEN SYNTHESIS OF ADIPIC ACID USING <i>IN SITU</i> H ₂ O ₂ IN CO ₂	116
7.1	EXPERIMENTAL.....	117
7.1.1	Chemicals and catalysts.....	117
7.1.2	General procedures for the green synthesis of adipic acid in CO ₂	119
7.2	RESULTS AND DISCUSSION FOR THE GREEN SYNTHESIS OF ADIPIC ACID.....	119
7.2.1	Using precious metal loaded TS-1 as the catalyst	119
7.2.2	Using precious metal loaded W-MCM-41 as the catalyst	121
7.3	SUMMARY	128
8.0	CONCLUSIONS	129

9.0	RECOMMENDED FUTURE WORK	131
	APPENDIX	133
	BIBLIOGRAPHY	136

LIST OF TABLES

Table 1	Twelve principles of green chemistry.....	2
Table 2	Some commonly used oxidants	4
Table 3	Active AQ left in the AO process after circulations without regeneration (g/L)	13
Table 4	Typical working solution composition in the AO process	15
Table 5	Consumption of major raw materials used in the synthesis of EAQ.....	17
Table 6	Consumption of major raw materials used in the synthesis of TOP.....	18
Table 7	Consumption of major raw materials used in the synthesis of TBU	18
Table 8	Typical experimental results for the direct synthesis of H ₂ O ₂ in literature	20
Table 9	Solubility of H ₂ and O ₂ in various solvents at room temperature.....	27
Table 10	Comparison of mass transfer rates between H ₂ -Methanol and H ₂ -Water	28
Table 11	Direct oxidation of propylene by the mixture of oxygen and hydrogen in literature ...	37
Table 12	Current N ₂ O abatement technologies	41
Table 13	Literature results for the oxidation of cyclohexene by H ₂ O ₂	43
Table 14	Some representatives of Type I metrics in green chemistry	49
Table 15	Application of Type I metrics in the production of adipic acid using different oxidants	51
Table 16	Experimental data used for calculating RME.....	51
Table 17	Hazardous ratings defined by HMIS	54
Table 18	Calculation of weighted values for the global warming index (GWI) and ozone depletion index (ODI).....	57

Table 19	Weighted values for different impact factors in calculating GIC	58
Table 20	Calculation of greenness index for a chemical (GIC).....	58
Table 21	Calculation of greenness index for a chemical formula GIF	59
Table 22	The greenness index GIO for various oxidants	61
Table 23	Calculation of GIC for the production of adipic acid with different oxidants.....	63
Table 24	Calculation of GIR and GIP for the production of adipic acid with different oxidants	64
Table 25	Comparison of greenness in producing BaSO ₄ obtained by different metrics	65
Table 26	Calculation of GIC for the production of BaSO ₄ by different methods	65
Table 27	Comparison of greenness in the production of TDI with different methods	67
Table 28	Greenness index for the reactions in the synthesis of H ₂ O ₂	70
Table 29	The GIC values for the chemicals used in the synthesis of H ₂ O ₂	71
Table 30	Relative crystallinities of TS-1 before and after impregnation of precious metal.....	81
Table 31	The standard Gibbs free energy changes for the reactions in direct synthesis of H ₂ O ₂	84
Table 32	Thermodynamic data of chemicals used in reaction (5- 8).....	85
Table 33	Experimental conditions in determining the calibration curve in CO ₂	97
Table 34	Comparison of experimental results with and without the consideration of calibration curve.....	98
Table 35	Greenness index GIR values of the chemical reactions in the synthesis of PO.....	100
Table 36	GIC values of the substances used in the synthesis of PO by various processes	101
Table 37	Green synthesis of PO using <i>in situ</i> generated H ₂ O ₂ in CO ₂	107
Table 38	Experimental results using selected inhibitors with different interaction ability in the green synthesis of PO in CO ₂	110
Table 39	Effect of reaction temperature on the green synthesis of PO in CO ₂	114
Table 40	GIR values for the synthesis of adipic acid by various methods	117
Table 41	Oxidation of cyclohexene and its derivatives by <i>in situ</i> H ₂ O ₂ in CO ₂	121

Table 42 Oxidation of cyclohexene by H ₂ O ₂ with different catalysts	124
Table 43 GC conditions in the detection of H ₂ and indicator in direct synthesis of H ₂ O ₂ in compressed CO ₂	133
Table 44 GC conditions in the synthesis of PO using <i>in situ</i> generated H ₂ O ₂ in CO ₂	135

LIST OF FIGURES

Figure 1 Atlas of molecular sieve with MFI structure.....	7
Figure 2 Chemical principle of the AO process.....	10
Figure 3 Schematic diagram of the AO process	11
Figure 4 Flow sheet of a typical AO process for the production of H ₂ O ₂	11
Figure 5 Explosion of a H ₂ O ₂ plant caused by the decomposition of H ₂ O ₂	16
Figure 6 Concentration profiles in gas-liquid-solid three-phase reaction system.....	23
Figure 7 Major adipic acid producers and their market shares	38
Figure 8 Experimental setup for the direct synthesis of H ₂ O ₂ in CO ₂	73
Figure 9 FT-IR spectra of TS-1, 0.2%Pd/TS-1 and (0.2%Pd+0.02%Pt)/TS-1	76
Figure 10 FT-IR spectra of TS-1, 0.35%Pd/TS-1 and (0.35%Pd+0.035%Pt)/TS-1	77
Figure 11 FT-IR spectra of TS-1, 0.6%Pd/TS-1 and (0.6%Pd+0.06%Pt)/TS-1	77
Figure 12 FT-IR spectra of TS-1, 1.0%Pd/TS-1 and (1.0%Pd+0.1%Pt)/TS-1	78
Figure 13 Powder XRD spectra of TS-1, 0.2%Pd/TS-1, (0.2%Pd+0.02%Pt)/TS-1, 0.35%Pd/TS-1 and (0.35%Pd+0.035%Pt)/TS-1	79
Figure 14 Powder XRD spectra of TS-1, 0.6%Pd/TS-1, (0.6%Pd+0.06%Pt)/TS-1, 1.0%Pd/TS-1 and (1.0%Pd+0.1%Pt)/TS-1	80
Figure 15 Reactions involved in the direct synthesis of H ₂ O ₂ and its determination	84
Figure 16 Effect of stirring speed on the direct synthesis of H ₂ O ₂ in CO ₂	86
Figure 17 Effect of O ₂ /H ₂ molar ratio on the direct synthesis of H ₂ O ₂ in CO ₂	87

Figure 18 Effect of H ₂ concentration on the direct synthesis of H ₂ O ₂ in CO ₂	89
Figure 19 Effect of catalyst mass on the direct synthesis of H ₂ O ₂ in CO ₂	90
Figure 20 Effect of Pd content on the direct synthesis of H ₂ O ₂ in CO ₂	92
Figure 21 Experimental results for the decomposition of H ₂ O ₂ by different catalysts.....	93
Figure 22 Effect of adding Pt to the Pd/TS-1 catalysts in direct synthesis of H ₂ O ₂	95
Figure 23 Calibration curve for the measurement of H ₂ O ₂ in CO ₂	97
Figure 24 Experimental setup for the green synthesis of PO using <i>in situ</i> generated H ₂ O ₂ in CO ₂	104
Figure 25 Effect of different inhibitors on green synthesis of PO in CO ₂	108
Figure 26 Effect of the amounts of selected inhibitor on the synthesis of PO.....	111
Figure 27 Effect of reaction time on green synthesis of PO in CO ₂	112
Figure 28 Possible mechanistic pathways for the synthesis of MCM-41: (1) liquid crystal phase initiated; (2) silicate anion initiated	123
Figure 29 Oxidation of cyclohexene by 30% H ₂ O ₂ in CO ₂ with different acids.....	126
Figure 30 Oxidation of cyclohexene by <i>in situ</i> generated H ₂ O ₂ in CO ₂	127

PREFACE

I would like to express my sincere gratitude to Dr. Eric J. Beckman, my Ph. D. advisor, for his valuable guidance, precious advice and continuous support throughout the course of this study. His profound knowledge, innovative ideas and encouragement helped me to overcome all the difficulties I faced during these years.

I would like to thank Dr. Terrence J. Collins, Thomas Lord Professor of Chemistry at Carnegie Mellon University, Dr. Robert M. Enick, Bayer Professor and Chairman of the Department of Chemical and Petroleum Engineering at the University of Pittsburgh and Dr. Götz Vesper, Associate Professor of the Department of Chemical and Petroleum Engineering at the University of Pittsburgh for severing as members of my Ph.D. Committee, for their helpful suggestions and comments. I am also grateful to Dr. Liang-Shih Fan, Distinguished University Professor of Ohio State University, for his continuous support and encouragement.

I want to thank the faculty, staff and colleagues in the Department of Chemical and Petroleum Engineering and The Mascaro Sustainability Initiative for their support during my graduate study, especially, Heather R. MacPherson for the discussion and assistance during my graduate study, for her help in using FT-IR, Dr. Sarah Jones for her help in running high pressure experiments at the beginning of my graduate study and Dr. Jiangying Zhang for her assistance. I also want to thank the staff and faculty associated with the Materials Micro-Characterization

Laboratory of the Department of Mechanical Engineering and Material Science for assistance with the X-ray diffraction conducted during this study.

Finally, I would like to express my deep gratitude to my dear wife, Yan Xu, my lovely daughters, Wenqi Chen and Christina Chen, for their love, unconditional support. I also want to thank my parents-in-law, Guide Xu and Haiqin Shen. I dedicate this dissertation to my parents, Xiulin Chen and Qing Xie, especially my beloved father, Xiulin Chen, who passed away during my graduate study at the University of Pittsburgh.

1.0 INTRODUCTION

Green chemistry is defined^[1, 2] as the design of chemical products and processes that reduce or eliminate the use and generation of hazardous substances. It was introduced in the early 1990s along with the increased public concerns about human health and environment impacts of chemical substances. Before the 1960s, it was common to think that the “mere decrease of concentration of a substance in a particular medium would be sufficient to mitigate its ultimate impact.”^[2] Therefore, *dilution was considered to be the solution to pollution*. The book “Silent Spring” [which detailed the adverse effects of pesticides (especially DDT) on the eggs of various birds] published in 1962 by Rachael Carson and a series of environmental disasters caused by toxic chemicals^[2] had awakened the public to the environmental impact of toxic substances. In response, government passed various environmental laws to regulate the release of toxic substances. At this stage, *regulation was considered to be the solution to pollution*. The Pollution Prevention Act passed by US congress in 1990 marked the shift of public attitude toward pollution from treatment and abatement through command and control to the prevention of the formation of waste at the source. At present, it is believed that “*prevention is the solution to pollution*”. Ever since its first appearance, green chemistry is widely accepted as an effective strategy to the pollution prevention, and the 12 principles^[2] of green chemistry

listed in Table 1 are considered to be the guidelines in designing and developing environmentally benign chemical processes and products.

Table 1 Twelve principles of green chemistry

1	It is better to prevent waste than to treat or clean up waste after it is formed.
2	Synthetic methods should be designed to maximize the incorporation of all materials used in the process into the final product.
3	Wherever practicable, synthetic methodologies should be designed to use and generate substances that possess little or no toxicity to human health and the environment.
4	Chemical products should be designed to preserve efficacy of function while reducing toxicity.
5	The use of auxiliary substances (e.g. solvents, separation agents, etc.) should be made unnecessary wherever possible and, innocuous when used.
6	Energy requirements should be recognized for their environmental and economic impacts and should be minimized. Synthetic methods should be conducted at ambient temperature and pressure.
7	A raw material or feedstock should be renewable rather than depleting wherever technically and economically practicable.
8	Unnecessary derivatization (blocking group, protection/deprotection, temporary modification of physical/chemical processes) should be avoided whenever possible.
9	Catalytic reagents (as selective as possible) are superior to stoichiometric reagents.
10	Chemical products should be designed so that at the end of their function they do not persist in the environment and break down into innocuous degradation products.
11	Analytical methodologies need to be further developed to allow for real-time, in-process monitoring and control prior to the formation of hazardous substances.
12	Substances and the form of a substance used in a chemical process should be chosen so as to minimize the potential for chemical accidents, including releases, explosions, and fires.

Catalytic oxidation reactions play an important role in modern chemical, petroleum and pharmaceutical industries. According to Oyama et al,^[3] catalytic oxidation produced more than 60% of the chemicals and intermediates synthesized by catalytic processes, with a global commercial value of \$20~40 billion in the early 1990s. Hudlicky^[4] summarized that hundreds of chemicals could be used as the oxidants. Some commonly used oxidants and their decomposition by-products are listed in Table 2^[5]. If we use the 12 principles of green chemistry to examine catalytic oxidation reactions and the oxidants used therein, it is easy to conclude that catalytic oxidation is probably one of the biggest challenges to green chemistry due to the following reasons: (1) Except for a few oxidants (e.g. oxygen and hydrogen peroxide, etc.), most oxidants are not environmentally benign since they can either decompose or react with reactants (or products) to form by-products that are harmful to human health and (or) the environment. For example, in the production of adipic acid, nitric acid is used to oxidize the mixture of cyclohexanol and cyclohexanone. During this process, nitrous oxide, a greenhouse gas, is generated as a by-product. Adipic acid producers have had to develop various abatement technologies to decompose it prior to its emission.

(2) Many catalytic oxidation reactions suffer low conversion and selectivity because many oxidants used can also oxidize the desired final product. For example, in the oxidation of cyclohexane by O_2 to a mixture of cyclohexanone and cyclohexanol (important raw materials for producing adipic acid), the desired mixture is more easily oxidized (by O_2) than the parent hydrocarbon. Therefore, conversion has to be kept low (<10%) in order to minimize the over-oxidation of desired product. Even at this

conversion level, the selectivity is only in the range of 80~85%.^[6] The lower conversion and selectivity imply that large amounts of raw materials will inevitably go to the waste stream and extra separation steps have to be used to separate reactants from product and to purify final product.

Table 2 Some commonly used oxidants

Oxidant	Active oxygen, %	Comments
O ₂	50	Usually one oxygen atom goes to H ₂ O as the by-product. Widely used oxidant but suffers low conversion and selectivity
H ₂ O ₂	47.0	H ₂ O as the only by-product; limited use in selective oxidation due to its containing of water, and higher price
<i>t</i> -BuOOH	17.8	Generates <i>t</i> -BuOH as a by-product. Used in the production of propylene oxide, and as an initiator in polymerization.
NaClO	21.6	Generates inorganic salt NaCl as a by-product; in some cases, ClO ⁻ can produce toxic and carcinogenic chlorocarbon by-products
KHSO ₅	10.5	Generates KHSO ₄ as a by-product
Heavy metal salts and oxides, e.g. CrO ₃		Oxidant itself is highly toxic; also generates toxic heavy metal derivatives as the by-products

(3). Many conventional organic solvents used in oxidation reactions can be oxidized. This will cause the loss of organic solvents and the generation of solvent

degradation wastes. In many cases, the final products will be contaminated by solvents and their degradation wastes. Extra steps have to be used to purify the final products.

Due to these drawbacks, green oxidants should be used whenever it is possible in carrying out oxidation reactions.

Hydrogen peroxide (H_2O_2) is an important green oxidant since it contains a high fraction of active oxygen and forms water as the only by-product as shown in Table 2. In 2005, global H_2O_2 capacity reached 3.53 million metric tons per year (in 100% H_2O_2) and the demand in North America and Europe is growing at 3%~5% per year.^[7] At present, China is the world's largest H_2O_2 producer and its annual growth is expected to maintain a double-digit trend in the next 5~10 years.^[8] Although the current major application of H_2O_2 is in the bleaching of pulp/paper and textiles—both non-selective oxidations, it is becoming more attractive in chemical synthesis in both academia and industry because of its “green” character, especially in selective oxidation.^[9, 10]

Industrially, H_2O_2 is produced by an anthraquinone auto-oxidation (AO) process. This process was first commercialized by Du Pont in 1953 and became the dominant technology in producing H_2O_2 ever since. However, because of the complicity of the AO process, the current H_2O_2 price is high enough such that many oxidation reactions can not be carried out economically, even though the reactions themselves are attractive, such as that given by Sato et al^[11] using 30% H_2O_2 to oxidize cyclohexene for the green synthesis of adipic acid.

Direct synthesis of H_2O_2 from O_2 and H_2 is an attractive green technology to replace the current AO process since it is the most atom-efficient approach by which H_2O_2 can be prepared. The study of direct synthesis of H_2O_2 began at the beginning of

last century. In 1914, Henkel and Weber^[12] were awarded probably the first patent on direct synthesis of H₂O₂ from O₂ and H₂ with a precious metal as the catalyst. However, little progress was made following 1914 because of safety issues (the mixture of O₂ and H₂ is explosive in the range of 4%~95.2% of H₂ in O₂ at 20°C and 1bar). It was almost completely ignored after the AO process was commercialized in the 1950s. There was renewed interest in direct synthesis of H₂O₂ after 1980 driven by the strong demand for H₂O₂, especially in recent years. If the safety issues associated with direct synthesis could be solved, direct synthesis of H₂O₂ from O₂ and H₂ could greatly simplify the H₂O₂ production process, dramatically cut the production cost, and generate almost no waste.

A major problem in using H₂O₂ as the oxidant in catalytic oxidation reactions is that most readily available commercial H₂O₂ product is an aqueous solution. Water associated with H₂O₂ is detrimental to many conventional catalysts. The discovery of the titanium silicalite (TS-1) catalyst in 1983 by Taramasso et al^[13] provided a new platform using H₂O₂ as a green oxidant to conduct selective oxidation reactions. TS-1 is a ZSM-5 type molecular sieve with MFI [ZSM-Five] structure in which small amount of tetrahedral Si atoms are substituted by Ti atoms in a purely siliceous framework. It has a crystalline structure similar to ZSM-5 with a 3-dimensional channel structure: parallel channels in one direction, and zigzag type channels perpendicular to them (as shown in **Figure 1**^[14]). The size of the channels is 0.55~0.60nm. The hydrophobic micropores of TS-1 are assumed to exclude water from its internal voids, and thus protect the active sites from deactivation.^[9] Therefore, TS-1 has become one of the most studied molecular sieve catalysts in using H₂O₂ to conduct selective oxidations, especially in the epoxidation of alkenes, oxidation of alcohols, hydroxylation of aromatics, ammoxidation

of cyclohexanone and oxidation of alkane etc.^[5, 9, 15] However, the major drawback of TS-1 is its small pore size which presents a diffusional limitation to relatively bulky chemicals.

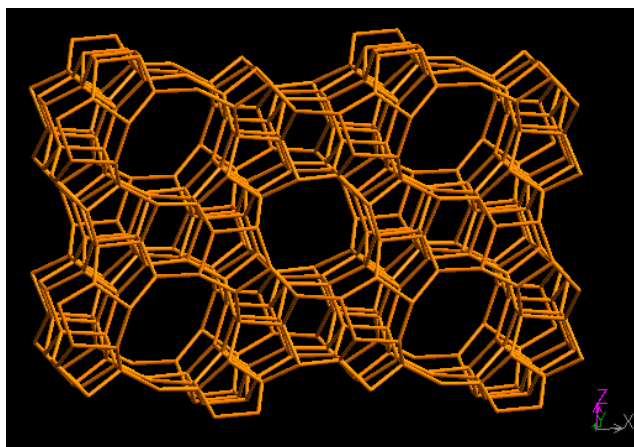


Figure 1 Atlas of molecular sieve with MFI structure

“Fluids near their critical point have dissolving power comparable to that of liquids, are much more compressible than dilute gases, and have transport properties intermediate between gas- and liquid-like. This unusual combination of physical properties can be advantageously exploited in environmentally benign separation and reaction processes, as well as for new kinds of materials processing”^[16] Compressed (liquefied or supercritical) carbon dioxide (CO₂) is well recognized as one of these fluids and has been used in separation and chemical reaction processes to replace the conventional organic solvents. Mild critical values ($T_C=31.1^{\circ}\text{C}$, $P_C=73.8$ bar), environmentally benign character (non-flammable, relatively non-toxic, relatively inert) and low cost of the material itself make compressed CO₂ an attractive solvent in both

academia and industry. Early studies mainly focused on using it as a solvent in extraction processes. The successful stories include coffee decaffeination by supercritical CO₂ and dry cleaning with liquid CO₂. In recent years, using CO₂ as a solvent in chemical reaction has been a research focus, especially in hydrogenation, oxidation and polymerization etc.^[17]

Although compressed CO₂ has the potential to be used as an environmentally benign solvent, the literature^[18, 19] shows contradictory conclusions in using CO₂ as a solvent in direct synthesis of H₂O₂ from O₂ and H₂. The aim of this study is to establish a method to identify if H₂O₂ could be effectively synthesized from a mixture of O₂ and H₂ over precious metal loaded TS-1 by using compressed CO₂ as a solvent; and to explore the possibility of using this *in situ* generated H₂O₂ in CO₂ to epoxidize propylene to propylene oxide, to oxidize cyclohexene to adipic acid etc.

2.0 LITERATURE REVIEW AND BACKGROUND

2.1 PRODUCTION OF H₂O₂ VIA ANTHRAQUINONE (AO) PROCESS

The chemical principle, schematic diagram and flow sheet of the AO process are shown in **Figure 2**, **Figure 3** and **Figure 4**, respectively.^[20-22] In this process, 2-alkylanthraquinone [AQ, **1**; most commonly used 2-alkylanthraquinones are 2-ethylanthraquinone (EAQ), 2-*tert*-butylanthraquinone and 2-amylanthraquinone] is dissolved in a mixture of non-polar solvent (C₉-C₁₁ alkylbenzene) and polar solvent [Trioctyl phosphate (TOP), or tetrabutyl urea (TBU), or diisobutyl carbinol (DIBC)]^[20, 22] to form a “working solution” and then hydrogenated over a precious metal (Pd or Ni) catalyst in a three-phase reactor (trickle bed or slurry bubble column) under mild reaction conditions (<5 bars, <80°C) to generate 2-alkylanthrahydroquinone (AQH₂, **2**). AQH₂ is then auto-oxidized by compressed air in a two-phase reactor (packed column or bubble column) to produce H₂O₂ and regenerate AQ. During this process, small amounts of AQ can be further hydrogenated to form mainly 2-alkyltetrahydroanthrahydroquinone (H₄AQH₂, **4**; it can also be oxidized to produce H₂O₂ and regenerate 2-alkyltetrahydroanthraquinone, H₄AQ, **3**). The generated H₂O₂ is then extracted by deionized water from the working solution in a countercurrent extraction column to obtain crude H₂O₂, which can be further treated in the purification and concentration step

under vacuum to produce final products [27.5%~70% (wt) H₂O₂ in concentration]. The working solution from the extraction step is treated in the post-treatment step in order to regenerate by-products and adjust its pH value, and is then circulated back to the hydrogenation step to begin next circulation.

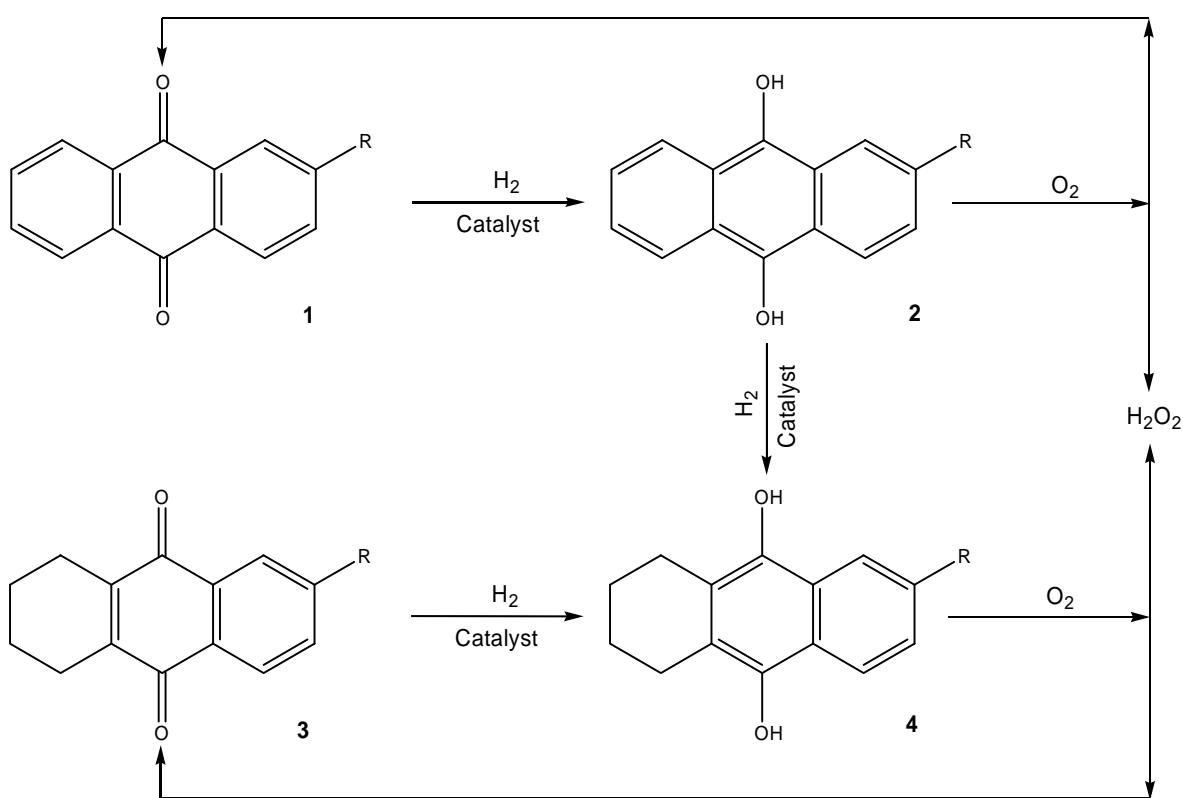


Figure 2 Chemical principle of the AO process

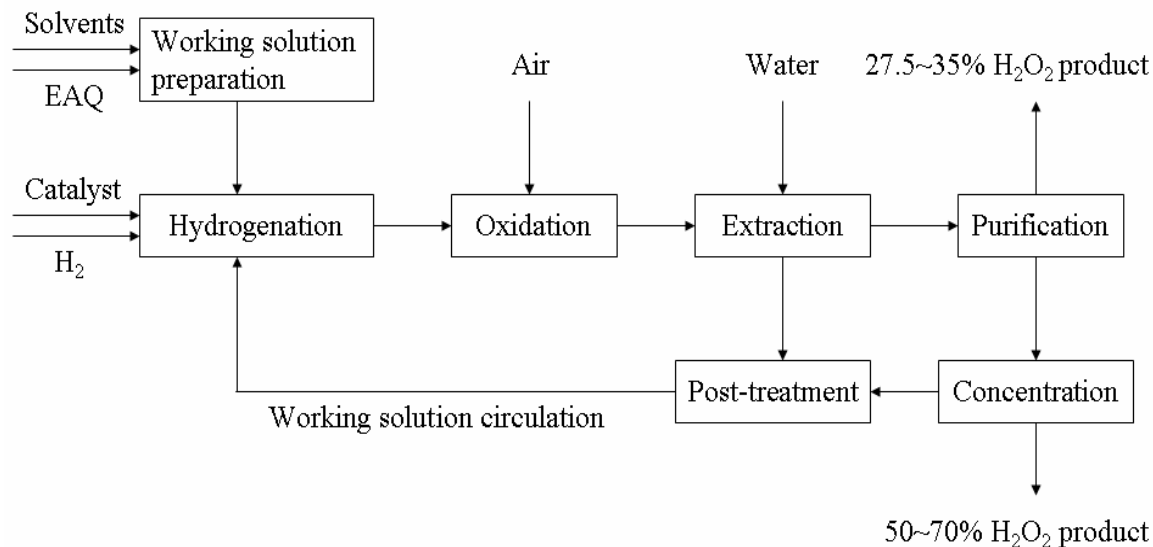
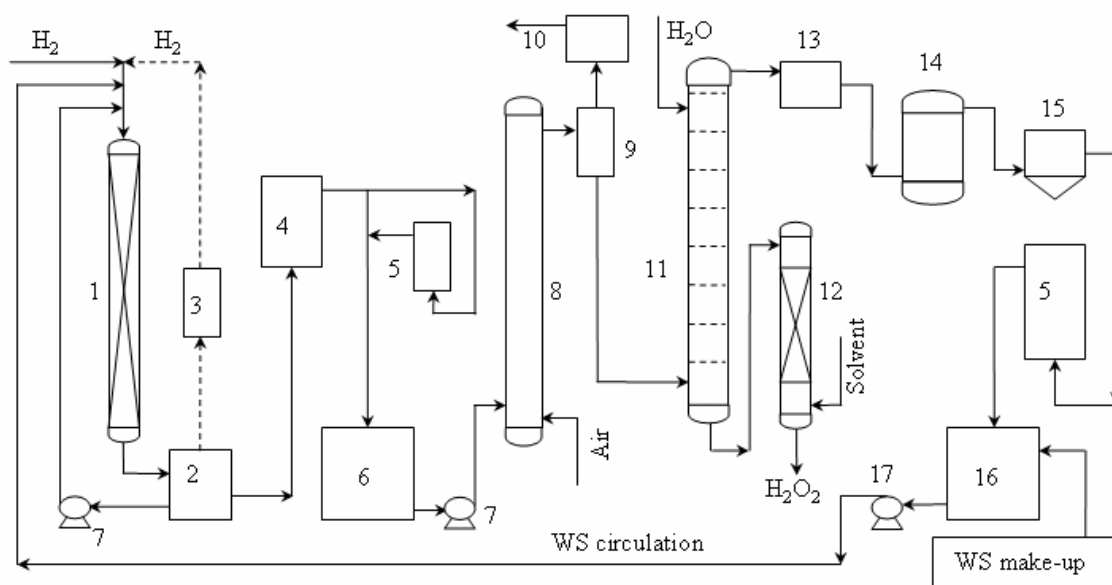


Figure 3 Schematic diagram of the AO process



1. Hydrogenation reactor; 2. Separator; 3. H₂ circulation facility; 4. Filter; 5. Alumina bed; 6. Hydrogenated WS storage tank; 7. Hydrogenated WS pump; 8. Oxidation reactor; 9. Separator; 10. Solvent recovery facility; 11. Extraction tower; 12. Purification column; 13. Separator; 14. Dryer; 15. Separator; 16. WS storage tank; 17. WS pump

Figure 4 Flow sheet of a typical AO process for the production of H₂O₂

This AO process is successfully used to produce most of the world's H₂O₂ because it prevents the direct contact between O₂ and H₂ and can be operated continuously under mild reaction conditions.^[23] However, the AO process is far from green in view of the 12 principles of green chemistry due to the following reasons:

(1). Generation of wastes

The current AO process generates several wastes because of the sequential hydrogenation and oxidation of AQ, the unintended oxidation of organic solvents, and the phase behavior in each reactor.^[23, 24] The AO process is unique compared to other chemical process in that AQ in the working solution has to be sequentially hydrogenated and oxidized continuously in order to produce commercially viable H₂O₂. This requires that the selectivity of both the hydrogenation reaction and oxidation reaction must be as close to unity as possible. Industrially, the initial AQ content in the working solution is in the range of 120~150g/L and the total selectivity is above 99%.^[21, 25] The importance of total selectivity in the AO process for the production of H₂O₂ is illustrated in **Table 3**. As can be seen that even if the total selectivity is as high as 99.5%, after each circulation, 0.5% of AQ in the working solution will be degraded to inert AQ derivatives (this is called degradation and the formed AQ derivatives are called degradation by-products) which lose the ability to generate H₂O₂. If there is no addition of makeup AQ and no regeneration of degradation by-products, after 100 circulations (about several weeks' operation in practice), over one third of AQ will be converted to the degradation by-products. This is obviously unacceptable in industrial practice. **Table 3** also shows that

slight decrease in total selectivity from 99.5% to 98.5% could result in dramatic decrease in AQ content from 73~91g/L to 26~33g/L after 100 circulations.

Table 3 Active AQ left in the AO process after circulations without regeneration (g/L)

Number of circulations	Total selectivity in the AO process, %				
	99.5	99	98.5	98	95
50	93~117	73~91	56~70	44~55	9~12
100	73~91	44~55	26~33	16~20	0.7~0.9

The degradation of AQ is mainly caused by the deep hydrogenation of its aromatic rings, hydrolysis of the C=O bounds and over-oxidation of H₄AQH₂, which generate mainly hydroxyanthrones of AQ and H₄AQ, anthrones of AQ and H₄AQ, anthracenes of AQ and H₄AQ, H₈AQ and H₄AQ-11,12-epoxide etc.^[20, 21, 26-28] Only part of these by-products can be regenerated back to AQ and H₄AQ in the post-treatment step, the rest of them will go to the waste water and crude H₂O₂ product. Therefore, makeup AQ has to be added to the working solution periodically to compensate the loss of AQ.

Although the solvents used in the AO process are relatively stable, small amounts of them could still be hydrogenated or oxidized by generated H₂O₂ to form solvent-based by-products during operation. These solvent by-products will lose the ability to dissolve AQ and AQH₂ and have to be removed from the working solution. Furthermore, some solvent can be carried out by off-gassing during the oxidation step.^[20] Therefore, makeup solvents have to be added to the system periodically.

Even though the solubility of AQ and the solvents in aqueous H₂O₂ is relatively low,^[20] small amounts of them, together with the water-soluble degradation by-products, will dissolve in crude H₂O₂ in the extraction step. This will lead to the further loss of AQ and solvents and, more seriously, the contamination of crude H₂O₂.

The lost AQ and solvents will eventually go to waste streams, which are waste water and tail gas from the oxidation step.^[20] The waste water needs to be treated to decompose AQ (and its derivatives), solvents (and their derivatives) prior to its discharge. The organic solvents in tail gas have to be recovered by an adsorption method prior to its emission.^[20]

(2). Low efficiency and high energy consumption

Although the AO process avoids the direct contact between O₂ and H₂, it uses AQ as a working carrier. Since 2-ethylanthraquinone (EAQ) is widely used by major H₂O₂ producers, we use it as an example in the following discussion.

The low efficiency is mainly due to the following reasons: (1). the limited solubility of AQ in the solvents, (2). controlled hydrogenation conversion, and (3) low H₂O₂ concentration in the working solution. As shown in **Table 4**, the solubility of EAQ in the solvents is in the range of 120~150g EAQ/L of working solution. In order to minimize side reactions in the hydrogenation step, the hydrogenation conversion is usually controlled at less than 70%. This means that only 80~105g EAQ/L of working solution participate in the reaction; therefore, the corresponding H₂O₂ concentration in the working solution is usually less than 1.5% (wt). Substantial extraction equipment has to be used and a large amount of working solution has to be circulated in order to obtain

commercially viable H₂O₂ solution, which is in the range of 27.5~70% (wt). For example, in order to obtain 1 metric ton of 50% H₂O₂, 40~50m³ of working solution has to be used or 1m³ of working solution has to be circulated for 40~50 times (this will result in the loss of significant amounts of EAQ if there is no regeneration).

Table 4 Typical working solution composition in the AO process

Item	Component	Amount in 1 liter of working solution, g
Working carrier	EAQ, H ₄ EAQ	120~150
Product	H ₂ O ₂	10~12
Solvents	C ₉ ~C ₁₁ alkyl-benzenes, TOP (or TBU, or DIBC)	~800 (the density of working solution is ca. 0.93~0.95g/ml)

As mentioned earlier, the crude H₂O₂ obtained in the AO process is contaminated by the organics in the working solution. This contaminated crude H₂O₂ has to be purified and concentrated prior to its commercial use. The purification and concentration process consumes large amounts of steam (approximately 10~20 pounds steam per pound H₂O₂^[29]) in order to almost completely evaporate crude H₂O₂ solution.

(3). Use of large amounts of solvents and working carrier (AQ)

There are two major issues associated with the use of large amounts of solvents and AQ in the production of H₂O₂: (a) Process safety—the solvents (C₉~C₁₁ aromatics, TOP, TBU, or DIBC) and working carrier (AQ) used in the AO process are either flammable or combustible. Although safety measures are designed and installed in the commercial

plants, the risk still exists mainly due to the easy decomposition of H_2O_2 . **Figure 5** shows how severe the pollution (caused by the combustion of working solution ignited by an explosion) could be when the safety measures failed in a commercial H_2O_2 plant.^[30]



Figure 5 Explosion of a H_2O_2 plant caused by the decomposition of H_2O_2

(b). Large amounts of wastes are generated during the production of major raw materials used in the AO process: 2-ethylanthraquinone (EAQ) is widely used as the working carrier, and trioctylphosphate (TOP) and tetrabutyl-urea (TBU) are widely used as the polar solvent. However, the production of these raw materials uses substantial quantity of toxic chemicals and generates large amounts of wastes as shown by equations (2- 1) to (2- 4) and **Table 5** to **Table 7**. For example, EAQ is produced by a Friedel-Crafts acylation reaction. The synthesis of 1 ton of EAQ will consume about 2 tons of aluminum chloride ($AlCl_3$) anhydride and 4~5 tons of oleum (20% in SO_3) and generate

tens of tons of highly toxic wastewater (containing AlCl_3 , H_2SO_4 , chlorobenzene and other organics).^[31] The synthesis of TOP uses highly toxic phosphorus oxychloride (POCl_3) and generates toxic hydrogen chloride (HCl).^[32] The synthesis of TBU uses extremely toxic phosgene and also generates HCl .^[33]

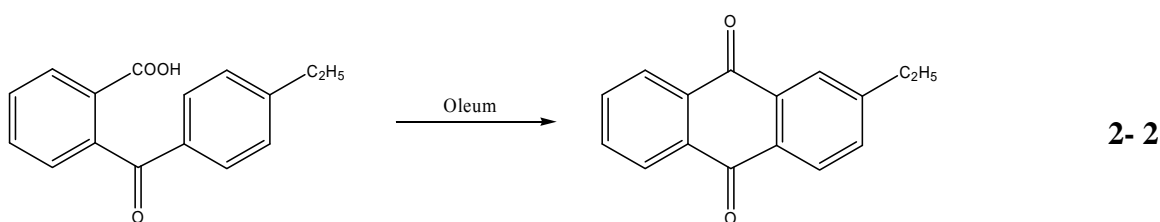
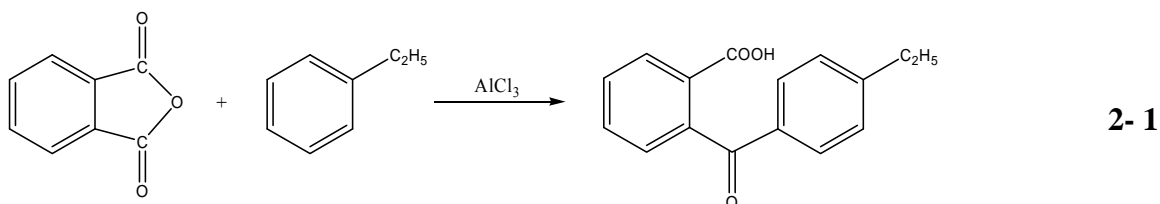


Table 5 Consumption of major raw materials used in the synthesis of EAQ

Raw material	Chemical formula	Amount, kg/ton of EAQ
Phthalic anhydride	$\text{C}_8\text{H}_4\text{O}_3$	975
Ethylbenzene	$\text{C}_6\text{H}_5\text{C}_2\text{H}_5$	725
Aluminum chloride anhydride	AlCl_3	1,760
Oleum (20% in SO_3)	$\text{H}_2\text{SO}_4 \cdot \text{SO}_3$	4,200
Chlorobenzene	$\text{C}_6\text{H}_5\text{Cl}$	400
Sodium hydroxide	NaOH	200

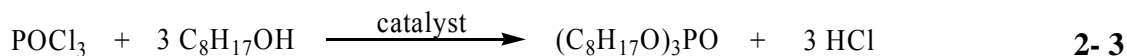


Table 6 Consumption of major raw materials used in the synthesis of TOP

Raw material	Chemical formula	Amount, kg/ton of TOP
Phosphorus oxychloride	POCl ₃	590
2-Ethyl-1-hexanol	CH ₃ (CH ₂) ₃ CH(C ₂ H ₅)CH ₂ OH	1,600
Titanium butoxide	Ti(OCH ₂ CH ₂ CH ₂ CH ₃) ₄	Catalyst
Sodium carbonate	Na ₂ CO ₃	150
Sodium chloride	NaCl	200
Adsorbent		60

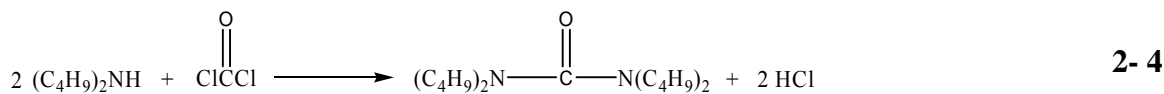


Table 7 Consumption of major raw materials used in the synthesis of TBU

Raw material	Chemical formula	Amount, kg/ton of TBU
Di-butylamine	(C ₄ H ₉) ₂ NH	769
Phosgene	COCl ₂	360
15% Sodium hydroxide	NaOH	2,088

2.2 DIRECT SYNTHESIS OF H₂O₂ FROM O₂ AND H₂

The issues associated with the production of H₂O₂ via the AO process have led to the exploration of other possible methods in preparing H₂O₂. Direct synthesis of H₂O₂ from O₂ and H₂ is an attractive alternative to the current AO process. However, direct synthesis is also one of the most dangerous alternatives because the mixture of O₂ and H₂ is explosive in a broad concentration range. Although direct synthesis of H₂O₂ from O₂ and H₂ has been a research focus for decades, early research was performed almost exclusively by companies and the results were published in form of patents. Because of the strong demand for H₂O₂ and the increased interest in using H₂O₂ as an environmentally benign oxidant in recent years, researchers from academia started to examine direct synthesis of H₂O₂ from O₂ and H₂. This trend was confirmed by the dramatic increase in the number of papers published by researchers in academia recently. **Table 8** summarizes the typical experimental results and related reaction conditions in the literature on direct synthesis of H₂O₂ from O₂ and H₂. As can be seen, the examined reaction systems can be homogeneous but are usually heterogeneous. The homogeneous reaction system was reported by Hancu et al.^[34, 35] using CO₂ as the solvent and a CO₂-soluble palladium complex as the catalyst to synthesize H₂O₂ from O₂ and H₂. Because the mass transfer resistance was completely eliminated in this homogeneous system, the H₂O₂ yield reached as high as 38%. However, the synthesis of the CO₂-soluble palladium catalyst was tedious and expensive.

Table 8 Typical experimental results for the direct synthesis of H₂O₂ in literature

Catalyst	Solvent (promoter)	T, °C	P, bar	Time, hrs	O ₂ /H ₂ ratio	Inert gas	H ₂ O ₂ yield, %	H ₂ O ₂ select.,%	Reference	
Homogeneous reaction system										
[Pd(P(C ₆ H ₄ -C ₂ H ₄ -C ₆ F ₁₃) ₃) ₂]Cl ₂	CO ₂ /H ₂ O (H ₂ SO ₄ /NH ₄ Cl)	25	172.4	3	7	CO ₂	~38		Hancu et al ^[34, 35]	
Heterogeneous reaction system										
Pd/Porous clay pipe	H ₂ O	No details were given								Henkel et al ^[12]
5%Pd/Silica gel	Acetone/H ₂ O (HCl/H ₂ SO ₄)	0	1	5	1	N ₂	7.5		Hooper ^[36]	
Pd/acid ion exchange resin	MeCN/H ₂ O	5	9.7	0.5	1	none		47.9	Kim et al ^[37]	
5%Pd/C	Acetone/H ₂ O (HCl/H ₂ SO ₄)	0	8.6	4	3.4	none	~14.1		Dalton et al ^[38]	
Pd+Pt/Al ₂ O ₃	H ₂ O (HCl)	5-8	137.9	3	4.6	none	40.1	69	Gosser et al ^[39]	
1%Pd,1.8%EAQ/Y zeolite	H ₂ O (HCl)	28	1	1	1	N ₂	4.1		Park et al ^[40]	

Table 8 (continued)

1%Pd+0.1%Pt/TS-1	MeOH/H ₂ O	10	32		1.56	N ₂	<1		Meiers et al ^[41]
0.6%Pd/Zeolite beta	H ₂ O (HCl)	r.t.	1	1	1	He	13		Park et al ^[42, 43]
Pd film/Pd-Ag alloy /alumina membrane	H ₂ O (H ₂ SO ₄)	29		3			20~50	20~50	Choudhary et al ^[44]
Pd:Au(1:1)/Al ₂ O ₃	MeOH/H ₂ O	2	37	0.5	1.2	CO ₂	8.8	14	Landon et al ^[18, 45]
Pd, Au/C or SiO ₂	H ₂ O (H ₂ SO ₄ , NaBr)	8	60~80	2~8	11.3~ 21.2	N ₂		72~89	Bertsch-Frank et al ^[46]
Au/SiO ₂	H ₂ O (HCl)	15	10	2	0.43	none	0.64		Okumura et al ^[47]
5%Pd/C	H ₂ O/MeCN (H ₃ PO ₄ , NaBr)	r.t.	80	2	32.6	N ₂	30.7	64	Burch et al ^[48]
5%Pd/SiO ₂	H ₂ O (HCl, NaBr)	10	1	5~20	4	none	>8.1	>90	Lunsford et al ^[49, 50]
Pd-Au/Al ₂ O ₃	H ₂ O or MeOH (H ₂ SO ₄ , NaBr)	25	50		6.67	N ₂	13.6~49.7	29~72	Haas et al ^[51]

Table 8 (continued)

Pd/Sulfonic acid polystyrene resin	MeOH/H ₂ O (HBr)	40	100	2	24	N ₂	~69.3	77	Blanco-Brieva et al ^[52]
2.5%Pd-2.5%Au/ α -Fe ₂ O ₃	MeOH/H ₂ O	2	37	0.5	2	CO ₂	15.6	22	Edwards et al ^[53]
2.5%Pd-2.5%Au/TiO ₂	MeOH/H ₂ O	2	37	0.5	2	CO ₂	12.8~40.9	61-89	Edwards et al ^[54]
1%Pd-1%Au/SiO ₂	H ₂ O (H ⁺)	10	1	2	6	none		30	Ishihara et al ^[55]
5%Pd/SiO ₂	Ethanol/H ₂ O (H ₂ SO ₄)	10	1	5	4	none	19.6	40	Han et al ^[56, 57]
Pd+Pt/C	H ₂ O/MeOH (H ₂ SO ₄ , NaBr)	35	51.7		6.1	Inert gas	11.26	56	Rueter et al ^[58]
Pd+Pt/C	H ₂ O/MeOH (H ₂ SO ₄ , NaBr)		34.5		1	none	36.0	60	Rueter et al ^[58]

Heterogeneous reaction systems were widely used by many researchers to directly synthesize H_2O_2 from O_2 and H_2 . Typically, a gas-liquid-solid three-phase reactor was used with the gas phase being the mixture of O_2 and H_2 (with or without the addition of an inert gas), liquid phase being either alcohol, water or their mixture, and solid phase being precious metal loaded catalyst. The most widely used catalysts were palladium (Pd) and/or platinum (Pt) loaded on SiO_2 , Al_2O_3 , TiO_2 , carbon or zeolite etc. Recently, nano-sized gold was found to exhibit high activity in catalyzing the direct synthesis of H_2O_2 , especially when it was used together with Pd.^[18, 53, 59, 60] Although a palladium membrane reactor^[44] gave high yield in the direct synthesis of H_2O_2 , it is too expensive to be used in large-scale applications due to its preparation process and its high palladium loading.

For the direct synthesis of H_2O_2 in a gas-liquid-solid three-phase reactor, the following steps are necessary before O_2 and H_2 can react with each other on the active site of the catalyst, as illustrated by **Figure 6**:^[61]

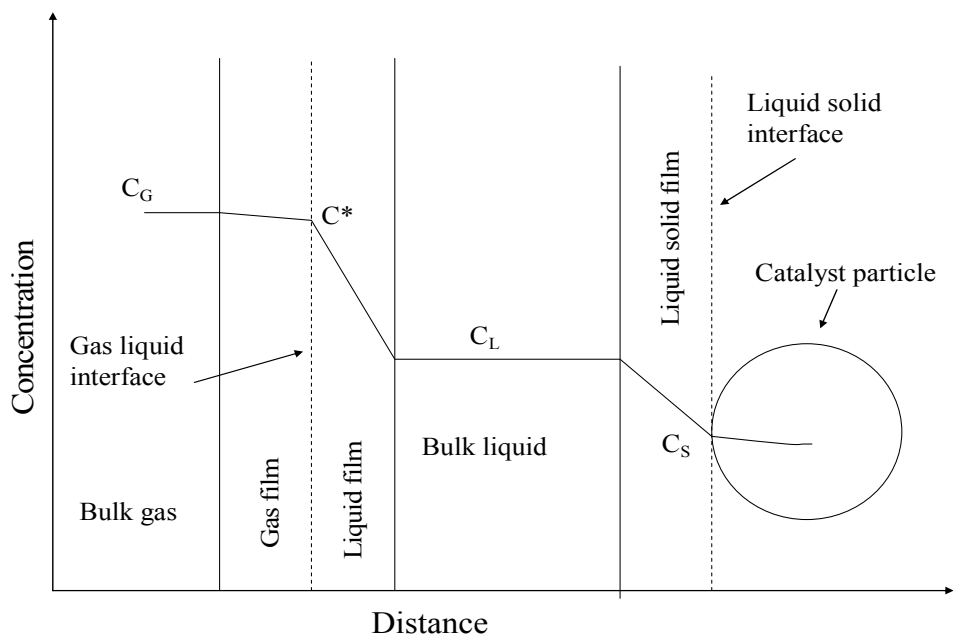


Figure 6 Concentration profiles in gas-liquid-solid three-phase reaction system

1. Transport of O₂ and H₂ from bulk gas to the gas film;
2. Transport of O₂ and H₂ from the gas film to the gas-liquid interface;
3. Transport of O₂ and H₂ from gas-liquid interface to the liquid film;
4. Transport of O₂ and H₂ from the liquid film to the bulk liquid;
5. Transport of O₂ and H₂ from the bulk liquid to the liquid-solid interface;
6. Transport of O₂ and H₂ from the liquid-solid interface to the surface of catalyst;
7. Intra-particle diffusion of O₂ and H₂ in the pores of the catalyst;
8. Adsorption of O₂ and H₂ on the active sites of the catalyst;
9. O₂ and H₂ react with each other to generate H₂O₂ on the active sites of the catalyst.

In general, compared with the resistances in other steps, the mass transfer resistances in step 1, 4, 5 can be neglected. The resistances in step 7~9 depend on the physical properties of the catalyst and the reaction kinetics. The rate of mass transfer from gas to liquid can be written as ($i=H_2$ or O₂)

$$N_i = (K_L a)_i (C_i^* - C_{Li}) \quad 2-5$$

Where N_i is the rate of mass transfer per unit volume of the reactor, C_i^* is the solubility of gas i , C_{Li} is the concentration of gas i in the bulk liquid, a is the gas-liquid interfacial area, and K_L is the overall gas-liquid mass transfer coefficient. K_L can be related to the individual gas-side and liquid-side mass transfer coefficient by the following equation

$$\frac{1}{(K_L a)_i} = \frac{1}{H e_i (k_G a)_i} + \frac{1}{(k_L a)_i} \quad 2-6$$

Where $H e_i$ is the Henry's Law constant, k_G is the gas-side mass transfer coefficient and k_L is the liquid-side mass transfer coefficient. For sparingly soluble gases, such as H_2 and O_2 , the term $K_L a$ can be approximated to $k_L a$ since the value of $(H e k_G a)$ is much larger than that of $k_L a$.

$$K_L a \cong k_L a \quad 2-7$$

The rate of mass transfer from the bulk liquid to the surface of the solid catalyst can be expressed as

$$N_i = (k_S a_S)_i (C_{L_i} - C_{S_i}) \quad 2-8$$

Where k_S is the liquid-solid mass transfer coefficient, a_S is the external surface area of catalyst per unit volume of the reactor and C_{S_i} is the concentration of gas i at the catalyst surface.

By combining equation (2-5) and equation (2-8), the overall rate of mass transfer of gas i from the gas phase to the surface of catalyst can be expressed as

$$N_i = \frac{(C_i^* - C_{S_i})}{\frac{1}{(k_L a)_i} + \frac{1}{(k_S a_S)_i}} \quad 2-9$$

Where k_L and a can be estimated by the following equations:^[62, 63]

$$k_L = 0.5g^{5/8} D_{AB}^{1/2} \rho_L^{3/8} \sigma^{-3/8} d_{vs}^{1/2} \quad \text{2- 10}$$

$$a = \frac{6\varepsilon_g}{d_{vs}} \quad \text{2- 11}$$

Where g is gravitational constant, D_{AB} is liquid phase diffusivity, ρ_L is liquid density, σ is surface tension, d_{vs} is the Sauter mean bubble diameter and ε_g is gas holdup. Bubble size d_{vs} decreases with increasing operating pressure and decreasing surface tension of liquid phase. Many experimental conditions can affect ε_g ,^[62] e.g. increasing operating pressure will increase gas holdup ε_g . The properties of the liquid phase also influence gas holdup: gas holdup increases with a decrease in liquid viscosity, or surface tension. The surface properties of the liquid phase play an important role in gas holdup. For example, the addition of small amount of short chain alcohols into pure water could cause great increase in gas holdup.^[64]

For sparingly soluble gases O_2 and H_2 , the overall rate of mass transfer plays a key role in carrying out the direct synthesis of H_2O_2 in three-phase reactors since the reaction itself is relatively fast. And also, in general, the $k_s a_s$ value is much larger than the $k_L a$ value. The effect of $k_s a_s$ on overall rate of mass transfer can be, therefore, omitted. Any methods that can cause the increase in the overall rate of mass transfer will lead to an increase in the H_2O_2 yield. These include (1) increasing the solubility of the gases by increasing reaction pressure or by using solvents that have higher gas solubility, (2) increasing gas holdup and decreasing bubble size by adding short chain alcohols to water or by increasing reaction pressure, (3) using solvents with lower viscosity and surface tension.

From **Table 8**, we can find that many researchers followed these guidelines by (1) using high reaction pressure since higher pressure leads to higher gas solubility, smaller bubble size and higher gas holdup; (2) using acetone or alcohols as the solvent since O₂ and H₂ are more soluble in them as shown in **Table 9**.^[65] The comparison of estimated overall rate of mass transfer between an H₂-water system and the H₂-methanol system given by Krishnan et al^[65] clearly showed (see **Table 10** for details) the advantages of using alcohol as the reaction solvent. The $k_s a_s$ and $k_L a$ values given in **Table 10** also proved that the contribution of $k_s a_s$ toward the overall rate of mass transfer was negligible.

The results disclosed by Rueter et al^[58] also verified that the addition of small amounts of methanol had significant influence on the direct synthesis of H₂O₂ from O₂ and H₂ in water with precious metal as the catalyst: In one example, the H₂ conversion was increased from 13.6% to 20.1%, while the H₂O₂ selectivity was increased from 46% to 56% when 2% methanol was added to water containing 1% H₂SO₄ and 5ppm NaBr; in another example, the H₂ conversion was increased from 33% to 60% under similar H₂O₂ selectivity (60~65%).

Table 9 Solubility of H₂ and O₂ in various solvents at room temperature

Solvent	Solubility of H ₂ , mg/L	Solubility of O ₂ , mg/L
Water (H ₂ O)	1.62	40
Methanol (MeOH)	7.91	324
Ethanol (EtOH)	7.50	320
Acetone	8.15	364

Table 10 Comparison of mass transfer rates between H₂-Methanol and H₂-Water

Item	H ₂ -Methanol	H ₂ -Water
Liquid diffusivity, D_{AB} , cm ² /s	4.5×10^{-3}	2.4×10^{-3}
Viscosity, cP	0.54	0.89
Mass transfer coefficient, k_L , cm/s	0.467	0.28
Gas-liquid interfacial area, a , cm ²	0.71	0.38
$k_L a$, cm ³ /s	0.33	0.11
Minimum $k_s a_s$, cm ³ /s (Assume mean catalyst diameter=100μm, suspended in stagnant liquid)	9.6	5.1
Overall rate of mass transfer, N_{H_2} , mmol/min	0.079	0.0053

Mineral acid (HCl, H₂SO₄, or H₃PO₄) and bromide were widely used as the promoters. Mild temperatures were used by most researchers in order to minimize H₂O₂ decomposition.

The O₂/H₂ molar ratios used in direct synthesis were usually high enough to avoid operating in the explosive range. For lower O₂/H₂ molar ratio, an inert gas was used to dilute the O₂ and H₂ mixture.

The latest progress in direct synthesis was recently reported by Degussa/ Headwaters:^[66] a pilot plant was reported to be undergoing testing and the process could be commercialized soon. The companies disclosed that methanol was used as the solvent in this new process; safety issue could still exist since methanol is a flammable and volatile organic solvent, and furthermore methanol will likely be oxidized during the synthetic process, forming formaldehyde and other by-products.^[67, 68] The product obtained in this direct synthetic process was dilute H₂O₂ in methanol (implying the need of large amounts of methanol); concentration and separation

processes are required in order to obtain a commercially viable aqueous H₂O₂ solution. Therefore, this new process was not intended to replace the current AO process; it was rather to be used as an *in situ* H₂O₂ source for a new propylene oxide production process.

CO₂ could be used to replace methanol as the solvent for *in situ* generation of H₂O₂ from O₂ and H₂. A CO₂-based system has the following advantages.^[17] (1) As mentioned before, the mixture of O₂ and H₂ is explosive in a broad concentration range. Recently Pande and Tonheim^[69] pointed out that the non-explosive limit for a gas mixture of O₂ and H₂ in CO₂ is significantly higher than that in N₂. (2) CO₂ can not be further oxidized. (3) Since O₂ and H₂ are all miscible with CO₂ at temperature above 31°C, the mixture of O₂, H₂ and CO₂ will form a homogeneous fluid phase. This will dramatically reduce, or even eliminate, mass transfer resistances. (4) CO₂ is non-flammable (a significant safety advantage over conventional organic solvents), naturally abundant, easy to obtain and less toxic than many other organic solvents [the threshold limit value (TLV) of CO₂ is 5000ppm, while the TLV values for acetone, methanol and benzene are 750ppm, 200ppm and 0.5ppm, respectively]. Therefore, it is expected that the direct synthesis of H₂O₂ from O₂ and H₂ in compressed CO₂ could be carried out more effectively than that in the conventional solvents.

However, some contradictory conclusions have been reported in the literature. Beckman^[23] and Danciu et al^[19] had previously found that propylene oxide (PO) could be effectively generated from the oxidation of propylene by *in situ* generated H₂O₂ from O₂ and H₂ using Pd/TS-1 as the catalyst and compressed CO₂ as the solvent. However, Landon et al^[18] reported that the generation of H₂O₂ in CO₂ was not as effect as that in the conventional solvents. The reason is that, until now, there has not been a reliable method available to measure the amount of *in situ* generated H₂O₂ in compressed CO₂ since: (1) it is difficult to accurately take

H₂O₂ sample from a high pressure reactor filled with compressed CO₂; (2) the precious metal catalyst used in the direct synthesis of H₂O₂ can also catalyze the decomposition of generated H₂O₂, as was observed by Landon et al.^[18] Therefore, simply releasing the reaction pressure and then taking H₂O₂ samples for titration after reaction is not likely to be the best method to accurately measure the amount of *in situ* generated H₂O₂ in compressed CO₂.

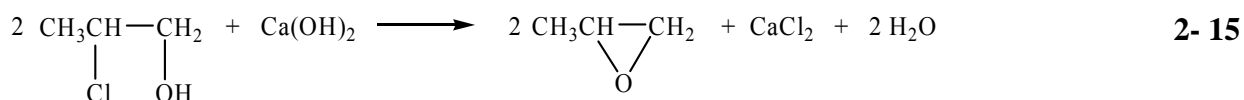
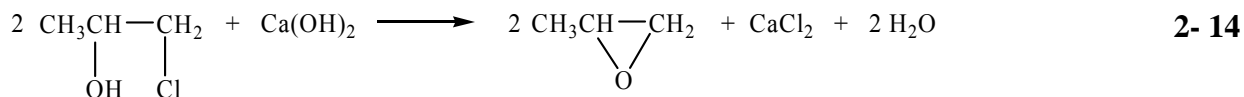
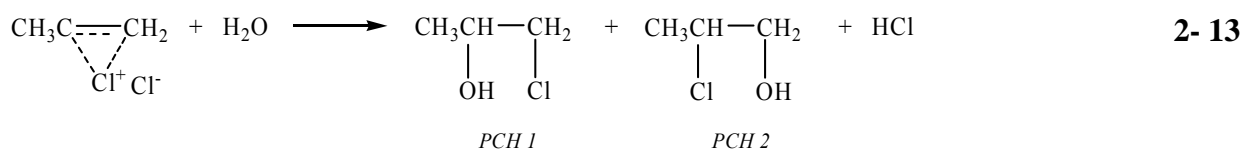
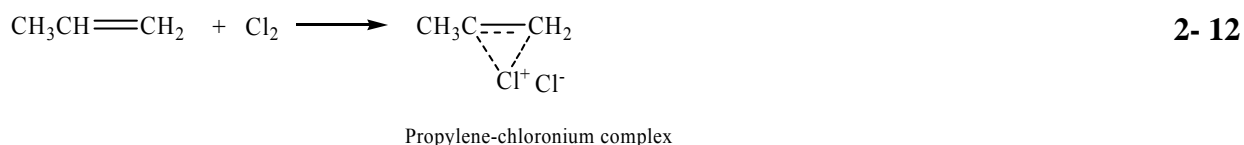
2.3 APPLICATION OF *IN SITU* GENERATED H₂O₂ IN GREEN OXIDATION

2.3.1 Green synthesis of propylene oxide

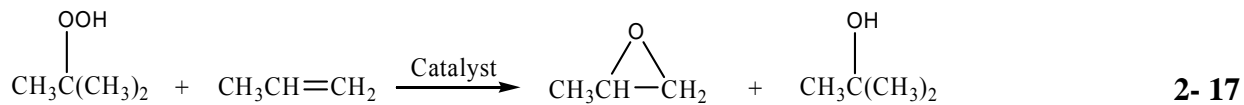
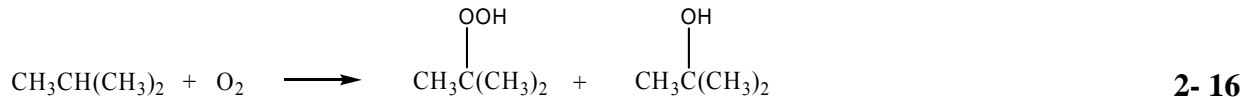
Propylene oxide (PO) is an important bulk chemical with a global annual capacity of ca. 7 million metric tons.^[70] It is used primarily as a reaction intermediate in the production of polyether polyols (ca. 60%, a raw material for polyurethanes), followed by propylene glycol (PG, 21%, a raw material for unsaturated polyester resins). Other uses include the production of propylene glycol ethers, flame retardants, synthetic lubricants, oilfield drilling chemicals, propylene carbonate, allyl alcohol, isopropanolamines etc.

PO is currently produced by two major industrial methods:^[71] namely the chlorohydrin and hydroperoxide processes. In the chlorohydrin process, propylene is reacted first with chlorine to generate a propylene-chloronium complex. This complex is then reacted with water to form 1-chloro-2-propanol (*PCH 1*, ca. 90%) and 2-chloro-1-propanol (*PCH 2*, ca. 10%) as the intermediates. During this process, some by-products (e.g. 1,2-dichloropropane, 1,3-dichloro-2-propanol, 2,3-dichloro-1-propanol and 2,2'-dichlorodiisopropyl ether etc.) can also be generated. *PCH 1* and *PCH 2* both are able to react with a base (e.g. lime) to produce PO. The major

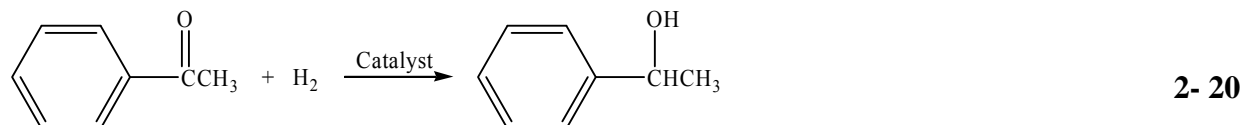
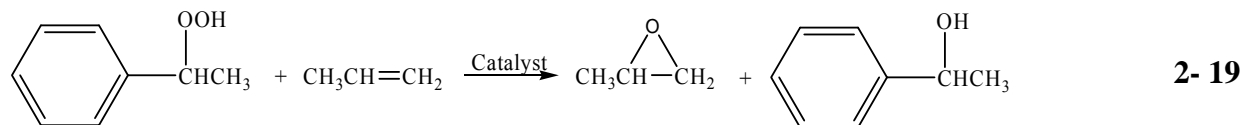
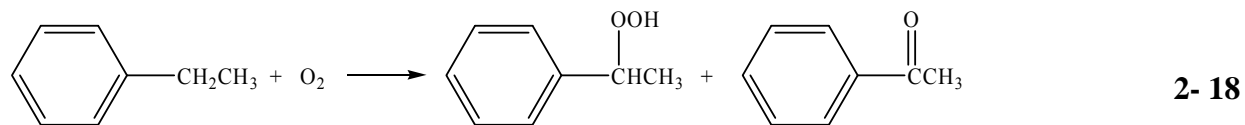
chemical reactions are given by equations (2- 12) to (2- 15). The issues associated with the chlorohydrin process are the use of chlorine, the complicated reaction mechanism leading to the formation of several wastes, and the generation of a stoichiometric amount of salt waste. The total waste generated during the production of PO by the chlorohydrin method is roughly about 40 times that of the PO produced.^[19]

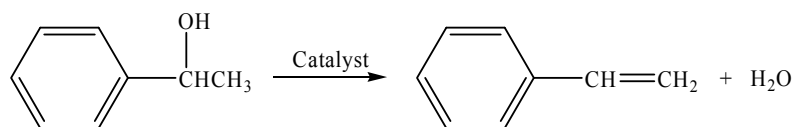


The hydroperoxide process uses either *tert*-butyl hydroperoxide or ethylbenzene hydroperoxide as the oxidant to epoxidize propylene. In the *tert*-butyl hydroperoxide process, *iso*-butane is first oxidized by oxygen in liquid phase to generate a mixture of *tert*-butyl hydroperoxide (ca. 50% in selectivity and 20~30% in yield) and *tert*-butanol (ca. 46% in selectivity). After separation, *tert*-butyl hydroperoxide is then reacted with propylene to produce PO. The major reactions are given by equations (2- 16) and (2- 17).



In the ethylbenzene hydroperoxide process, ethylbenzene is first oxidized by oxygen in the liquid phase to generate a mixture of ethylbenzene hydroperoxide and acetophenone etc.; the generated hydroperoxide is then used to oxidize propylene over a catalyst to form PO and 1-phenylethanol. The co-product, 1-phenylethanol, together with acetophenone (which is first converted to 1-phenylethanol via hydrogenation), is dehydrated to styrene in a vapor phase reaction over a catalyst. These major reactions are expressed by the following equations (2- 18) and (2- 21).

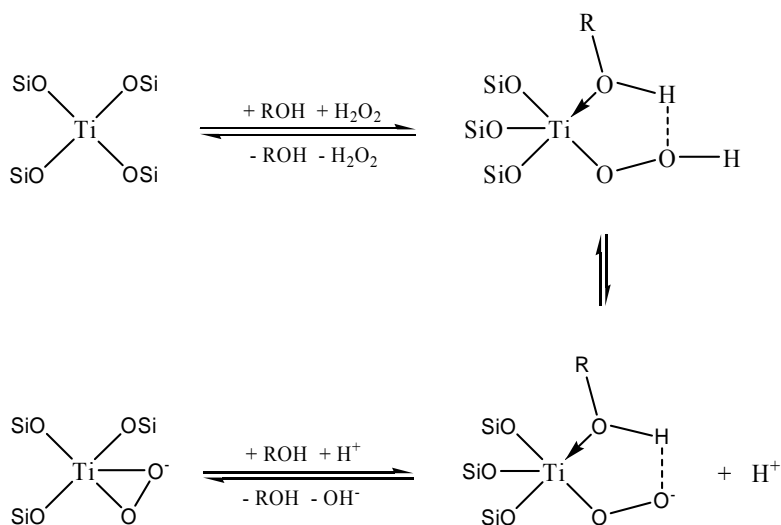




2- 21

The problems associated with these hydroperoxide processes are (1) low hydroperoxide yields due to the low selectivity and safety concerns. Therefore complicated separation and purification measures have to be used in order to obtain the desired hydroperoxides; (2) the generation of large quantity of *tert*-butanol or styrene as co-product. The production of 1 ton of PO is usually accompanied by the generation of 3~4 tons of *tert*-butanol or 2.4 tons of styrene.^[71] Therefore, the PO market is strongly affected by the market for *tert*-butanol and styrene.

In order to avoid the generation of waste and co-products, extensive studies^[67, 71, 72] have been conducted to find means by which to use hydrogen peroxide (H₂O₂), a green oxidant, to replace chlorine and hydroperoxides, especially after the discovery of titanium silicalite (TS-1) in 1980s.^[13] TS-1 has unique catalytic activity for the selective oxidation of some organic compounds with aqueous H₂O₂, especially in the epoxidation of lower olefins. Experimental results^[67] have showed an almost quantitative yield of PO (from propylene) under mild reaction conditions using a dilute methanol solution of H₂O₂. The preferred solvent in carrying out this epoxidation reaction is methanol or the mixture of methanol and water. Without methanol, a significant decrease in PO selectivity could be observed. The proposed mechanism is that methanol could actively interact with H₂O₂ and TS-1 to form a cyclic structure according to **Scheme 1**^[73], in which methanol coordinates with the Ti centers and stabilizes the Ti-peroxo complex through hydrogen bonding, thus enhances the propylene conversion and PO selectivity.



Scheme 1 Interaction between methanol and TS-1 in using H₂O₂ as the oxidant

Recently, Dow and BASF^[70] announced the construction of the first commercial PO plant using pre-manufactured H₂O₂ to epoxidize propylene. Nevertheless, there are several issues associated with using pre-manufactured H₂O₂ according to the 12 principles of green chemistry. As described earlier that the current industrial production method of H₂O₂, the anthraquinone auto-oxidation (AO) process, is not as green as one would prefer due to the generation of wastes, use of large volumes of organic solvents, low efficiency and high energy consumption. More seriously, the production of major raw materials [2-alkylanthraquinone, trioctylphosphate (TOP) and tetrabutyl urea (TBU)] used in the AO process uses toxic chemicals and generates various wastes. From **Section 2.1** we know that the production of 1 ton of 2-ethylanthraquinone (EAQ) will consume about 2 tons of aluminum chloride anhydride and 4~5 tons of oleum (20% in SO₃) and generate tens of tons of wastewater (containing AlCl₃, H₂SO₄ and various organics). The production of TOP uses phosphorus oxychloride and generates hydrogen chloride (HCl) as waste. The production of TBU uses extremely toxic phosgene and also generates HCl. Therefore, using pre-manufactured H₂O₂ to produce PO would mean the shift of human health and

environmental burden from the manufacture of PO (by either the chlorohydrin or hydroperoxide processes) to the production of H₂O₂ and the raw materials used in the AO process.

From both environmental and economic points of view, it is attractive to use *in situ* generated H₂O₂ (synthesized from O₂ and H₂) to replace pre-manufactured H₂O₂ and hence this route has been investigated extensively over the past decade.^[19, 68, 74, 75] The major achievements are summarized in **Table 11**. In general a bifunctional catalyst is used to epoxidize propylene by the *in situ* generated H₂O₂: Here precious metal (Pd, Pt, Au or their combination) loaded on a “support” functions as the catalyst for the *in situ* generation of H₂O₂ from O₂ and H₂, while the “support”, usually a titanium silicalite (TS-1) molecular sieve, catalyzes the epoxidation of propylene. The reaction can be carried out in either gas phase or liquid phase. Gas phase oxidation usually was operated in a continuous mode with relatively high reaction temperature (>100°C), and, an inert gas was used to dilute the reactants for safety. In general, the obtained propylene conversion was less than 10% in order to maintain PO selectivity. Recent results given by Chowdhury et al^[75] showed ca. 7% of propylene conversion and ca. 90% of PO selectivity with the PO production rate of 0.064-0.08g h⁻¹(g cat)⁻¹ when trimethylamine was used as a promoter. In the liquid phase oxidation, a mixture of methanol and water was used as the solvent because, as proposed by Clerici et al,^[73] methanol could interact with the active site of TS-1 to enhance the selectivity of epoxidation. Attempts to increase propylene conversion usually led to a considerable decrease in PO selectivity due to the hydrogenation of propylene and other side-reactions. For example, Laufer and Hoelderich^[76] reported that at a propylene conversion of 21%, the PO selectivity was only 71% in a semi-batch reactor. Using compressed CO₂ as the solvent was also explored by Danciu et al^[19] and Beckman^[23]. Similar to the results obtained in

gas and liquid phase oxidation, the attempts to increase propylene conversion also resulted in the considerable decrease in PO selectivity.

Table 11 Direct oxidation of propylene by the mixture of oxygen and hydrogen in literature

Catalyst	Solvent (promoter)	T, °C	P, bar	Time, hrs	O ₂ /H ₂ /C ₃ H ₆ ratio	Inert gas	C ₃ H ₆ conv. %	PO select.,%	Reference
8.0%Au/Ti-MCM-41	-	100	1	Cont.	1/1/1	Ar	3.1	92	Uphade et al ^[77]
16%Au/Ti-MCM-48	-	100	1	Cont.	1/1/1	Ar	3.0	92	Uphade et al ^[78]
0.05%Au/TS-1	-	200	-	Cont.	1/1/1	He	8.8	81w	Taylor et al ^[79]
Au/TS-1	- (trimethylamine)	150	1	Cont.	1/1/1	Ar	~7	~90	Chowdhury et al ^[75]
0.47%Pd/TS-1	Compressed CO ₂	45	131	4.5	2.08/0.32/1	-	7.5 9.5	94.3 77.1	Danciu et al ^[19] , Beckman ^[23]
(1.0%Pd+0.1%Pt)/TS-1	MeOH/H ₂ O	43	32	2	1.4/1/?	N ₂	11.7	46.0	Meiers et al ^[74]
(1%Pt+0.02%Pd)/TS-1	MeOH/H ₂ O	43	50	~1	0.4/0.25/1	N ₂	3.5	99	Jenzer et al ^[68]
(1%Pd+0.02%Pt)/TS-1	MeOH/H ₂ O	43	7	2	13.1/13.1/1	N ₂	21	71	Rueter et al ^[58]

2.3.2 Green synthesis of adipic acid using H₂O₂

Adipic acid is the most important dicarboxylic acid; its global annual capacity is ca. 2.99 million metric tons.^[80, 81] It is mainly used as a raw material in the production of nylon-6,6 fiber (62%), nylon-6,6 engineering resin (22%), polyester polyols (9%) and plasticizers (4%) etc. The dominant technology for the production of adipic acid is the liquid phase oxidation of KA oil (a mixture of cyclohexanone and cyclohexanol) by nitric acid. The major producers and their market shares are shown in **Figure 7**^[81]. It can be seen that, even after being commercialized for over 50 years, this technology is still highly controlled by several companies. For example, the capacities of Koch (formerly owned by DuPont), Rhodia, Solutia and BASF accounts for ca. 80% of global capacity.

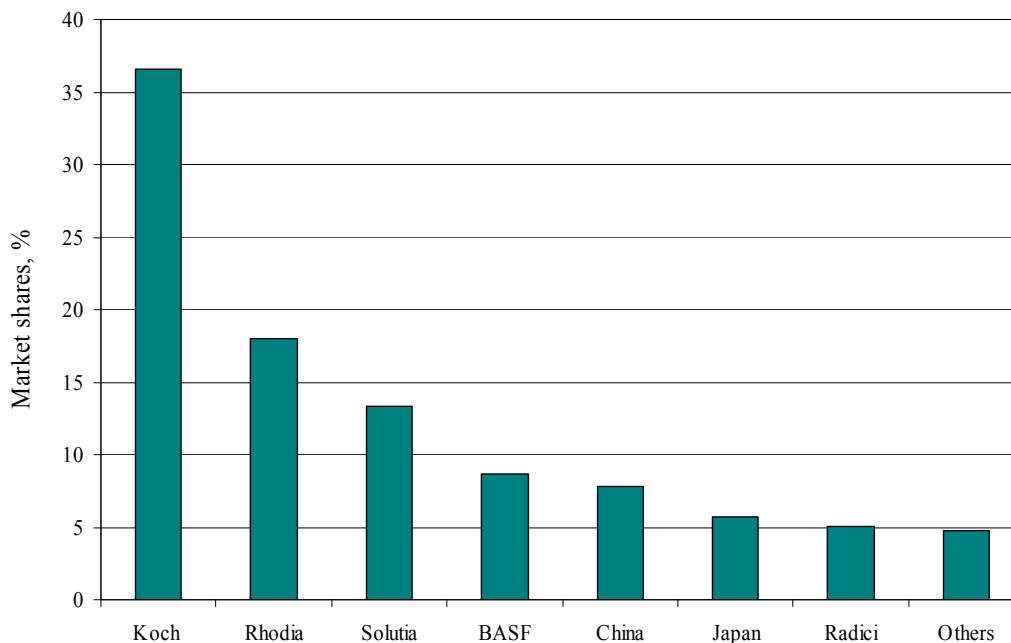
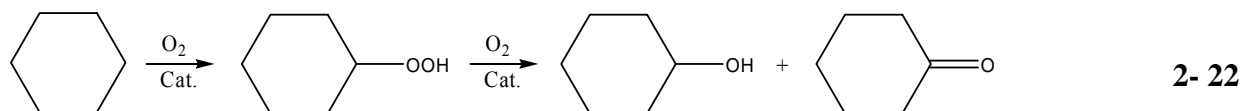


Figure 7 Major adipic acid producers and their market shares

The starting materials for the industrial production of adipic acid are either cyclohexane or phenol, but cyclohexane is dominant. The oxidation of cyclohexane to adipic acid involves two typical oxidation reactions. The first reaction is the catalytic oxidation of cyclohexane by air to a mixture of cyclohexanone/cyclohexanol—referred to as KA (Ketone/ Alcohol) oil. The second reaction is the oxidation of KA oil to adipic acid by nitric acid with the generation of nitrous oxide as a waste.

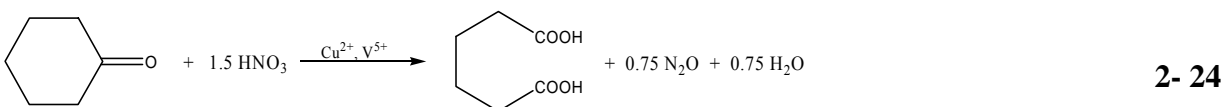
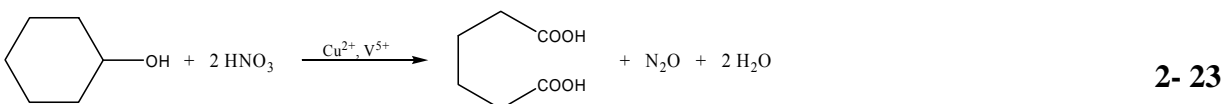
The liquid phase oxidation of cyclohexane by air is usually carried out over cobalt or manganese naphthenate or octanoate in an oxidation tower, or a series of agitated reactors at 125~165°C and 8~15bar.^[82, 83] The reaction pathways are shown by equation (2- 22), cyclohexane was first oxidized to form cyclohexylhydroperoxide; this intermediate can be catalytically converted to the KA oil. The conversion of cyclohexane is usually less than 10% in order to avoid the formation of by-products, even though the selectivity to KA oil is only in the range of 80~85%. When boric acid is used as the oxidation promoter, the selectivity can be further improved under similar cyclohexane conversion.



As an intermediate, KA oil is further catalytically oxidized by nitric acid through the complicated reaction pathways^[6, 84] to adipic acid. The adipic acid yield is ca. 93~95% and the major by-products are glutaric acid and succinic acid.

The environmentally undesirable features of this multi-step process are:

(1). Generation of stoichiometric amount of nitrous oxide as a by-product shown by equations (2- 23) and (2- 24). Theoretically, in order to obtain one kilogram of adipic acid, 0.32kg of nitrous oxide will be generated.^[82] The industrial survey conducted in an adipic acid plant in Japan showed that the emission coefficient of nitrous oxide (N₂O) is 0.25kg N₂O/kg of adipic acid.^[85] Thus the annual emission of N₂O from adipic acid production is ca. 0.7 million tons.



(2). The chemical reactions shown by equations (2- 23) and (2- 24) also imply that at least stoichiometric amount of nitric acid is needed in the production of adipic acid. This makes it the only industrial process using nitric acid to produce a bulk chemical. Furthermore, the production of nitric acid also generates nitrous oxide with the emission coefficient of 2.9kg N₂O/ton of nitric acid.

Nitrous oxide is a harmful gas to the environment by contributing to the greenhouse effect and the ozone layer depletion (although the mechanism is complicated, there is no doubt on the negative effect of nitrous oxide on the ozone layer). As a greenhouse gas, nitrous oxide is very stable with a life time of about 150 years, its global warming potential is 310 times higher than that of carbon dioxide.^[86] Therefore it has to be destroyed prior to its emission.

Various abatement technologies developed by the adipic acid producers to cut the N₂O emissions are listed in **Table 12**.^[85, 87-89] It can be seen that thermal and catalytic decompositions are the dominant technologies. Although these abatement technologies can cut N₂O emission, they will also increase the operating cost^[87] or initial investment dedicated to environmental protection facilities.

Table 12 Current N₂O abatement technologies

Company	Technology	Start-up date	Characteristics
DuPont	Thermal decompose	1958, 1976	No increased cost
	Catalytic decompose	1997	98% decomposed
Rhodia	Partially recycle		20% N ₂ O recycled
Solutia	Oxidize benzene	No industrial operation	To produce phenol
BASF	Catalytic decompose	1997	Increased cost 90~95% decomposed
Asahi Kasei	Thermal decompose	1999	Increased cost 98% decomposed
Radici Chimica	Catalytic decompose	2001	Increased cost

(3). Low conversion and selectivity in the oxidation of cyclohexane makes it one the least effective industrial processes in operation. Therefore, complicated facilities have to be used in

order to separate KA oil, un-reacted cyclohexane and by-products, and to recycle the un-reacted cyclohexane.

(4). The chromium and cobalt salts in waste stream need to be treated before their discharge.

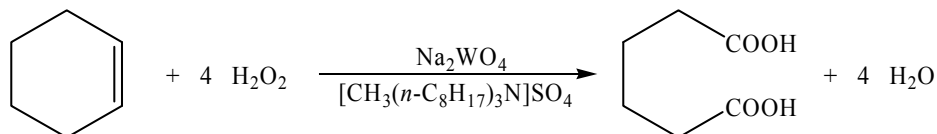
Cyclohexene could be considered as a potential alternative raw material to replace cyclohexane in the synthesis of adipic acid using green oxidant, H₂O₂, as the oxidant. This has been a research focus for years and the recent major achievements are summarized in **Table 13**. Sato et al^[11] first reported that cyclohexene could be effectively oxidized by 30% H₂O₂ using Na₂WO₄·2H₂O as a catalyst and [CH₃(*n*-C₈H₁₇)₃N]HSO₄ as a phase transfer catalyst (PTC); adipic acid yield could reach as high as 93%. The reaction pathway was shown by **Scheme 2** and the total reaction can be expressed by equation (**2- 25**). The detection of intermediates **3** and **5** supported this reaction pathway. However, one of the drawbacks of this process is the use of expensive and harmful phase transfer catalyst (PTC). The improvement had been made by using organic acids to replace PTC since tungstate and selected organic acids could form a peroxytungstate-organic complex.^[90, 91]

Recently Lee et al^[92] experimentally proved that a titanium framework-substituted aluminophosphate number 5 (TAPO-5) zeolite was also an effective catalyst in carrying out the oxidation of cyclohexene to adipic acid using aqueous H₂O₂ as the oxidant, the mechanistic reaction pathway given by Lee et al^[92] was shown in **Scheme 3**. The significance of Lee et al's work is they identified that (1) the oxidation of *cis*-cyclohexanediol was faster than that of *trans*-cyclohexanediol; (2) *trans*-cyclohexanediol was generated through the hydrolysis of cyclohexene oxide, while *cis*-cyclohexanediol was generate via a radical mechanism directly from

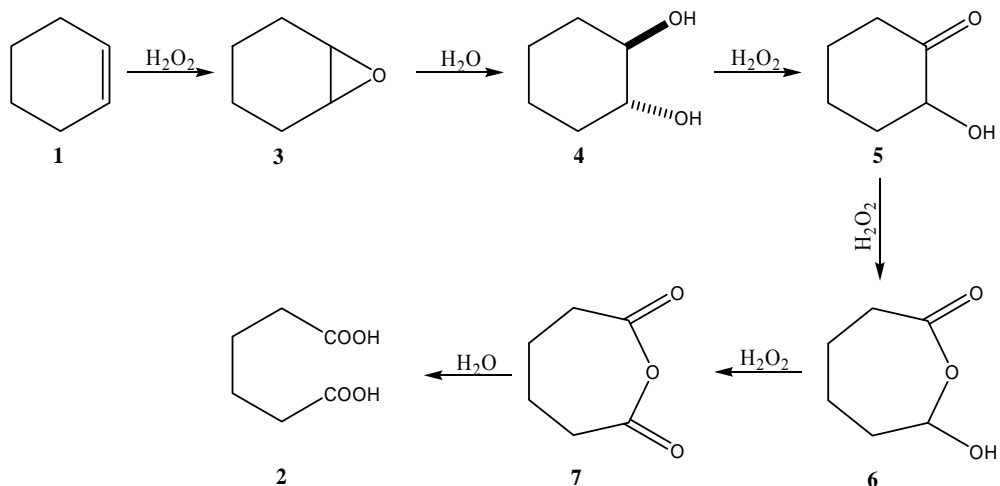
cyclohexene, (3) the proposed mechanistic pathway was based on the identification of each intermediate.

Table 13 Literature results for the oxidation of cyclohexene by H₂O₂

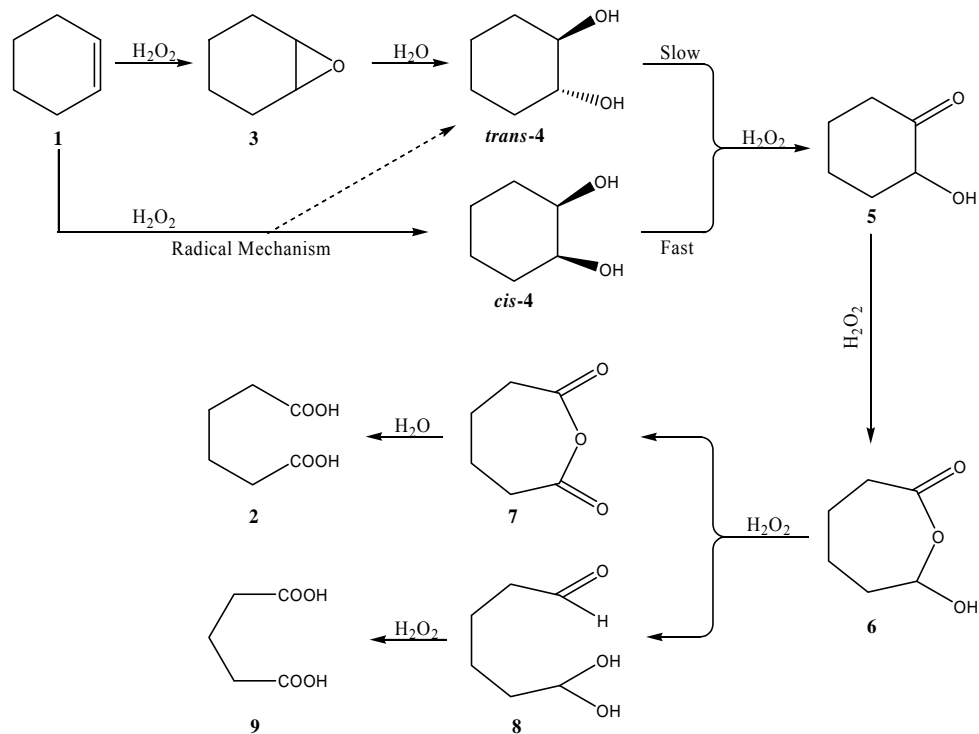
Catalyst	Solvent	T, °C	Time, h	Molar ratio	Conv., %	AA Yield, %	Reference
Na ₂ WO ₄ /PTC	-	75~90	8	4.4:1		93	Sato et al ^[11]
Na ₂ WO ₄ /ligand	-	94	8	4.4:1		93~95	Deng et al ^[90]
OsO ₄ /NMM/Flavin	TEAA/ Acetone	20	26	1.5:1		91 (diols)	Jonsson et al ^[93]
Na ₂ WO ₄ /ligand	-	Reflux	8	4.4:1		88.0	Jiang et al ^[91]
Fe(TPA)	MeCN	4	0.5	4:1	75	45/30(diols /epoxide)	Ryu et al ^[94]
TAPO-5	-	80	72	3.6:1(?)	100	30.3	Lee et al ^[92]
W-MCM-41	HOAc	80	1	1:1	90-95	~80 (diol)	Zhang et al ^[95]



2- 25



Scheme 2 Reaction pathways for the direct oxidation of cyclohexene to adipic acid using tungstate and phase transfer catalyst



Scheme 3 Mechanistic reaction pathway for the oxidation of cyclohexene to adipic acid over TAPO-5 catalyst

However, one of the major obstacles in using cyclohexene as an alternative raw material to produce adipic acid is the use of large amount of pre-manufactured H_2O_2 : Theoretically, at least 4 moles of H_2O_2 are needed in order to oxidize 1 mole of cyclohexene to adipic acid. Therefore, even though the oxidation of cyclohexene by H_2O_2 is a green method to adipic acid, it can not compete with current industrial method economically since the current price of pre-manufactured H_2O_2 is too high.

3.0 RESEARCH OBJECTIVES

The primary research objective of this study is, using the principles of green chemistry as a guideline, to conduct research on the direct synthesis of H_2O_2 from O_2 and H_2 using compressed CO_2 as the solvent over precious metal loaded titanium silicalite (TS-1) and its application in green oxidation reactions, e.g. the epoxidation of propylene to propylene oxide, the oxidation of cyclohexene to adipic acid etc. In order to achieve this objective, the following research were conducted:

1. develop a new green chemistry metric with the consideration of both quality (hazards to both human health and the environment) and quantity of involved chemicals to guide the exploration of green technologies in the direct synthesis of H_2O_2 , oxidation of propylene and cyclohexene by *in situ* generated H_2O_2 ;
2. establish a method to measure the amount of *in situ* generated H_2O_2 from O_2 and H_2 in compressed CO_2 over precious metal loaded TS-1;
3. synthesize bi-functional catalysts, precious metal loaded molecular sieves (TS-1 and W-MCM-41), in order to carry out the direct synthesis of H_2O_2 and green oxidation simultaneously;
4. verify whether H_2O_2 can be effectively synthesized from O_2 and H_2 in compressed CO_2 over precious metal loaded TS-1;

5. examine the effects of the following experimental conditions on H₂ conversion, H₂O₂ selectivity and yields in direct synthesis of H₂O₂ from O₂ and H₂ in compressed CO₂: stirring speed, O₂/H₂ molar ratio, H₂ concentration, catalyst mass, palladium content and the addition of platinum;
6. use the *in situ* generated H₂O₂ from O₂ and H₂ in compressed CO₂ over precious metal loaded TS-1 to epoxidize propylene to propylene oxide; the focus is to develop a method to effectively suppress the side-reactions encountered during epoxidation;
7. explore the possibility to oxidize cyclohexene to adipic acid using *in situ* generated H₂O₂ from O₂ and H₂ in compressed CO₂ over precious metal loaded TS-1 and W-MCM-41.

4.0 DEVELOPMENT OF A GREEN CHEMISTRY METRIC

“When you can measure what you are speaking about, and express it in numbers, you know something about it; but when you cannot measure it, when you cannot express it in numbers, your knowledge is of a meagre and unsatisfactory kind; it may be the beginning of knowledge, but you have scarcely, in your thoughts, advanced to the stage of science.” This famous quote by Lord Kelvin (1824-1907) clearly stated the importance in using numbers in scientific studies. This is also true to green chemistry since whenever you talk about a green technology, the following question will be raised naturally: “So you think your process (or product) is green, how do you know?”^[96] Green chemistry metrics should be used as a tool to address this question. Green chemistry metrics emerged along with the introduction of green chemistry. At present, various green chemistry metrics have been developed to carry out this task. In general, these metrics can be divided into two types: Type I metrics are represented by E-factor,^[97] atom economy (AE)^[98] and reaction mass efficiency (RME)^[96] etc. The definition of these metrics and their calculation methods are summarized in **Table 14**.

Table 14 Some representatives of Type I metrics in green chemistry

Metric	Definition	Calculation	Reference
E-factor	Amount of waste (anything that is not the desired product) produced per kilogram of product	$\frac{\text{amount of waste (kg)}}{\text{kg product}}$	Sheldon ^[97]
Atom efficiency (AE)	How much of the reactants end up in the product	$\frac{\text{m. w. of product}}{\text{m. w. of reactants}} \times 100$	Trost ^[98]
Reaction mass efficiency (RME)	Percentage of the mass of the reactants that remain in the product	$\frac{\text{mass of product}}{\text{mass of reactants}} \times 100$	Constable et al ^[96]

Because of their simplicity, these metrics are widely used by many researchers. However, when examining these metrics, we can find that they consider only one aspect of green chemistry—the quantity of involved chemicals, while ignoring another important aspect of green chemistry—the quality (hazards to both human health and the environment) of these chemicals. This ignorance could, in some case, result in a false conclusion when we use them to compare the greenness of different synthetic methods. For example, we assume a product can be synthesized by two different processes \mathbf{P}_A and \mathbf{P}_B ; in order to produce 1 mole of this product, process \mathbf{P}_A will generate 1 mole of NaCl (58.45g) as waste, while process \mathbf{P}_B generates 1 mole of NaCN (49g) as waste. The application of E-factor shows that process \mathbf{P}_B is greener than \mathbf{P}_A .

However, in industrial practice, the cost of treating NaCN will be much higher than that of NaCl since NaCN is more toxic than NaCl.

As we mentioned earlier, in the industrial production of adipic acid (AA), HNO₃ is used to oxidize cyclohexanol (CHANol), cyclohexanone (CHAO) or their mixture (KA oil) as shown by equations (4- 1) and (4- 2). Many researchers have explored the possibility to use a green oxidant to replace nitric acid. H₂O₂ is one of the more interesting oxidants since water is the only by-product in using H₂O₂ to oxidize CHANol and CHAO^[99] [see reactions (4- 3) and (4- 4)]. However, the application of E-factor, AE and RME given in **Table 15** shows the contradictory conclusion that HNO₃ was greener than H₂O₂ in the synthesis of adipic acid (AA). The calculation of RME was based on data listed in **Table 16**.

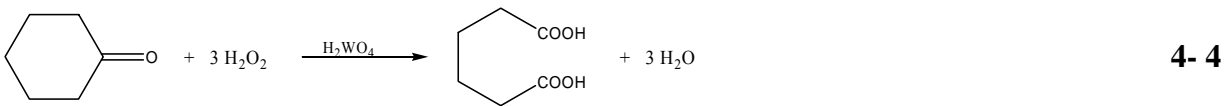
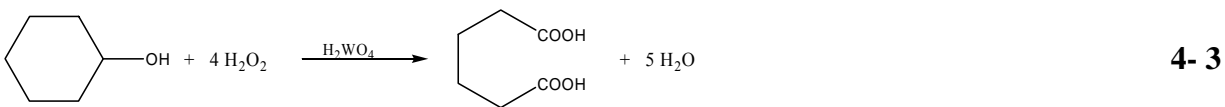
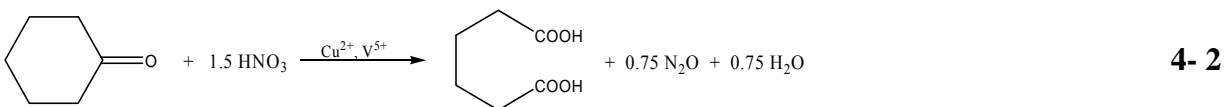
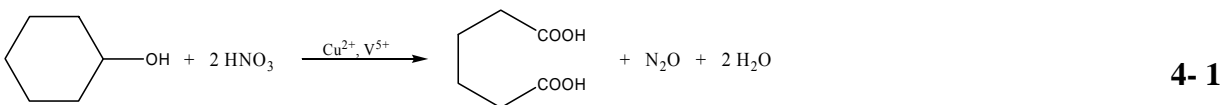


Table 15 Application of Type I metrics in the production of adipic acid using different oxidants

Reactant	Oxidant	E-factor	AE, %	RME, %
CHANol	50~70% HNO ₃	0.55	64.6	59.0
	30% H ₂ O ₂	0.62	61.9	50.9
CHAO	50~70% HNO ₃	0.32	75.9	
	30% H ₂ O ₂	0.37	73.0	62.9
KA oil (1:1)	50~70% HNO ₃			68.4

Table 16 Experimental data used for calculating RME

H ₂ O ₂ as the oxidant ^[99]				HNO ₃ as the oxidant ^[100, 101]			
Chemical	Wt, g	Chemical	Wt, g	Chemical	Wt, kg	Chemical	Wt, kg
CHANol	100	CHAO	100	CHANol	727.3	KA oil	751
H ₂ O ₂	149.4	H ₂ O ₂	114.6	HNO ₃	967	HNO ₃	710
AA	127	AA	135	AA	1000	AA	1000
H ₂ WO ₄ ^a	2.5	H ₂ WO ₄ ^a	2.5	NH ₄ VO ₃ ^a	1.15	NH ₄ VO ₃ ^a	2.3
H ₂ O ^b	97.1	H ₂ O ^b	60.7	Cu ^a	3	Cu ^a	5
				N ₂ O ^b	337.7	N ₂ O ^b	248
				H ₂ O ^b	269	H ₂ O ^b	173

Note: a: Chemicals served as the catalysts;

b. Values calculated according to the related chemical reactions.

Type II metrics are represented by TRACI (**T**ool for the **R**eduction and **A**ssessment of **C**hemical and Other Environmental **I**mpact)^[102] and BASF's eco-efficiency.^[103] TRACI is a computer program developed by the U.S. Environmental Protection Agency (EPA) with the consideration of impact of a product on sustainable development. The 12 impact categories selected by TRACI are: ozone depletion, global warming, smog formation, acidification, eutrophication, human health cancer, human health non-cancer, human health criteria pollutants, eco-toxicity, fossil fuel depletion, land use and water use. BASF's eco-efficiency selects the following five environmental impact categories: energy consumption, emissions, material consumption, toxicity potential, and abuse and risk potential. The emissions include emissions to air (the impact category for emissions to air includes global warming potential, ozone depletion potential, photochemical ozone creation potential and acidification potential), emissions to water and solid wastes. Furthermore, overall weighting factors (which include relevance factors and societal weighting factors) were used to obtain environmental fingerprint.

The following are issues associated with Type II metrics: (1) Due to the complexity of these metrics, the collection of required data could be a tedious burden to a researcher at the early stage of designing and developing a new synthetic method; (2) Anastas and Warner^[2] pointed out that “the goal of green chemistry must involve the full range of hazards (toxicity, explosivity, and flammability) and not be focused simply on pollution or ecotoxicity.” However, Type II metrics consider toxicity of a chemical, but fail to address both flammability and reactivity (or physical hazard) of a chemical—two important impact factors in the design and development of a chemical product and process.

Therefore, it is necessary to develop a new green chemistry metric with the consideration of both quantity and quality of involved chemicals. Furthermore, it should be easy to use.

4.1 DEFINITION OF GREENNESS INDEX FOR A CHEMICAL (GIC)

The core concept of green chemistry is to reduce or eliminate the use or generation of hazardous substances (chemicals). A green chemistry metric which can properly address this concept should consider both quantity and quality of chemicals involved in a chemical process. The quantities of chemicals are easy to determine based on either stoichiometric relationship or the amounts of chemicals used in a chemical process. The quality of chemicals should be expressed by their impacts on both human health and the environment. In this study, the selected impact factors were the persistent and bioaccumulation, hazard (health, flammability, reactivity or physical hazard etc), global warming and ozone depletion etc. The persistent and bioaccumulation issue will be discussed latter. All the parameters used to address hazard should be simple to use and easy to access. The following available hazardous information systems are potential candidates: HMIS (Hazardous Materials Identification System^[104]), NFPA (National Fire Protection Association^[105]), SAF-T-DATA (developed by J. T. Baker^[106]) and WHMIS (Workplace Hazardous Materials Information System developed by the Canadian government^[107]) etc. One common feature of these systems is that numeric ratings are used to indicate the degree of hazard of a chemical. After comparing all these information systems, HMIS was adopted in this study. HMIS was developed by the National Paint & Coatings Association (NPCA) to help employers comply with OSHA's Hazard Communication Standard (HCS).^[108] It includes three hazard factors: health, flammability and reactivity (or physical hazard in the newly released third edition). As can be seen from **Table 17** the rating scale for each factor is in the range of 0~4 for different chemicals according to their hazards.^[109] This system has been widely adopted by major reagent and gas suppliers in their MSDS's. In this

study, the adopted hazardous ratings were from the MSDS's given by Sigma-Aldrich, Praxair and BOC Gases etc.

Table 17 Hazardous ratings defined by HMIS

Rating	Health rating (HR)	Flammability rating (FR)	Physical hazard (or Reactivity, RR)
4	Life-threatening, major or permanent damage may result from single or repeated overexposures.	Flammable gases, or very volatile flammable liquids with flash points below 73 °F, and boiling points below 100°F. Materials may ignite spontaneously with air.	Materials that are readily capable of explosive water reaction, detonation or explosive decomposition, polymerization, or self-reaction at normal temperature and pressure.
3	Major injury likely unless prompt action is taken and medical treatment is given.	Materials capable of ignition under almost all normal temperature conditions. Includes flammable liquids with flash points below 73°F and boiling points above 100°F, as well as liquids with flash points between 73°F and 100 °F.	Materials that may form explosive mixtures with water and are capable of detonation or explosive reaction in the presence of a strong initiating source. Materials may polymerize, decompose, self-react, or undergo other chemical change at normal temperature and pressure with moderate risk of explosion.

Table 17 (continued)

2	Temporary or minor injury may occur.	Materials which must be moderately heated or exposed to high ambient temperatures before ignition will occur. Includes liquids having a flash point at or above 100°F but below 200 °F.	Materials that are unstable and may undergo violent chemical changes at normal temperature and pressure with low risk for explosion. Materials may react violently with water or form peroxides upon exposure to air.
1	Irritation or minor reversible injury possible.	Materials that must be preheated before ignition will occur. Includes liquids, solids and semi solids having a flash point above 200°F.	Materials that are normally stable but can become unstable (self-react) at high temperatures and pressures. Materials may react non-violently with water or undergo hazardous polymerization in the absence of inhibitors.
0	No significant risk to health.	Materials that will not burn.	Materials that are normally stable, even under fire conditions, and will not react with water, polymerize, decompose, condense, or self-react. Non-explosives.

The Montreal Protocol and Kyoto Protocol are globally recognized as efforts to control ozone depletion and global warming. In this study, Ozone Depletion Potential (ODP) was used to address the ozone depletion issue and Global Warming Potential (GWP) was used to address the global warming issue. ODP is defined by the *United Nations Environmental Programme (UNEP)*^[110, 111] as the ratio of the impact on ozone of a chemical compared to the impact of a similar mass of CFC-11. Thus, the ODP of CFC-11 is designated as 1.0. GWP is defined by the *Intergovernmental Panel on Climate Change (IPCC)*^[112] as an index describing the radiative characteristics of well-mixed greenhouse gases that represents the combined effect of the differing times these gases remain in the atmosphere and their relative effectiveness in absorbing outgoing infrared radiation. This index approximates the time-integrated warming effect of a unit mass of a given greenhouse gas in today's atmosphere, relative to that of CO₂. Therefore, the GWP of CO₂ is defined as 1.0. The GWP values over 100-year time horizon are adopted in this study since they are used by United States for policy making and reporting.^[102]

The information about persistent and bioaccumulative chemicals can be found in the US EPA's *Persistent Bioaccumulative and Toxic (PBT) Chemical Program*.^[113] EPA has also developed an evaluation tool, the PBT Profiler,^[114] to predict PBT potential of various chemicals. From the viewpoint of green chemistry, all the priority PBT chemicals listed by EPA should be prohibited when designing and developing a new synthetic process. Therefore, a weighting factor of 2 was assigned to its health, flammability and reactivity ratings if a persistent and bioaccumulative chemical appeared in a synthetic process. Since the health rating was directly related to human health, exponent 2 was assigned to its rating as weighting factor for a chemical used in a synthetic process. For ozone depletion potential (ODP) and global warming potential (GWP), an arithmetic calculation was used to bring them down to similar scale (0~4) as that for

the hazard ratings. The ODP values are in the range of 0~10s, exponent 0.6 was used to adjust their values. The GWP values are in the range of 0 ~several 10,000s, a weighting factor of general logarithm was assigned to those chemicals when their GWP values are greater than 10. For those chemicals with GWPs<10, a weighting factor of 1/10 was assigned to them (see **Table 18** for some examples in calculating the weighted values for the global warming index and ozone depletion index). By assigning different weighting factors, the weighted value for each impact factor is listed in **Table 19**. Thus, a greenness index for a chemical GIC can be calculated according to the definition given in **Table 20**.

Table 18 Calculation of weighted values for the global warming index (GWI) and ozone depletion index (ODI)

Global warming index (GWI)			
Substance	CO ₂	N ₂ O	SF ₆
Global warming potential (GWP)	1	310	22,000
Weighted value	=1/10=0.1 (GWP≤10)	=Log(310)=2.5 (GWP>10)	=Log(22000)=4.3 (GWP>10)
Ozone depletion index (ODI)			
Substance	HCFC-251	Halon-1211	Halon-1301
Ozone depletion potential (ODP)	0.001	3.0	10.0
Weighted value	=0.001 ^{0.6} =0.16	=3.0 ^{0.6} =1.9	=10.0 ^{0.6} =4.0

Table 19 Weighted values for different impact factors in calculating GIC

Item	Chemical	Data source	Factor	Value	Weighted Value
Hazard index (HI)	Non-persistent and non-bioaccumulative chemicals	HMIS	Health rating	HR	HR ²
			Flammability rating	FR	FR
			Reactivity rating	RR	RR
	Persistent and bioaccumulative chemicals	HMIS	Health rating	HR	(2HR) ²
			Flammability rating	FR	2FR
			Reactivity rating	RR	2RR
Ozone depletion index (ODI)	Ozone depletion substances	UNEP	Ozone depletion potential	ODP	(ODP) ^{0.6}
Global warming index (GWI)	Greenhouse gases	IPCC	Global warming potential	GWP	$\frac{GWP}{10}$ if GWP ≤ 10 Log(GWP) if GWP > 10

Table 20 Calculation of greenness index for a chemical (GIC)

Chemical	GIC (greenness index for a chemical)
Non-persistent & non-bioaccumulative chemicals	$GIC = HI + ODI + GWI$ $= \begin{cases} HR^2 + FR + RR + (ODP)^{0.6} + \frac{GWP}{10} & \text{if } GWP \leq 10 \\ HR^2 + FR + RR + (ODP)^{0.6} + \text{Log}(GWP) & \text{if } GWP > 10 \end{cases}$
Persistent & bioaccumulative chemicals	$GIC = HI + ODI + GWI$ $= \begin{cases} (2HR)^2 + 2FR + 2RR + (ODP)^{0.6} + \frac{GWP}{10} & \text{if } GWP \leq 10 \\ (2HR)^2 + 2FR + 2RR + (ODP)^{0.6} + \text{Log}(GWP) & \text{if } GWP > 10 \end{cases}$

4.2 DEFINITIONS OF GIF, GIO, GIR AND GIP

As being mentioned earlier, a proper green chemistry metric should consider both quantity and quality of a chemical. In this study, the greenness index for a chemical GIC was adopted to express the quality of a chemical, while the quantity of a chemical can be obtained according to the chemical reaction or the amounts of chemicals added in a chemical process. Here, four new concepts were defined to address different situations accordingly: greenness index for a chemical formula (GIF), greenness index for an oxidant (GIO), greenness index for a chemical reaction (GIR), and greenness index for a product (GIP).

As shown in **Table 21**, a chemical formula usually contains certain amounts of various chemicals. The greenness index for this chemical formula GIF, is defined by equation (4- 5) in this study.

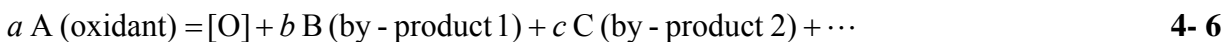
Table 21 Calculation of greenness index for a chemical formula GIF

Compound	A	B	C	D	...
Mass, g	M_A	M_B	M_C	M_D	...
GIC	GIC_A	GIC_B	GIC_C	GIC_D	...

$$GIF = \frac{GIC_A M_A + GIC_B M_B + GIC_C M_C + GIC_D M_D + \dots}{M_A + M_B + M_C + M_D + \dots} \quad 4- 5$$

By using equation (4- 5), we can easily compare the greenness of two different chemical formulas. The smaller the GIF number, the greener a chemical formula will be.

One of the biggest issues associated with oxidation reactions is the use of many toxic oxidants. Therefore, “the key to the new green oxidation chemistry will be the use and generation of little or no hazardous substances.”^[2] However, until now, there is no practical guideline to evaluate the greenness of an oxidant. In this study, the greenness index for an oxidant (GIO) was defined to address this issue. For a generic oxidant A, its decomposition can be expressed by equation (4- 6) during an oxidation reaction. The greenness index, GIO, for oxidant A is, therefore, defined by equation (4- 7) in this study.



$$\text{GIO} = \frac{a \text{GIC}_A \text{MW}_A + b \text{GIC}_B \text{MW}_B + c \text{GIC}_C \text{MW}_C + \dots}{a \text{MW}_A + b \text{MW}_B + c \text{MW}_C + \dots} \quad 4- 7$$

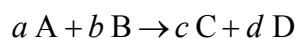
Where MW is molecular weight of a chemical.

The comparison of GIO values for various oxidants is given in **Table 22**. It can be seen that the greenness of different oxidants could be easily evaluated according to their GIO values. For example, the GIO value of 30% H₂O₂ (6.5) was smaller than that of 50%~70% HNO₃ (7.6), therefore, as an oxidant, 30% H₂O₂ is greener than 50%~70% HNO₃ in the production of adipic acid. It is also concluded from **Table 22** that due to their high GIO values, heavy metal oxides and salts are less green when compared with other commonly used oxidants.

Table 22 The greenness index GIO for various oxidants

Oxidant	Decomposition by-product	GIO
O ₂	H ₂ O	1.9
3% H ₂ O ₂	H ₂ O	0.7
30%~50% H ₂ O ₂	H ₂ O	6.5
50%~70% HNO ₃	N ₂ O and H ₂ O (in the production of adipic acid)	7.6
<i>t</i> -BuOOH	<i>t</i> -BuOH	7.7
NaClO	NaCl	5.5
KHSO ₅	KHSO ₄	11.1
CrO ₃	Cr ₂ O ₃	9.0

For a generic chemical reaction shown by equation (4- 8), the greenness index of this reaction, GIR, is defined by equation (4- 9) if the information about solvent and catalyst was not available. If the information was available, the GIR for this generic reaction was given by equation (4- 10). This calculated GIR considered both stoichiometric quantities of reactants, product, by-products, solvent and catalyst (if information was available) and their greenness index GIC values. We assume D was the desired product, then the greenness index for product D, GIP, was defined by equation (4- 11) based on the amounts of reactants, solvent and catalyst added, the amounts of product and by-product generated, and solvent and catalyst used in the reaction.

**4- 8**

$$\text{GIR} = \frac{c \text{GIC}_C \text{MW}_C + d \text{GIC}_D \text{MW}_D + a \text{GIC}_A \text{MW}_A + b \text{GIC}_B \text{MW}_B}{c \text{MW}_C + d \text{MW}_D + a \text{MW}_A + b \text{MW}_B} \quad 4-9$$

$$\text{GIR} = \frac{c \text{GIC}_C \text{MW}_C + d \text{GIC}_D \text{MW}_D + a \text{GIC}_A \text{MW}_A + b \text{GIC}_B \text{MW}_B + \text{GIC}_{\text{Sol}} \text{MW}_{\text{Sol}} + \text{GIC}_{\text{Cat}} \text{MW}_{\text{Cat}}}{c \text{MW}_C + d \text{MW}_D + a \text{MW}_A + b \text{MW}_B + \text{MW}_{\text{Sol}} + \text{MW}_{\text{Cat}}} \quad 4-10$$

$$\text{GIP} = \frac{\text{GIC}_C M_C + \text{GIC}_D M_D + \text{GIC}_A M_A + \text{GIC}_B M_B + \text{GIC}_{\text{Sol}} M_{\text{Sol}} + \text{GIC}_{\text{Cat}} M_{\text{Cat}}}{M_D + M_{\text{Sol}} + M_{\text{Cat}}} \quad 4-11$$

Where MW is molecular weight and M is mass of a chemical.

4.3 APPLICATION OF THE NEW GREEN CHEMISTRY METRIC

Using the definitions described above to express the greenness index for a reaction GIR and greenness index for a desired product GIP, the greenness of different processes in the production of adipic acid was re-evaluated. The calculated results of GIC, GIR and GIP values are given in **Table 23** and **Table 24**, respectively. It can be seen that the GIR values for the production of adipic acid using H₂O₂ as the oxidant were smaller than that using HNO₃. This meant that H₂O₂ was greener than HNO₃ in the production of adipic acid. However, the calculated GIP values for the production of adipic acid using H₂O₂ were larger than that using HNO₃ due to the lower adipic acid yields in using H₂O₂ (when CHANol was used as the starting material, adipic acid yield was only 87%, while for CHAO, the yield was 91%;^[99] when HNO₃ was used, the adipic acid yield was 94.2%^[100, 101]). If the same yields were considered, the GIP value using H₂O₂ would be smaller than that using HNO₃. For example, at adipic acid yield of 94.2%, if CHANol was used as the starting material, the GIP using H₂O₂ would be 15.03, while using HNO₃, it was

15.20. This suggests that even if a new synthetic method is greener than the previous one according to the chemical reaction itself, the yield of desired product from this new method should reach a certain value in order to ensure the greenness of this new process. However, even at adipic acid yield of 94.2%, the application of RME still showed that HNO₃ was greener than H₂O₂.

Table 23 Calculation of GIC for the production of adipic acid with different oxidants

Substrate	HR	FR	RR	ODP	GWP	<i>GIC</i>	MW
CHANol	2	2	0	0	0	6	100.2
CHAO	2	2	0	0	0	6	98.2
Cyclohexene	1	3	0	0	0	4	82.2
HNO ₃ , 50~70%	3	0	0	0	0	9	63.0
H ₂ O ₂ , 30%	3	0	1	0	0	10	34.0
Adipic acid	2	0	0	0	0	4	146.1
N ₂ O	2	0	0	0	310	6.5	44
H ₂ O	0	0	0	0	0	0	18
H ₂ WO ₄	2	0	0	0	0	4	249.9
Cu granular	0	3	1	0	0	4	63.5
NH ₄ VO ₃	4	0	0	0	0	16	117

Table 24 Calculation of GIR and GIP for the production of adipic acid with different oxidants

Substrate	CHANol		CHAO		ol/one mixture (1:1 in wt)
Oxidant	50~70%HNO ₃	30% H ₂ O ₂	50~70%HNO ₃	30% H ₂ O ₂	50~70%HNO ₃
GIR	5.76	5.39	5.81	5.48	
GIP	15.20	16.25		12.77	12.47

Two more examples were given below to demonstrate the use of this new green chemistry metric: the first one is an inorganic reaction and the second one is an organic reaction.

Example I: Production of precipitated barium sulfate

Precipitated barium sulfate (BaSO₄, also called blanc fixe) is an important barium salt. It is mainly used as a filler and extender, in some fields also as a white pigment. It is manufactured by adding dilute sulfuric acid or sodium sulfate to a solution of barium sulfide.^[115] The chemical reactions of these two methods can be expressed by the following two equations:



The comparison of greenness of these two methods obtained by Type I metrics and the new metric developed in this study is given in **Table 25**. **Table 26** lists the calculated GIC values, which were used to calculate GIR and GIP (assume reactants were in stoichiometric

amounts). From **Table 25**, we can draw the following conclusions: The results of E-factor, AE and RME showed that using H₂SO₄ was greener than using Na₂SO₄, while the results of GIR and GIP in this study suggested that using Na₂SO₄ was greener than using H₂SO₄. In industrial practice, when H₂SO₄ is used as a starting material, a base (e.g., sodium hydroxide) has to be used to neutralize generated by-product H₂S. This is because H₂S is a highly toxic chemical; its direct release to the environment is prohibited. Thus, it is obvious that using Na₂SO₄ is greener than using H₂SO₄, which agreed with the conclusion drawn according to the new green chemistry metric developed in this study.

Table 25 Comparison of greenness in producing BaSO₄ obtained by different metrics

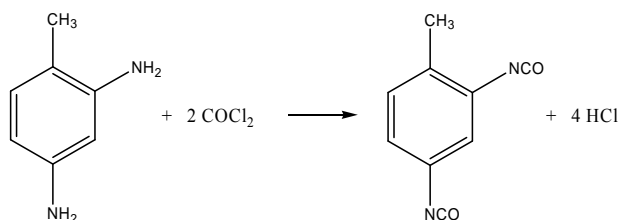
Method	E-factor	AE, %	RME, %	GIR	GIP
H ₂ SO ₄	0.15	87.3	87.3	4.7	9.7
Na ₂ SO ₄	0.33	74.9	74.9	2.7	6.1

Table 26 Calculation of GIC for the production of BaSO₄ by different methods

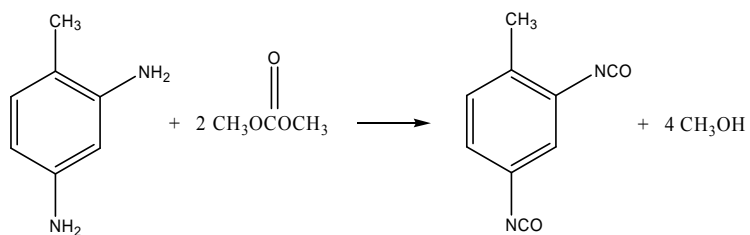
Chemical	HR	FR	RR	ODP	GWP	<i>GIC</i>	MW
BaS	1	0	2	0	0	3	169.4
H ₂ SO ₄	3	0	2	0	0	11	98.1
Na ₂ SO ₄	0	0	1	0	0	1	142.0
BaSO ₄	1	0	0	0	0	1	233.4
H ₂ S	4	4	0	0	0	20	34.1
Na ₂ S	3	0	1	0	0	10	78.0

Example II: Production of toluenediisocyanate (TDI)

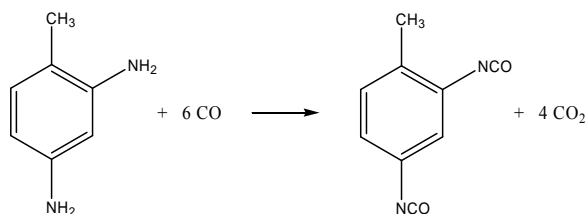
Toluenediisocyanate (TDI) is a major raw material in the production of polyurethane; it is industrially produced by a phosgene-based route. In this method, phosgene is reacted with toluenediamine to generate TDI and hydrochloride as a by-product [see equation (4- 14)]. This process is not environmentally benign due to the use of extremely toxic phosgene as a reactant and the generation of corrosive hydrochloride as a by-product. Many researchers are trying to develop new technologies to replace this phosgene process. Some of the potential processes are DMC method using dimethyl carbonate to react with toluenediamine^[116] and CO method using carbon monoxide to react with toluenediamine.^[117, 118] Their chemical principles are shown by equations (4- 15) and (4- 16), respectively. However, the application of E-factor, AE and RME (assume reactants are in stoichiometric amounts) showed that the greenness of these methods in the synthesis of TDI was in the following order: DMC method>Phosgene method>CO method (see **Table 27** for details). While the results from our newly developed metric GIR and GIP (assuming reactants were in stoichiometric amounts) disclosed that the greenness of these three methods was in the following order: CO method >DMC method>Phosgene method. In practice, whenever it is possible, phosgene should be avoided due to its extreme toxicity.



4- 14



4- 15



4- 16

Table 27 Comparison of greenness in the production of TDI with different methods

Method	E-factor	AE, %	RME, %	GIR	GIP
Phosgene	0.84	54.4	54.4	13.5	39.7
DMC	0.74	57.6	57.6	11.2	28.8
CO	1.01	49.7	49.7	4.8	9.1

4.4 SUMMARY

In this study, we classified current green chemistry metrics into two types: Type I is represented by E-factor, atom economy (AE) and reaction mass efficiency (RME). These widely used

metrics consider only quantity of involved chemicals. The ignorance of quality of involved chemicals could result in false conclusion as demonstrated by the production of adipic acid with both HNO_3 and H_2O_2 as the oxidant. Type II is represented by US EPA's TRACI (**T**ool for the **R**eduction and **A**ssessment of **C**hemical and Other Environmental **I**mpact) and BASF's eco-efficiency. However, they are too complicated to be used as a daily tool to evaluate the greenness of a synthetic method. Furthermore, they fail to address the reactivity (physical hazard) and flammability of a chemical—two important factors in designing and developing a chemical process.

Based on above analysis, a new green chemistry metric was developed in this study. This new metric not only considered both quantity and quality (hazards to both human health and the environment) of chemicals, but also easy to use. Greenness index for a chemical (GIC) was assigned to a chemical with the consideration of the following impact factors: persistence and bioaccumulation, hazards (including health, flammability, reactivity or physical hazard), ozone depletion and global warming. By considering the amounts of reactants, solvent and catalyst, desired product and by-product and their GIC values, greenness index for a chemical formula (GIF), for an oxidant (GIO), for a reaction (GIR), and for a product (GIP) were defined accordingly and used to evaluate the greenness of a chemical formula, an oxidant, a chemical reaction, and a desired product.

This new green chemistry metric was used as a guideline in this study for search of greener technologies in the synthesis of H_2O_2 , oxidation of propylene to propylene oxide and cyclohexene to adipic acid etc.

In a recently published editorial “It’s not easy being green” on *Chemical & Engineering News* (August 6, 2007), Acker^[119] pointed out that “*What is green? This important discussion is just beginning, and I predict it will be an issue for some time. I believe that at some point in the future, a consumer will pick up a product and be provided with an easy-to-understand way to determine the relative greenness of that product...*” The new green metric developed in this study could be considered as an attempt toward this future goal.

5.0 DIRECT SYNTHESIS OF H₂O₂ FROM O₂ AND H₂ IN CO₂

The new green chemistry metric developed in this study was used to evaluate the greenness of different methods for the synthesis of H₂O₂: (1) the AO process using EAQ as the working carrier and a mixture of trimethylbenzene and TOP as the solvent; (2) direct synthesis using a mixture of methanol and water as the solvent; (3) direct synthesis using compressed CO₂ as the solvent. The greenness index GIR values for these reactions are given in **Table 28** and the GIC values for the chemicals involved in these reactions are listed in **Table 29**. It is clear that using compressed CO₂ as the solvent had the lowest GIR value meaning that it was greener than other processes. Since methanol is a toxic, flammable and volatile chemical, using it as the solvent could considerably compromise the greenness of direct synthesis of H₂O₂ from O₂ and H₂.

Table 28 Greenness index for the reactions in the synthesis of H₂O₂

Method for the synthesis of H ₂ O ₂	GIR	
$\text{H}_2 + \text{O}_2 \xrightarrow[\text{EAQ}]{\text{Trimethylbenzene/TOP}} \text{H}_2\text{O}_2$	2.0	5-1
$\text{H}_2 + \text{O}_2 \xrightarrow{\text{MeOH/water}} \text{H}_2\text{O}_2$	3.1	5-2
$\text{H}_2 + \text{O}_2 \xrightarrow{\text{CO}_2} \text{H}_2\text{O}_2$	1.7	5-3

Table 29 The GIC values for the chemicals used in the synthesis of H₂O₂

Chemical	HR	FR	RR	ODP	GWP	<i>GIC</i>	MW
H ₂	0	4	3	0	0	7	2
O ₂	0	0	3	0	0	3	32
3% H ₂ O ₂	0	0	1	0	0	1	34
Trimethylbenzene	2	2	0	0	0	6	120.2
TOP	1	1	0	0	0	2	434.7
EAQ	0	0	0	0	0	0	236.3
Methanol	2	3	0	0	0	7	32
CO ₂	1	0	0	0	0.1	1.1	44

5.1 EXPERIMENTAL

5.1.1 Chemicals and Catalysts

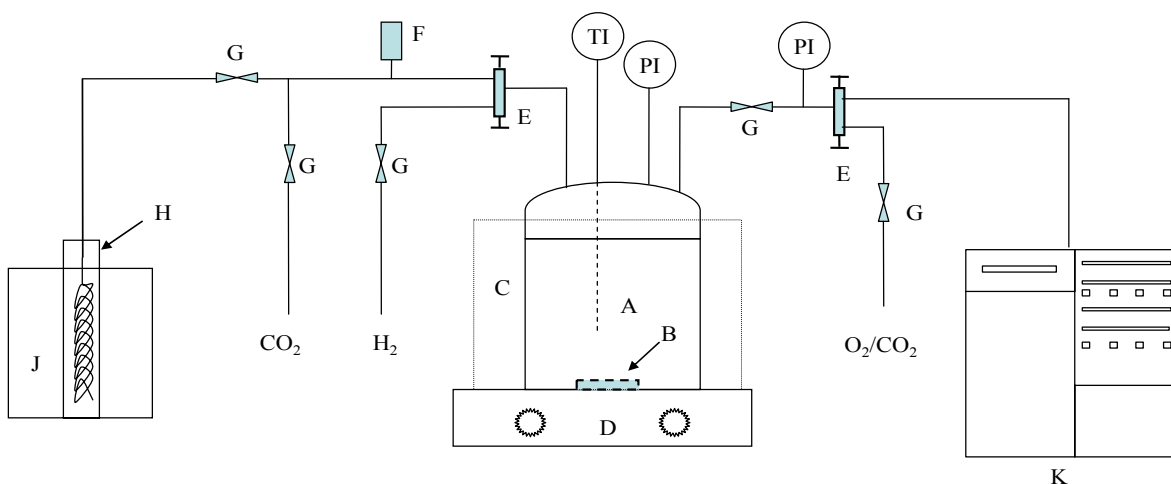
The purities of O₂, H₂ and CO₂ (from Penn Oxygen, Jeannette, PA) used in this study were all above 99.9%. Pyridine (99+%, Aldrich), pyridine *N*-oxide (95%, Aldrich), H₂O₂ (30%, J. T. Baker), methanol (99.9%, Fisher), [Pd(NH₃)₄](NO₃)₂ [10%(wt) solution in water, Aldrich], Pt(NH₃)₄Cl₂·H₂O (98%, Aldrich) and Mineral oil for IR spectroscopy (Aldrich) were all used as received without further purification.

TS-1 and 0.35%Pd/TS-1 were received as a gift from Lyondell Chemical Company. The methods for preparing 0.2%Pd/TS-1, (0.2%Pd+0.02%Pt)/TS-1, (0.35%Pd+0.035%Pt)/TS-1, 0.6%Pd/TS-1, (0.6%Pd+0.06%Pt)/TS-1, 1.0%Pd/TS-1 and (1.0%Pd+0.1%Pt)/TS-1 catalysts were similar to that given by Hancu et al.^[120] A typical procedure is described below with the preparation of (1.0%Pd+0.1%Pt)/TS-1 as an example: 3.0g of TS-1 and 12ml of deionized water were added to a glass flask and then heated to 80°C under continuous stirring. To this solution, 0.82ml of 10% (wt) [Pd(NH₃)₄](NO₃)₂ solution and 0.26ml of 2% (wt) Pt(NH₃)₄Cl₂ solution were added. This mixture was stirred for 24 hours and then cooled to room temperature. The solid was recovered by filtering and then washing 3 times with deionized water and then dried at 80°C overnight. It was then calcined in air at 150°C for 4 hours and reduced by H₂ at room temperature for 4 hours. The yield of as-synthesized (1.0%Pd+0.1%Pt)/TS-1 catalyst was 2.94g.

5.1.2 General procedures for direct synthesis of H₂O₂ in CO₂

The experimental setup is shown in **Figure 8**. Direct synthesis of H₂O₂ from O₂ and H₂ in compressed CO₂ was conducted in a 30ml stainless steel reactor **A** manufactured at the University of Pittsburgh. A cylindrical glass liner was used to prevent the decomposition of H₂O₂ by the metal wall. The net volume of reactor was therefore reduced to 25ml. Initially, the reactor and the glass liner were both passivated with 35% HNO₃ for 4 hours and 30% H₂O₂ for 10 hours; after each experiment, they were also passivated by 30% H₂O₂ for 4 hours. In a typical experiment, 0.5ml of “indicator” compound—pyridine, 0.5ml water and catalyst were loaded to the reactor **A**. A magnetic stirring bar **B** was placed inside the reactor in order to keep the reactants well-mixed. The reactor was first charged with a known amount of O₂/CO₂, followed by CO₂, and then a known amount of H₂. The reaction pressure was finally adjusted to 125bar by

adding more CO₂. The reaction temperature was controlled at 60°C by stirrer/ hotplate **D**. The direct synthesis of H₂O₂ was allowed to run for 5 hours, and the amount of un-reacted H₂ in the reactor was analyzed by using an online HP 5890A gas chromatograph (GC) equipped with a TCD detector and a HayeSep D packed column (20ft×1/8”) and controlled by a HP ChemStation. The reactor was then ice-cooled to 0~5°C and the gas mixture inside the reactor was vented into a known amount of methanol. This methanol solution was used to extract pyridine *N*-oxide and un-reacted pyridine from the reactor and analyzed by another 5890A GC equipped with a FID detector and a DB-1 capillary column (30m×0.253mm×0.50μm) to determine the quantities of pyridine *N*-oxide and pyridine (indicator). A proportional relief valve was installed for safety.



A. High pressure reactor, **B.** Stirring bar, **C.** Vessel, **D.** Stirrer/hotplate, **E.** Three-way valves, **F.** Proportional relief valve, **G.** Two-way valves, **H.** Venting vessel, **J.** Glass vessel, **K.** Online gas chromatograph

Figure 8 Experimental setup for the direct synthesis of H₂O₂ in CO₂

H₂ conversion, H₂O₂ selectivity and H₂O₂ yield were defined by the following equations, respectively.

$$\text{H}_2 \text{ conversion (\%)} = \frac{\text{the amount of H}_2 \text{ consumed during reaction (mmol)}}{\text{the amount of H}_2 \text{ added to the reactor (mmol)}} \times 100 \quad \text{5- 4}$$

$$\text{H}_2\text{O}_2 \text{ selectivity (\%)} = \frac{\text{the amount of } \textit{in situ} \text{ generated H}_2\text{O}_2 \text{ (mmol)}}{\text{the amount of H}_2 \text{ consumed during reaction (mmol)}} \times 100 \quad \text{5- 5}$$

$$\text{H}_2\text{O}_2 \text{ yield (\%)} = \frac{\text{the amount of } \textit{in situ} \text{ generated H}_2\text{O}_2 \text{ (mmol)}}{\text{the amount of H}_2 \text{ added to the reactor (mmol)}} \times 100 \quad \text{5- 6}$$

The experiments for obtaining calibration curve were similar to the direct synthesis of H₂O₂ except that the reactants were 0.5ml of “indicator” compound—pyridine, a known amount of 30% H₂O₂, 0.05g TS-1. If the total volume of reactants was less than 1.0ml, water was added to bring the total volume to 1.0 ml. The reaction pressure was adjusted to 125bar by using only compressed CO₂. The yield of pyridine *N*-oxide was analyzed using the GC.

5.1.3 General procedures for the decomposition of H₂O₂

The experiments used to investigate the decomposition of H₂O₂ were conducted at ambient pressure in a 50ml glass flask. The flask was placed in an oil bath in order to keep temperature at 60°C during experiment. 0.1g of catalyst and 12.4mmol of “indicator” compound (pyridine) were placed into this flask. 12.4mmol of 30%H₂O₂ was then added to above mixture and the reactor was stirred for 5 hours. During the decomposition experiment, the flask was connected to a

condenser to prevent the reactants from evaporating. After reaction, methanol was used to extract product and reactant. This methanol solution was analyzed by 5890A GC to determine the yield of pyridine *N*-oxide.

5.2 CATALYST CHARACTERIZATION

In order to examine the effect of impregnating precious metals Pd (and Pt) on TS-1, Fourier Transform Infrared Spectroscopy (FT-IR) and Powder X-ray Diffraction (XRD) techniques were used to identify the changes of functional groups of TS-1 and the crystallinity of TS-1 before and after the impregnation in this study.

5.2.1 FT-IR spectra

FT-IR spectra of TS-1, precious metal loaded TS-1 were recorded on a Genesis II FT-IR Spectrometer (Mattson Instruments, Wisconsin, USA) using a Nujol Mull technique. Compared with using a KBr wafer technique, the Nujol Mull technique is a rapid, inexpensive way to get an FT-IR spectrum of solid sample.^[121] Nujol is a commercially available mineral oil (saturated hydrocarbon) having medium molecular weights (higher than kerosene and lower than paraffin). Since its IR spectrum has no overlap with the fingerprint wavenumbers of TS-1, it is possible to use the Nujol Mull technique to examine TS-1 and precious metal loaded TS-1. To make a Nujol mull, one first places a small amount of solid sample in an agate mortar and pre-grinds it to a fine powder, then several drops of mineral oil are added and mixed thoroughly by grinding with a pestle. Thus, a Nujol Mull is a suspension of a fine solid powder in mineral oil. To measure its

IR, a few drops of this suspension are placed between two sodium chloride plates and then the plates are inserted into the instrument sample holder for scanning.

The catalytic activity of TS-1 is due to the incorporation of Ti atoms into the framework of silicalite, which is characterized by a band at 960 cm^{-1} on its FT-IR spectrum (this band is assigned to asymmetric Ti-O-Si stretch in the literature). The comparisons of FT-IR spectra of TS-1, 0.2%Pd/TS-1 and (0.2%Pd+0.02%Pt)/TS-1, 0.35%Pd/TS-1 and (0.35%Pd+0.035%Pt)/TS-1, 0.6%Pd/TS-1 and (0.6%Pd+0.06%Pt)/TS-1, and 1.0%Pd/TS-1 and (1.0%Pd+0.1%Pt)/TS-1 are shown in **Figure 9** to **Figure 12**. It can be seen that there was no change in all fingerprint bands in TS-1 before and after the impregnation of precious metals. This meant that the effect of impregnating Pd (and Pt) on the functional groups of TS-1 was negligible.

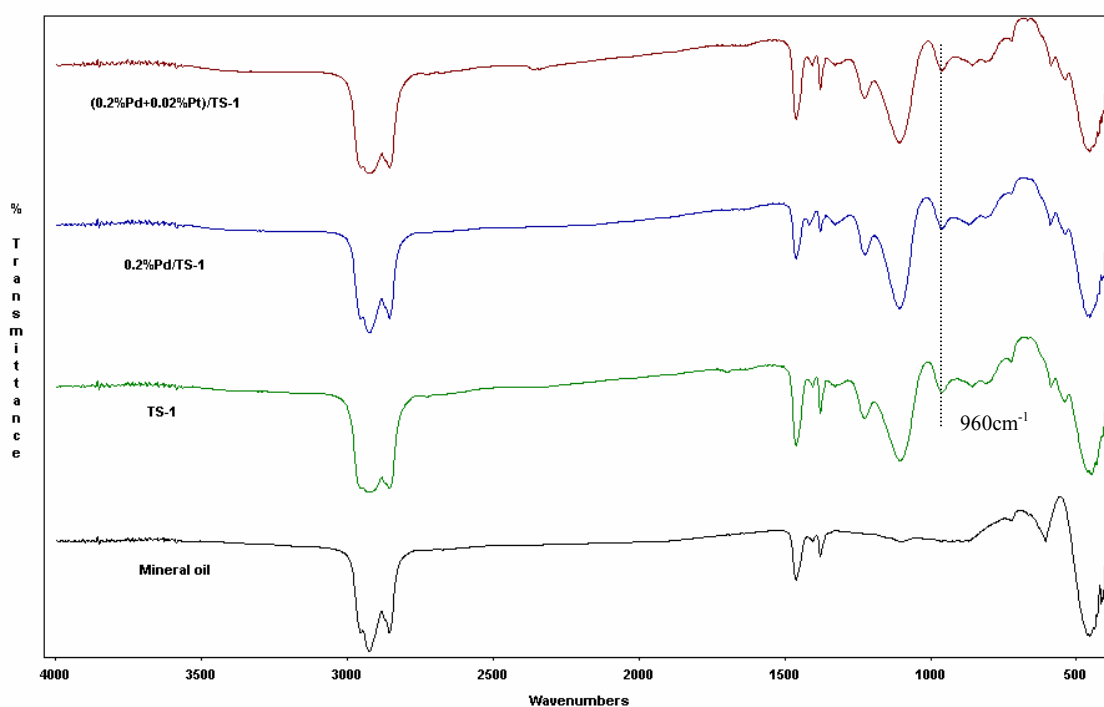


Figure 9 FT-IR spectra of TS-1, 0.2%Pd/TS-1 and (0.2%Pd+0.02%Pt)/TS-1

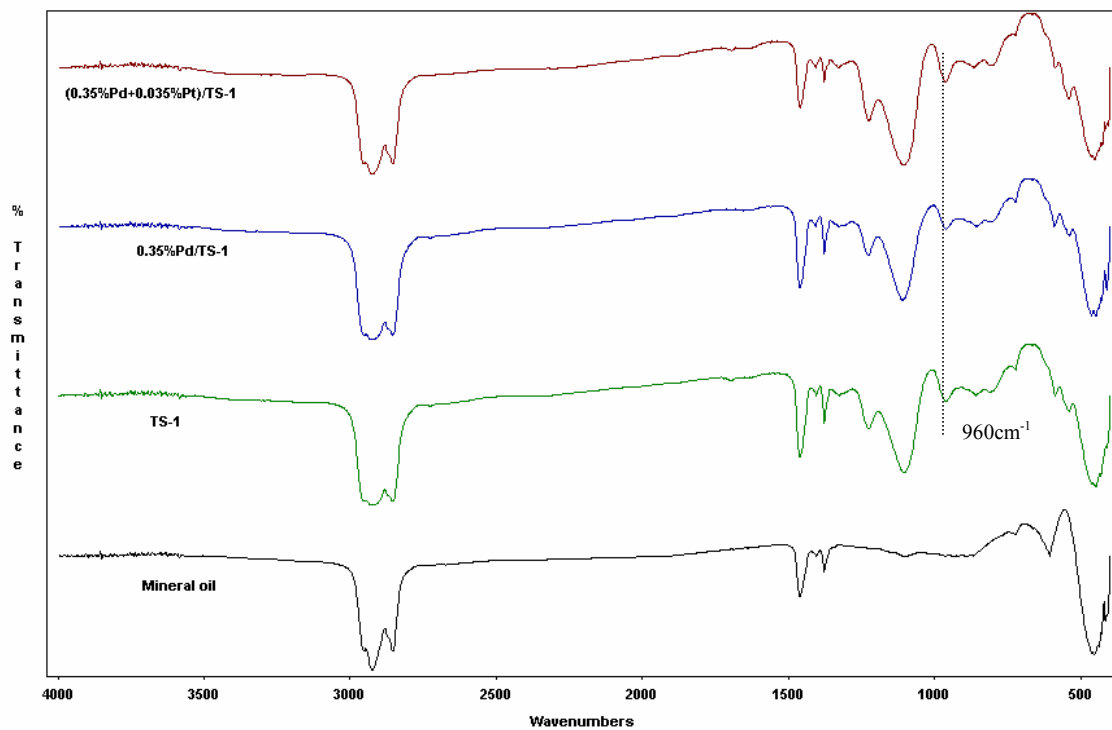


Figure 10 FT-IR spectra of TS-1, 0.35%Pd/TS-1 and (0.35%Pd+0.035%Pt)/TS-1

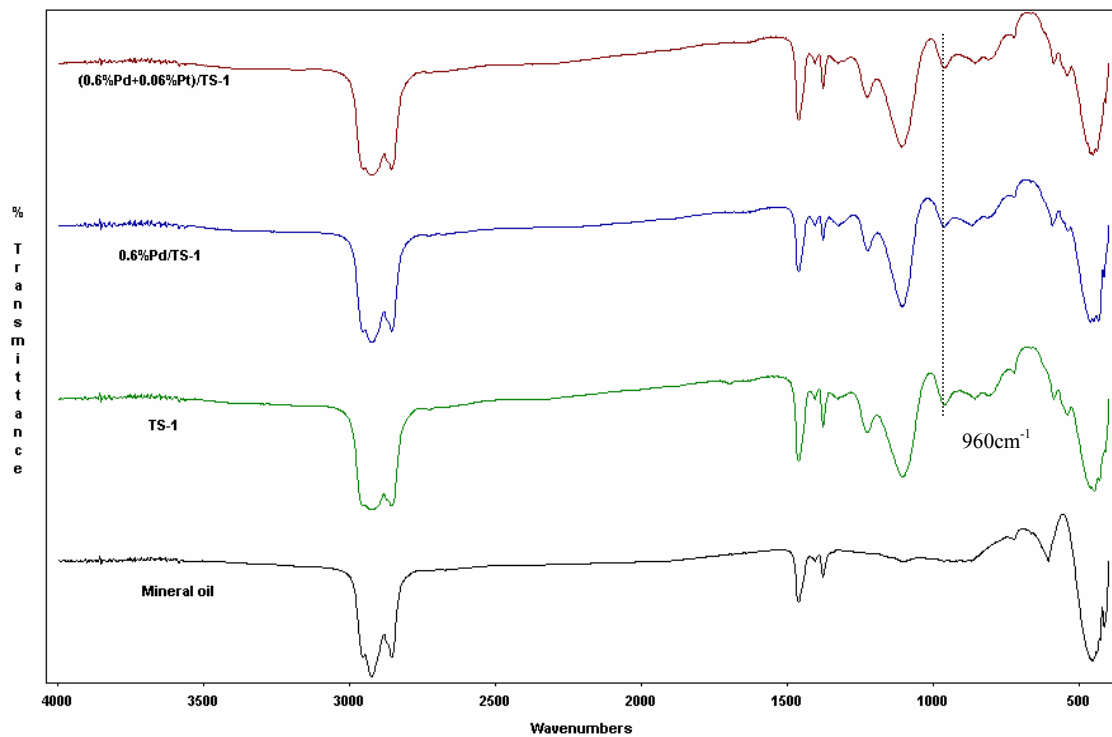


Figure 11 FT-IR spectra of TS-1, 0.6%Pd/TS-1 and (0.6%Pd+0.06%Pt)/TS-1

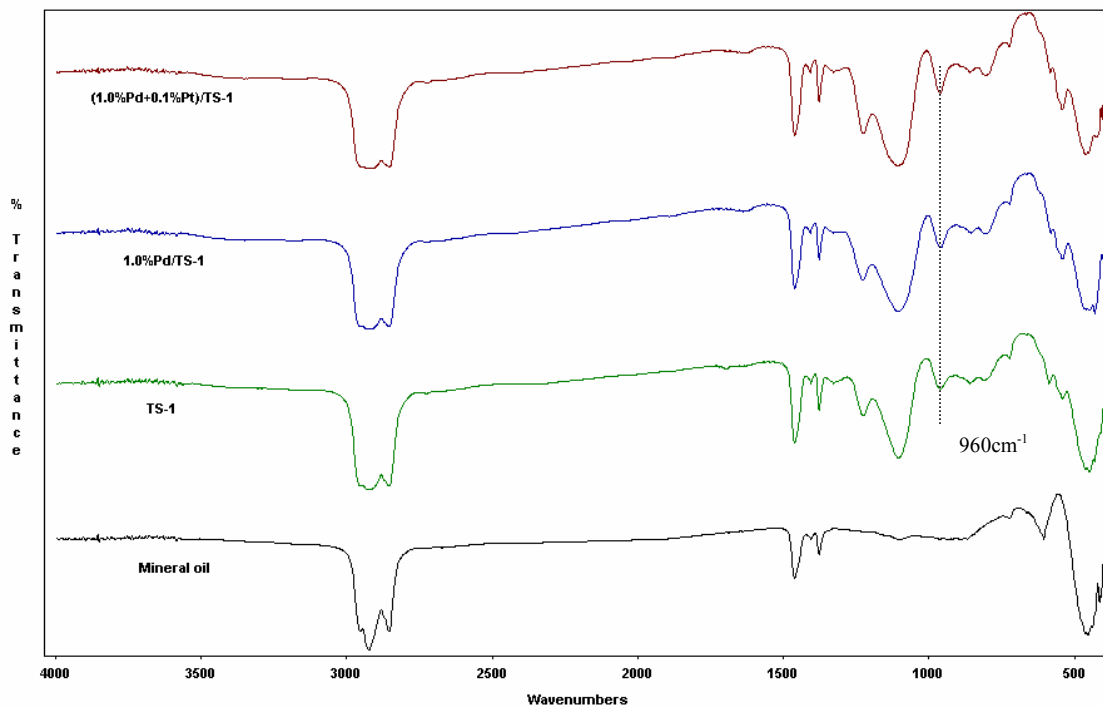


Figure 12 FT-IR spectra of TS-1, 1.0%Pd/TS-1 and (1.0%Pd+0.1%Pt)/TS-1

5.2.2 Powder X-ray diffraction (XRD) spectra

The three-dimensional structure of non-amorphous materials, like TS-1, is defined by regular, repeating planes of atoms that form a crystal lattice. When a focused X-ray beam interacts with these planes of atoms, parts of the beam is diffracted. This diffraction of an X-ray beam by a crystalline solid depends on what atoms make up the crystal lattice and how these atoms are arranged. Powder **X-Ray Diffraction (XRD)** is one of the most widely used techniques to characterize the structural properties of crystalline solids.

The X-ray diffraction patterns of TS-1 and precious metal loaded TS-1 were recorded on a Philips X'Pert PW3710 X-ray diffractometer using a Cu-K α radiation source ($\lambda=1.54056\text{\AA}$).

Bragg angles (2θ) between 5° and 50° were scanned with a step size of 0.02° . **Figure 13** shows the XRD spectra of TS-1, 0.2%Pd/TS-1, (0.2%Pd+0.02%Pt)/TS-1, 0.35%Pd/TS-1 and (0.35%Pd+0.035%Pt)/TS-1 and **Figure 14** shows the XRD spectra of 0.6%Pd/TS-1, (0.6%Pd+0.06%Pt)/TS-1, 1.0%Pd/TS-1 and (1.0%Pd+0.1%Pt)/TS-1. All the spectra obtained in this study showed the “fingerprint” peaks of a TS-1 molecular sieve given by Taramasso et al.^[13] The same patterns of TS-1 and precious metal loaded TS-1 indicated that the MFI crystal structure of TS-1 had no change before and after the impregnation.

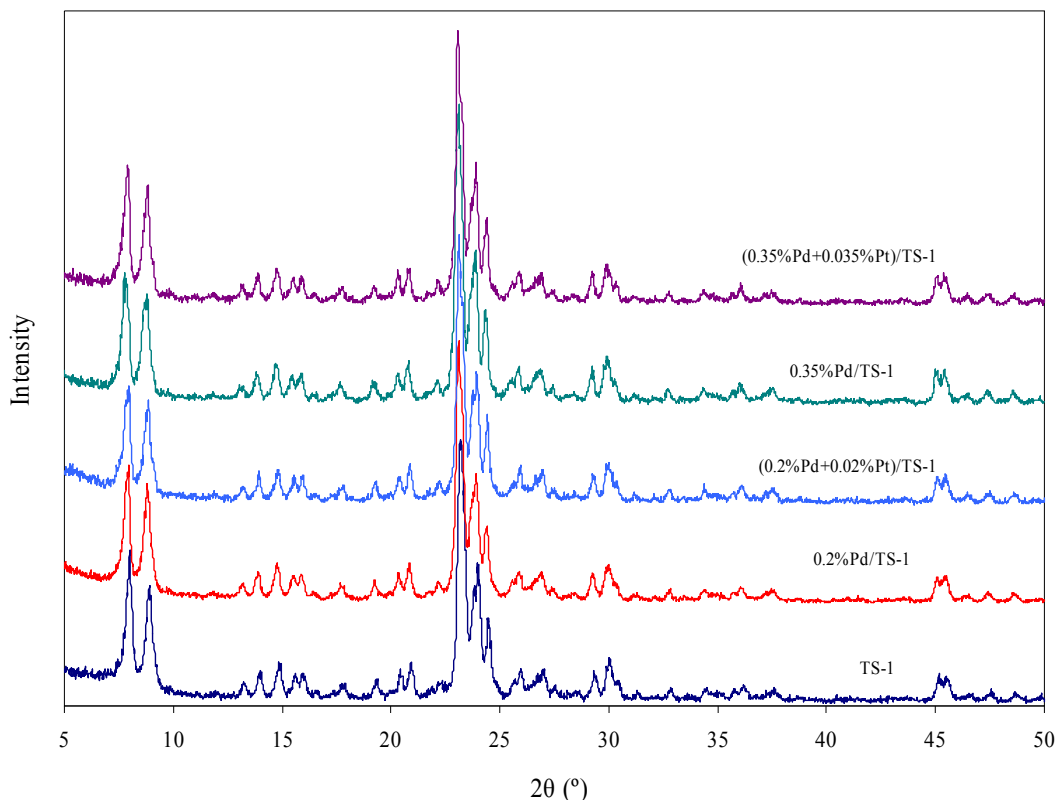


Figure 13 Powder XRD spectra of TS-1, 0.2%Pd/TS-1, (0.2%Pd+0.02%Pt)/TS-1, 0.35%Pd/TS-1 and (0.35%Pd+0.035%Pt)/TS-1

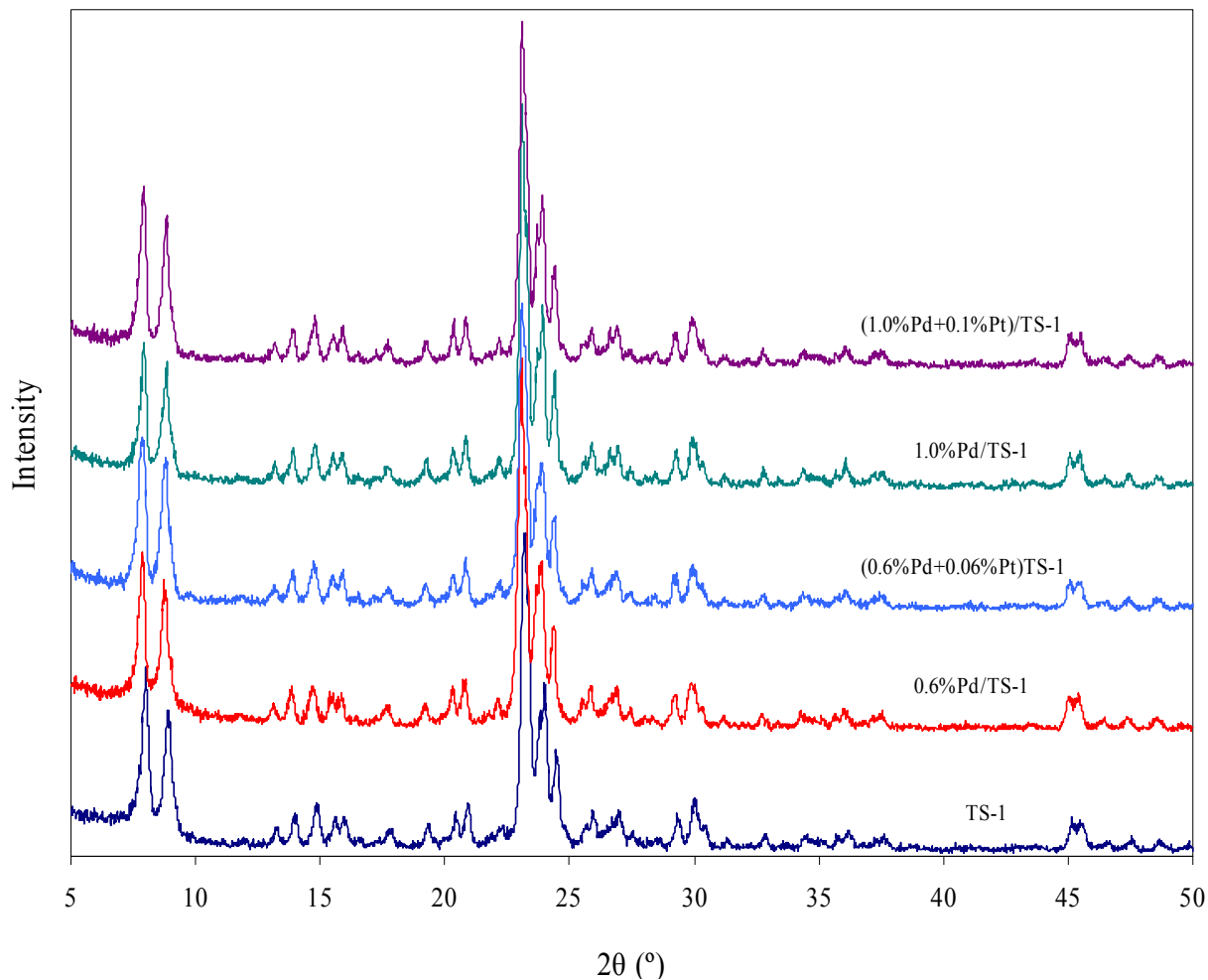


Figure 14 Powder XRD spectra of TS-1, 0.6%Pd/TS-1, (0.6%Pd+0.06%Pt)/TS-1, 1.0%Pd/TS-1 and (1.0%Pd+0.1%Pt)/TS-1

The obtained XRD spectra can also be used to compare the change of crystallinity of TS-1 before and after impregnation according to equation (5- 7).^[122] The crystallinities of the samples were calculated based on the intensity of the five strong reflections ($2\theta=7.99^\circ$, 8.91° , 23.21° , 24.01° , 24.47°)^[13, 123] and two other fingerprint peaks ($2\theta=29.33^\circ$, 30.07°).^[13] The crystallinity of TS-1 was assumed to be 100. The calculated relative crystallinities of precious metal loaded TS-1 used in this study are listed in **Table 30**. As can be seen that the changes of

crystallinities of TS-1 before and after impregnation of precious metal Pd (and Pt) were within 5%, implying that the effect of impregnation process adopted in this study on the crystallinity of TS-1 was minor. By contrast, the impregnation method used by Wang et al^[124] could result in the occurrence of crystal defects during the impregnation of precious metal Pd (and Pt) since considerable decrease in peak intensities was observed before and after the impregnation.

$$\text{Cryst., \%} = \frac{\text{Sum of peak heights of precious metal loaded TS -1}}{\text{Sum of peak heights of TS -1}} \times 100 \quad \text{5-7}$$

Table 30 Relative crystallinities of TS-1 before and after impregnation of precious metal

Entry	Catalyst	Crystallinity, %
1	TS-1	100
2	0.2%Pd/TS-1	97
3	(0.2%Pd+0.02%Pt)/TS-1	95
4	0.35%Pd/TS-1	105
5	(0.35%Pd+0.035%Pt)/TS-1	102
6	0.6%Pd/TS-1	105
7	(0.6%Pd+0.06%Pt)/TS-1	95
8	1.0%Pd/TS-1	104
9	(1.0%Pd+0.1%Pt)/TS-1	103

From the analysis of FT-IR and XRD, we conclude that the effect of impregnating precious metal Pd (and Pt) on the structure and crystalline of TS-1 was negligible. This ensured the catalytic characteristics of TS-1 after the impregnation of precious metal.

5.3 SELECTION OF AN “INDICATOR” COMPOUND

In this study, an “indicator” compound was used to measure the amount of *in situ* generated H₂O₂ in compressed CO₂ without the need to titrate samples. This “indicator” had to meet the following criteria: (1) It should be easily oxidized by H₂O₂ under mild reaction conditions with TS-1 as the catalyst. One problem associated with using H₂O₂ as a selective oxidant in carrying out green oxidation is the presence of water in H₂O₂ solution, since water usually can cause the deactivation of many catalysts, especially those used in organic oxidations. The discovery of TS-1 removed this obstacle because the hydrophobic nature of TS-1’s micropores favors the diffusion of organic substrates to the active site and protects the active site from deactivation by water.^[9] This makes TS-1 one of the most studied catalysts in carrying out green oxidation reactions with H₂O₂. Therefore, proving that precious metal loaded TS-1 is an effective catalyst in direct synthesis of H₂O₂ has special meaning in future applications. (2) The indicator should not be oxidized by oxygen alone or hydrogenated; this is obvious since the mixture of O₂ and H₂ is used for direct synthesis of H₂O₂. (3) The selectivity to its oxide should be high at reasonable H₂O₂ concentration, because the formation of more than one product will make the measurement complicated. (4) The “indicator” should be converted to its oxide proportional to the amount of H₂O₂ added. (5) The “indicator” and its oxide should be both soluble in CO₂. This proposed “indicator” compound can be selected from a list of various alcohols, tertiary amines and

sulfides.^[9] Ultimately, pyridine was selected as the “indicator” according to above mentioned criteria.

The chemical reactions involved in the direct synthesis of H₂O₂ from O₂ and H₂ and its determination by using pyridine as the “indicator” are given in **Figure 15**. The standard Gibbs free energy changes (ΔG^0) for these reactions are listed in **Table 31**. The thermodynamic data for H₂, O₂, H₂O₂, water and pyridine were all from Dean.^[125] Since the Gibbs free energy of formation for pyridine *N*-oxide could not be found in literature, equations (5- 13) to (5- 15) were used to calculate the Gibbs free energy change for chemical reaction (5- 8). The enthalpy of formation and the entropy of pyridine *N*-oxide under standard state were from Shaofeng and Pilcher^[126] and Varsanyi et al,^[127] respectively. We conclude that, thermodynamically, all these reactions are completely shifted to the right and the reverse reactions under normal reaction conditions are negligible. In order to effectively generate H₂O₂, the reactions for the formation of water, the hydrogenation and decomposition of synthesized H₂O₂ should be suppressed by using a selective catalyst and experimental conditions. Experimentally, Prasad et al.^[128] proved that the oxidation of pyridine by aqueous H₂O₂ was fast over TS-1. Therefore, it is reliable to choose pyridine as the “indicator” to determinate the amount of *in situ* generated H₂O₂ in compressed CO₂ in this study.

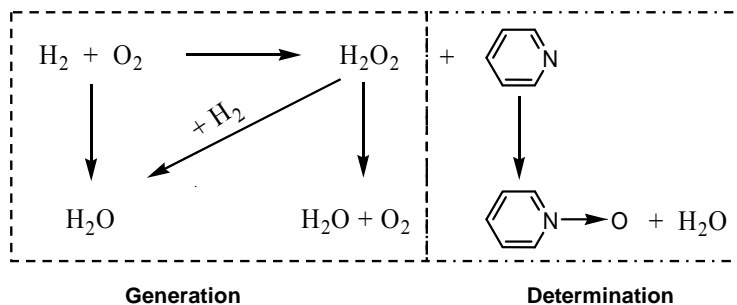


Figure 15 Reactions involved in the direct synthesis of H_2O_2 and its determination

Table 31 The standard Gibbs free energy changes for the reactions in direct synthesis of H_2O_2

Chemical reaction	ΔG^0 , kJ/mol	
$\text{C}_5\text{H}_5\text{N (l)} + \text{H}_2\text{O}_2 \text{ (l)} \longrightarrow \text{C}_5\text{H}_5\text{NO (s)} + \text{H}_2\text{O (l)}$	-213.6	5- 8
$\text{H}_2 \text{ (g)} + \text{O}_2 \text{ (g)} \longrightarrow \text{H}_2\text{O}_2 \text{ (l)}$	-120.4	5- 9
$\text{H}_2 \text{ (g)} + 0.5 \text{ O}_2 \text{ (g)} \longrightarrow \text{H}_2\text{O (l)}$	-237.4	5- 10
$\text{H}_2\text{O}_2 \text{ (l)} + \text{H}_2 \text{ (g)} \longrightarrow 2 \text{ H}_2\text{O (l)}$	-353.8	5- 11
$\text{H}_2\text{O}_2 \text{ (l)} \longrightarrow \text{H}_2\text{O (l)} + 0.5 \text{ O}_2 \text{ (g)}$	-116.7	5- 12

$$\Delta G^0 = \Delta H^0 - T \Delta S^0 \quad \mathbf{5- 13}$$

$$\Delta H^0 = \left(\sum_{i=1}^m \Delta H_f^0 \right)_{\text{products}} - \left(\sum_{j=1}^n \Delta H_f^0 \right)_{\text{reactants}} \quad \mathbf{5- 14}$$

$$\Delta S^0 = \left(\sum_{i=1}^m S^0 \right)_{\text{products}} - \left(\sum_{j=1}^n S^0 \right)_{\text{reactants}} \quad \mathbf{5- 15}$$

Table 32 Thermodynamic data of chemicals used in reaction (5- 8)

Compound	Pyridine (l)	H ₂ O ₂ (l)	Pyridine <i>N</i> -oxide (s)	H ₂ O (l)
ΔH_f^0 , kJ/mol	100.2	-187.78	8.6 ^[126]	-285.3
S^0 , J/(mol K)	177.9	109.6	299.78 ^[127]	69.95

In this study, the direct synthesis of H₂O₂ was carried out for 5 hours at 60°C in compressed CO₂ with pyridine as the “indicator”. Gas chromatographic (GC) analysis during control experiments using aqueous H₂O₂ under these conditions showed only two peaks: one for pyridine *N*-oxide, and another for un-reacted pyridine (indicator). Further control experiments also showed that pyridine was not oxidized by O₂ alone over TS-1 or Pd/TS-1, or by the mixture of O₂ and H₂ with or without TS-1 as the catalyst.

5.4 RESULTS AND DISCUSSION FOR THE DIRECT OF SYNTHESIS OF H₂O₂ IN CO₂

The direct synthesis of H₂O₂ was conducted using a mixture of O₂ and H₂ as the starting reactants over precious metal loaded TS-1 with pyridine as the “indicator” in compressed CO₂. The amounts of *in situ* generated H₂O₂ from O₂ and H₂ could be calculated according to the obtained pyridine *N*-oxide yields by applying the stoichiometric relationship between the *in situ* generated H₂O₂ and pyridine *N*-oxide shown in **Figure 15**. Here, precious metal loaded TS-1 is a bifunctional catalyst: the precious metal functioned as the catalyst for direct synthesis of H₂O₂

from O₂ and H₂, while TS-1 functioned as the catalyst for the oxidation of pyridine by *in situ* generated H₂O₂.

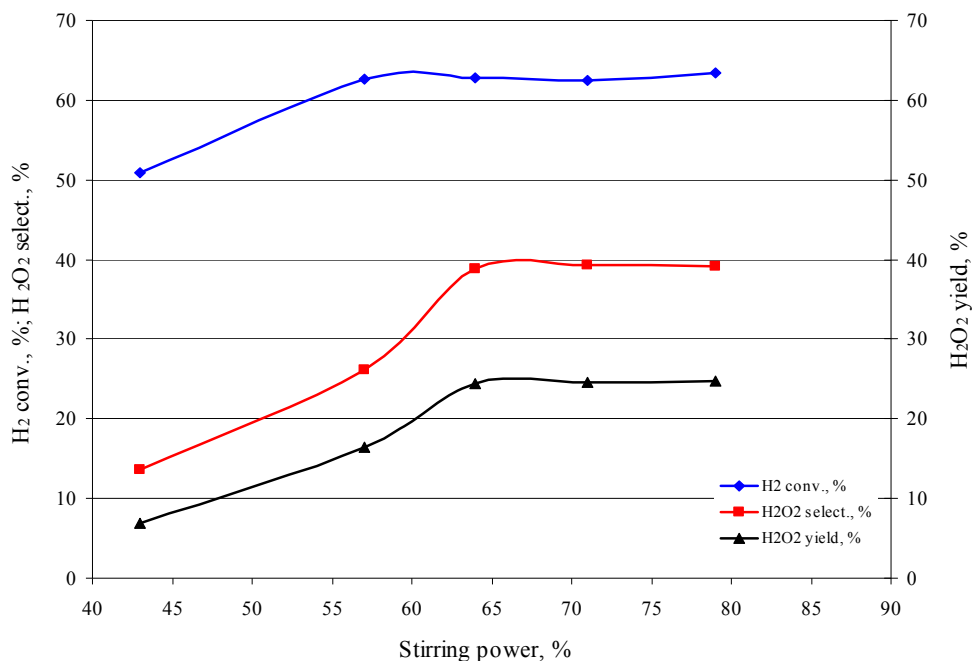


Figure 16 Effect of stirring speed on the direct synthesis of H₂O₂ in CO₂

Experimental conditions: H₂=6.2mmol, O₂/H₂=1, indicator=6.2mmol, water=27.8mmol,
0.35%Pd/TS-1=0.05g; P=125bar, T=60°C, reaction time=5 hours

For a heterogeneous catalytic reaction system under batch operation, external mass transfer resistance exists. Increasing stirring speed could reduce this resistance. In this study, the effect of stirring speed on the direct synthesis of H₂O₂ from O₂ and H₂ in CO₂ was examined and the results are presented in **Figure 16**. It is clear that stirring speed (expressed by the percentage of stirring power for stirrer/hotplate) had considerable influence on the H₂ conversion, H₂O₂ selectivity and yield: They were all increased along with the increase of stirring power until it reached 65% implying that the external mass transfer resistance for O₂ and H₂ decreased with an

increase in stirring speed. Further increase in stirring power had almost no effect on H₂ conversion, H₂O₂ selectivity and yield meaning that the external mass transfer resistance for the direct synthesis was completely eliminated when the stirring power reached 65%. Therefore, the stirring power for stirrer/hotplate in this study was kept at 70% (above the critical value) in the rest of this study.

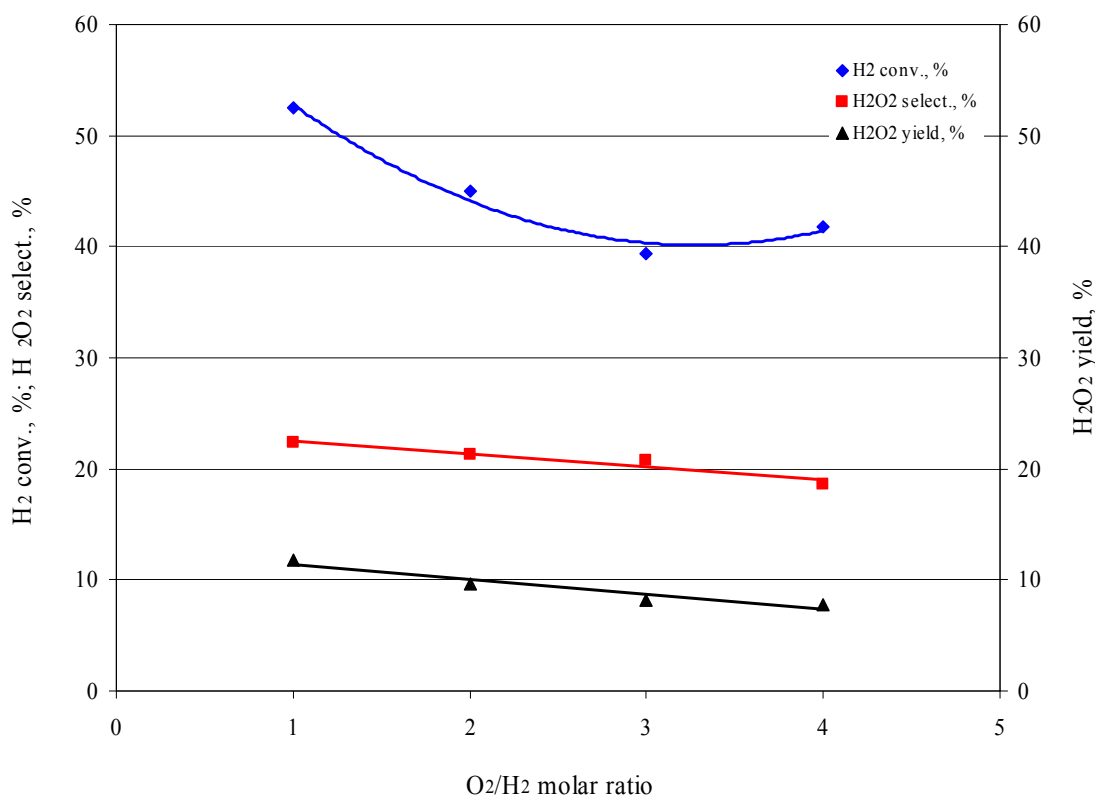


Figure 17 Effect of O₂/H₂ molar ratio on the direct synthesis of H₂O₂ in CO₂

Experimental conditions: H₂=6.2mmol, indicator=6.2mmol, water=27.8mmol, 0.35%Pd/TS-

1=0.05g; P=125bar, T=60°C, reaction time=5 hours

The O₂/H₂ molar ratio should have a significant effect on the direct synthesis of H₂O₂, although literature results in conventional solvents showed differing conclusions. Chinta and

Lunsford^[50] concluded that the selectivity for H₂O₂ decreased with the increase of the O₂/H₂ molar ratio, and Hwang et al^[43] found that a feed ratio of O₂:H₂=1:1 led to the optimal H₂O₂ production. By contrast, Dalton and Skinner^[38] stated that in order to improve the direct synthesis of H₂O₂ from O₂ and H₂ in an acidic medium containing an oxygenated or nitrogenous organic compound, the O₂/H₂ molar ratio should be higher than 3.4. Here we also examined the effect of O₂/H₂ molar ratio on the direct synthesis of H₂O₂ in CO₂ and the results are given in **Figure 17**. It reveals that H₂ conversion, H₂O₂ selectivity and H₂O₂ yield (see their definitions in **Section 5.1.2**) all decreased with an increase of O₂/H₂ molar ratio. The optimal H₂ conversion, H₂O₂ selectivity and H₂O₂ yield were obtained at an O₂/H₂ molar ratio of 1. Although the reason behind this phenomenon is not clear, the results in this study coincide with those of Chinta and Lunsford^[50] and Hwang et al.^[43] In the rest of this study, the O₂/H₂ molar ratio was kept at 1 in order to maximize the formation of H₂O₂ in CO₂.

The effect of H₂ concentration on direct synthesis of H₂O₂ has not been well explored in the literature. The results shown in **Figure 18** disclose the effect of H₂ concentration (defined as the amount of H₂ added to the reactor over the net volume of the reactor, mM) on H₂ conversion, H₂O₂ selectivity and H₂O₂ yield at constant O₂/H₂ ratio. It is concluded that with the increase of H₂ concentration in the reactor, H₂ conversion, H₂O₂ selectivity and H₂O₂ yield all increased until H₂ concentration reached 500 mM. When H₂ concentration was increased from 250 mM to 500 mM, H₂ conversion only increased about 20% (from 52.5% to 62.6%), while H₂O₂ selectivity almost doubled (from 22.4% to 39.3%). This in turn resulted in the increase of H₂O₂ yield from 11.8% to 24.6%. **Figure 18** also showed that when H₂ concentration was below 500mM, the relationship between H₂O₂ yield and H₂ concentration was linear implying that the reaction rate for the direct synthesis of H₂O₂ from O₂ and H₂ in CO₂ was first order with respect

to H₂ concentration. Further increase to H₂ concentration led to a decrease in H₂O₂ selectivity at similar H₂ conversions. The possible reason is that, at higher H₂ concentration, the existence of significant amounts of H₂ favored the hydrogenation of H₂O₂ in the presence of the Pd/TS-1 catalyst. Therefore, part of the *in situ* generated H₂O₂ was hydrogenated before it can react with the “indicator”.

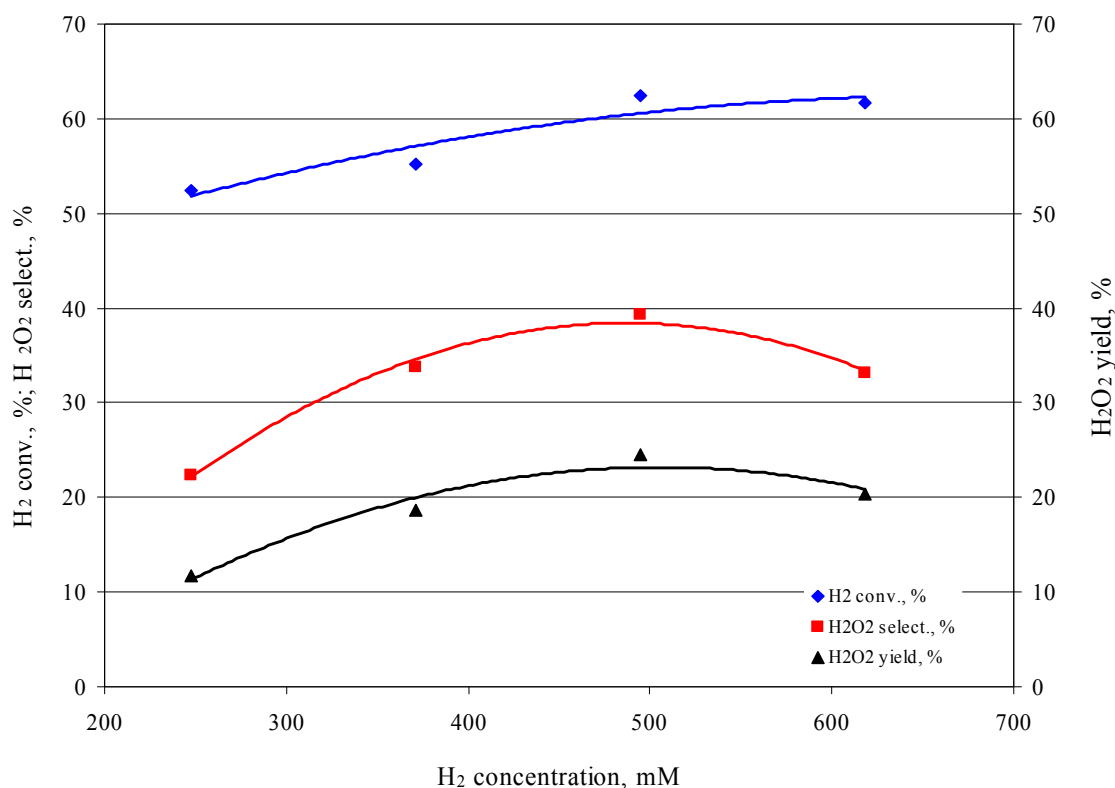


Figure 18 Effect of H₂ concentration on the direct synthesis of H₂O₂ in CO₂

Experimental conditions: O₂/H₂=1, indicator=6.2mmol, water=27.8mmol, 0.35%Pd/TS-1=0.05g;

P=125bar, T=60°C, reaction time=5 hours

The influence of catalyst mass on the formation of H₂O₂ is given in **Figure 19**. H₂ conversion increased with the increase of catalyst mass, especially at the lower catalyst mass ranges, while H₂O₂ selectivity initially increased with the increase of catalyst mass and then

steadily decreased. The combination of these effects resulted in an initial increase and then a plateau in H₂O₂ yield. This could be attributed to the occurrence of the hydrogenation of *in situ* generated H₂O₂ at higher catalyst concentration, which, in turn, led to the increase in H₂ conversion, the decrease in H₂O₂ selectivity and almost no change in H₂O₂ yield. When conducting direct synthesis of H₂O₂ using a palladium catalyst in an aqueous medium, Izumi et al^[129] also observed a similar phenomenon: the formation of H₂O₂ increased initially with the increase of catalyst concentration and then reached a plateau along with the further increase in the catalyst concentration.

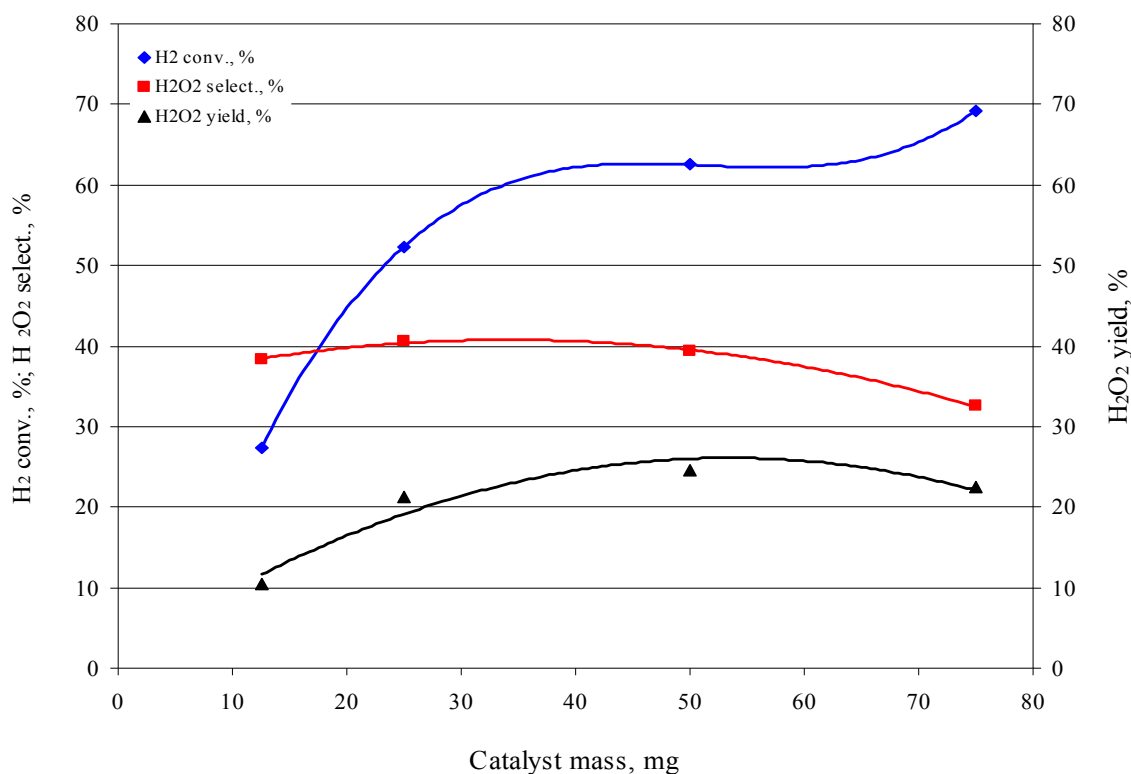


Figure 19 Effect of catalyst mass on the direct synthesis of H₂O₂ in CO₂

Experimental conditions: H₂=12.4mmol, O₂/H₂=1, indicator=6.2mmol, water= 27.8mmol,

0.35%Pd/TS-1; P=125bar, T=60°C, reaction time=5 hours

A survey of the literature showed that high palladium ($\geq 1\%$ Pd) contents were preferred by many researchers^[18, 41, 48, 54, 57] in carrying out direct synthesis of H_2O_2 from O_2 and H_2 . Few investigators^[43] examined the direct synthesis by using lower Pd content catalysts ($\leq 1\%$ Pd). From an economic viewpoint, for a similar H_2O_2 yield, the lower the Pd content in the catalyst, the more competitive the catalyst will be. In this study, a series of catalysts with Pd contents ranging from 0.2%~1.0% were used to conduct direct synthesis of H_2O_2 in CO_2 and the results are given in **Figure 20**. With the increase of Pd content in the catalyst, H_2 conversion increased while H_2O_2 selectivity decreased steadily. The combination of these changes led to almost no change in H_2O_2 yield until the Pd content reached 0.6%. Further increasing Pd content in the catalyst resulted in a decrease in H_2O_2 yield. In order to explore the reason behind this phenomenon, H_2O_2 decomposition experiments were conducted using catalysts with different Pd contents; the results are shown in **Figure 21**. We should point out that higher pyridine *N*-oxide yields in **Figure 21** mean that less H_2O_2 was decomposed by the catalyst. By comparing with TS-1 alone, we found that Pd on TS-1 can cause significant decomposition of H_2O_2 . The amounts of H_2O_2 decomposed by Pd/TS-1 increased with the increase in Pd contents in the catalysts. 1.0%Pd/TS-1 could decompose about 50% of H_2O_2 under the given experimental conditions. Therefore, the decrease in H_2O_2 yield when using the higher Pd loaded catalyst was likely because the higher Pd loaded catalyst could cause the partial decomposition of *in situ* generated H_2O_2 before it could react with the “indicator”. Finally, the lower selectivities observed upon raising Pd content could be due to hydrogenation of H_2O_2 as well.

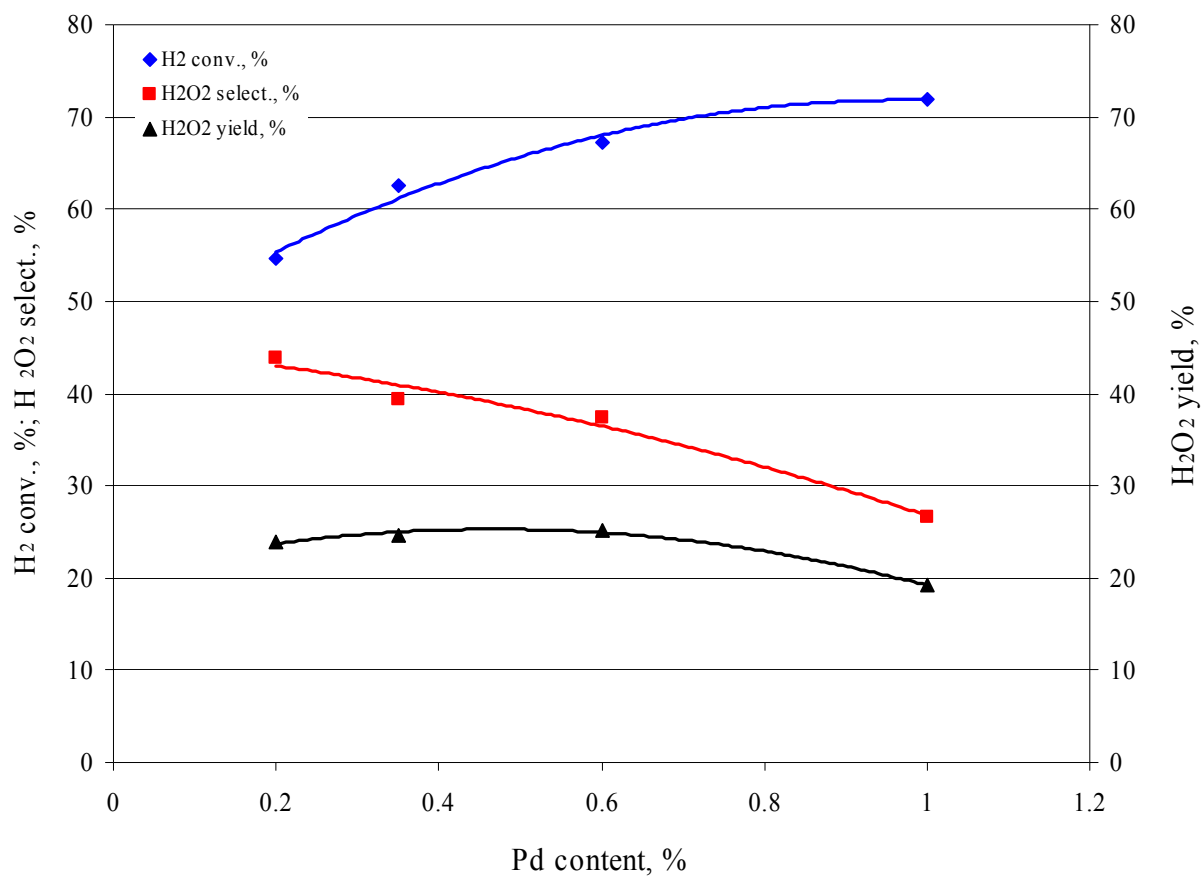


Figure 20 Effect of Pd content on the direct synthesis of H₂O₂ in CO₂

Experimental conditions: H₂=12.4mmol, O₂/H₂=1, indicator=6.2mmol, water=27.8mmol, Pd/TS-1= 0.05g; P=125bar, T=60°C, reaction time=5 hours

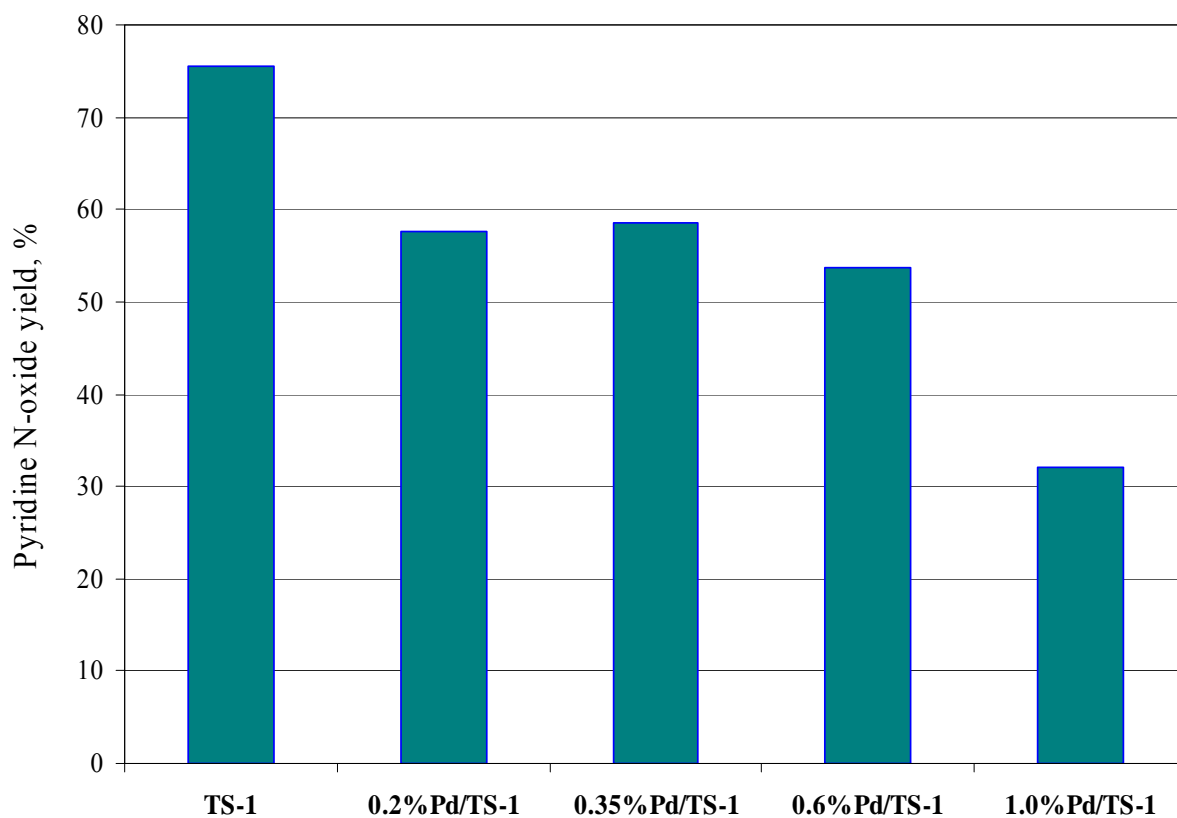


Figure 21 Experimental results for the decomposition of H_2O_2 by different catalysts

Experimental conditions: H_2O_2 /indicator=1, indicator =12.4 mmol, catalyst=0.1g; P=1bar,

T=60°C, reaction time=5 hours.

Platinum (Pt) has the ability to promote the direct synthesis of H_2O_2 from O_2 and H_2 over Pd catalysts, the optimal amount of Pt is typically about one tenth that of Pd.^[39, 41, 130] In this study, the influence of adding Pt (Pt/Pd=0.1 by weight) to Pd/TS-1 catalysts was investigated, the results given in **Figure 22** supported the previous literature conclusions. It can be seen from **Figure 22** that the addition of Pt to the Pd/TS-1 catalyst had significant influence on direct synthesis of H_2O_2 in compressed CO_2 , especially when Pd content was less than 0.6%. This influence was mainly on H_2O_2 selectivity, while for H_2 conversion, it was minor. The

combination of these effects led to an increase in H₂O₂ yield. For example, adding 0.02%Pt to 0.2%Pd/TS-1 could increase H₂O₂ selectivity from 43.8% to 56.1% with almost no change in H₂ conversion, which, in turn, resulted in the increase in H₂O₂ yield from 23.9% to 31.7%. As pointed out by Meiers et al,^[74] during the preparation of Pd/TS-1, the interaction of the Pd precursor, [Pd(NH₃)₄]²⁺, with TS-1 (support) created a new Pd species, Pd(II), with a binding energy in the range of 337.2~337.8eV. This new Pd species was neither Pd⁰ (binding energy in the range of 335.3~335.5eV) nor PdO (binding energy: 336.1~336.2eV), and it played an important role in epoxidation of propylene by the mixture of O₂ and H₂ (via the *in situ* generation of H₂O₂). Adding small amounts of Pt to Pd/TS-1 could dramatically increase the fraction of Pd(II) sites, thus, leading to an increase in H₂O₂ yield. However, one should be aware that the addition of Pt to Pd/TS-1 affects not only the Pd oxidation state but also particle features. A further increase in Pt content could only slightly increase the fraction of Pd(II), but significantly changed the surface morphology of the Pd aggregates from primarily needle-shaped to a mixture of needle-shaped crystallites and the undesirable spherical crystallites.^[74]

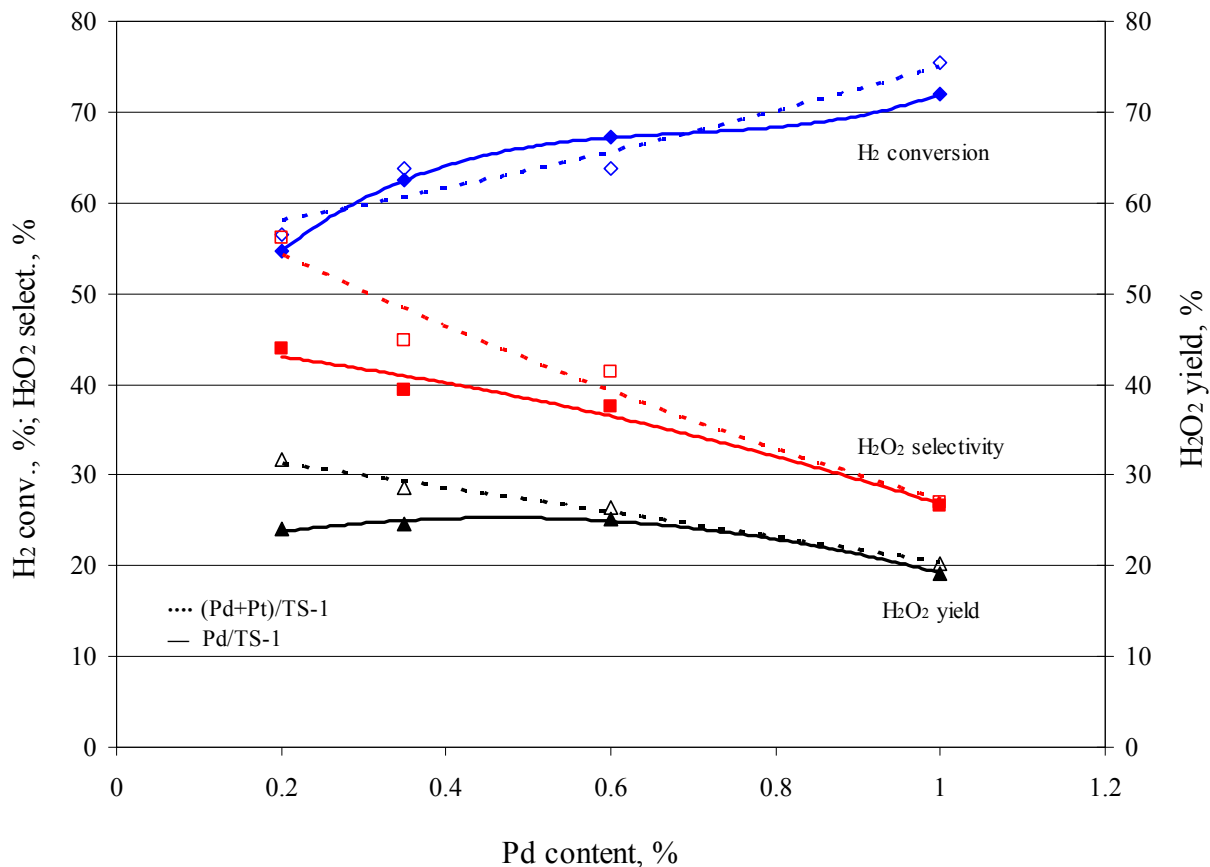


Figure 22 Effect of adding Pt to the Pd/TS-1 catalysts in direct synthesis of H₂O₂

Experimental conditions: H₂=12.4mmol, O₂/H₂=1, indicator=6.2mmol, water=27.8mmol, catalyst=0.05g; P=125bar, T=60°C, reaction time=5 hours

5.5 INTERACTION BETWEEN H₂O₂ AND TS-1

Upon contact between H₂O₂ (pre-manufactured or *in situ* generated) and TS-1, two reactions occur simultaneously. The first reaction, as disclosed by Antcliff et al,^[131] could be called “self-degradation” of H₂O₂ catalyzed by TS-1 to generate HOO[•], with subsequent deprotonation to

form superoxide (O_2^- or OO^*) radicals. Some of these radicals could eventually form O_2 , especially when TS-1 was loaded with a metal. The second reaction (and also the dominant one) was the formation of Ti-peroxo species—which were active in oxidation reactions. However, Bonino et al^[132] observed that a small fraction (about 10%) of peroxo species (characterized by a cream color) appeared to be poorly reactive toward organic substrates. This implies that, in any oxidation reaction involving H_2O_2 and TS-1, part of the consumed H_2O_2 will not play any role in catalytic oxidation reactions owing to the degradation over TS-1.

We conducted a series of experiments using different amounts of pre-manufactured 30% aqueous H_2O_2 solution in compressed CO_2 to oxidize the “indicator” under the reaction conditions given in Error! Reference source not found.. The relationship between H_2O_2 /pyridine molar ratios and the pyridine *N*-oxide yields is shown in **Figure 23**. It is clear from these results that in the case of using pre-manufactured H_2O_2 , only about 70% of the consumed H_2O_2 reacted with the “indicator” to generate pyridine *N*-oxide in compressed CO_2 . It should be pointed out that there might be a difference in pyridine *N*-oxide yield found using pre-manufactured H_2O_2 versus using *in situ* generated H_2O_2 . By adding small aliquots (10~20 μ L) of pre-manufactured H_2O_2 every 5 minutes into the reactor, we could possibly mimic the *in situ* generation of H_2O_2 from O_2 and H_2 . The result at ambient pressure and 60°C showed that the difference in pyridine *N*-oxide yield between adding pre-manufactured H_2O_2 at the beginning and adding it aliquot by aliquot was within 10%. Therefore, we might say that the H_2O_2 yields obtained in this study during direct synthesis in compressed CO_2 was the minimum amount of *in situ* generated H_2O_2 , while the H_2O_2 selectivity was the minimum selectivity toward the direct synthesis of H_2O_2 from O_2 and H_2 in compressed CO_2 over precious metal loaded TS-1. In comparison, we recalculated the H_2O_2 selectivity and yield by using the calibration curve given in **Figure 23**. The results are

listed in **Table 34**. Naturally, at the same H₂ conversion, H₂O₂ selectivity and yield calculated using the calibration curve were each higher than those obtained before—these results might represent an upper bound to these values.

Table 33 Experimental conditions in determining the calibration curve in CO₂

H ₂ O ₂ , mmol	0.29	0.49	0.97	1.55	3.11	6.21	8.73
H ₂ O ₂ /pyridine, (mol/mol)	0.047	0.079	0.16	0.25	0.50	1.01	1.41
Water ^a , ml	0.47	0.45	0.40	0.34	0.18	-	-

Note: Other conditions: Indicator=6.2mmol, TS-1=0.05g; P=125bar, T=60°C, time=5 hours.

^a: Water was used to compensate the total volume of liquid reactants if it was less than 1.0ml.

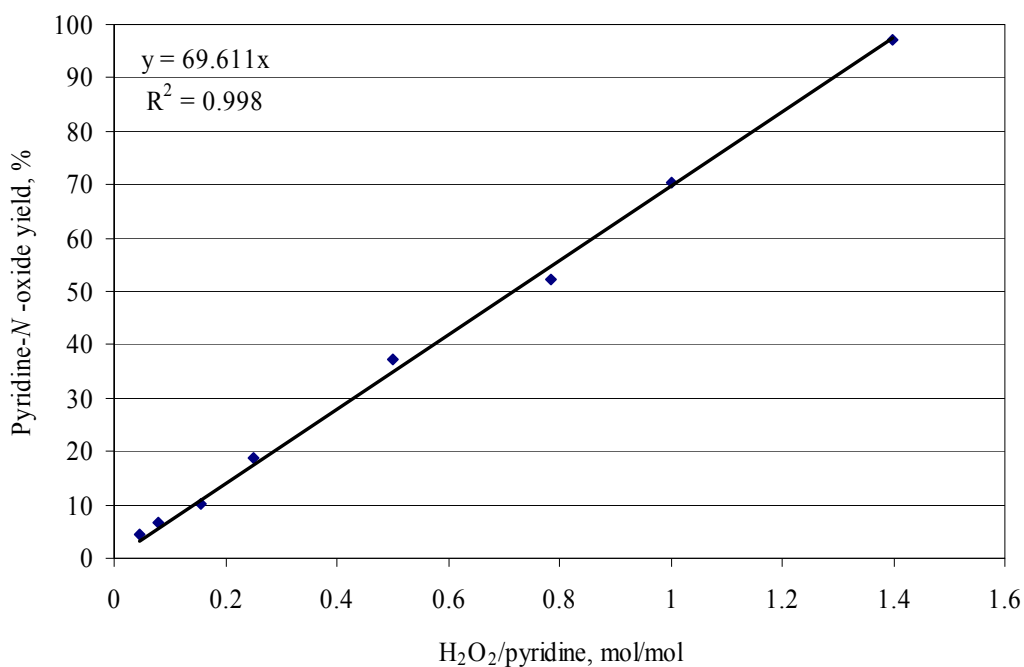


Figure 23 Calibration curve for the measurement of H₂O₂ in CO₂

Indicator=6.2mmol, TS-1=0.05g; P=125bar, T=60°C, reaction time=5 hours.

Table 34 Comparison of experimental results with and without the consideration of calibration curve

Catalyst	H ₂ conversion, %	H ₂ O ₂ selectivity, %		H ₂ O ₂ yield, %	
		A	B	A	B
0.2%Pd/TS-1	54.7	43.8	62.9	24.0	34.4
0.35%Pd/TS-1	62.5	39.3	56.4	24.6	35.3
0.6%Pd/TS-1	67.2	37.5	53.8	25.2	36.1
1.0%Pd/TS-1	72.0	26.6	38.2	19.2	27.5
(0.2%Pd+0.02%Pt)/TS-1	56.5	56.1	80.4	31.7	45.5
(0.35%Pd+0.035%Pt)/TS-1	63.7	44.8	64.3	28.5	41.0
(0.6%Pd+0.06%Pt)/TS-1	63.8	41.4	59.4	26.4	37.8
(1.0%Pd+0.1%Pt)/TS-1	75.4	26.9	38.7	20.3	29.1

Note: 1. Experimental conditions: H₂=12.4mmol, O₂/H₂=1, indicator=6.2mmol, water=27.8mmol, catalyst=0.05g; P=125bar, T=60°C, reaction time=5 hours;

2. A is the results without considering degradation of H₂O₂ on TS-1 and the calibration curve; B is the results with the consideration of calibration curve.

5.6 SUMMARY

Based on the criteria given in this study, pyridine was selected as an “indicator” compound to react immediately with directly synthesized H₂O₂ from O₂ and H₂ over precious metal loaded

TS-1. By quantifying the conversion of this indicator, the amount of *in situ* generated H₂O₂ in compressed CO₂ was obtained.

The experimental results in this study showed, for the first time, that H₂O₂ could be effectively synthesized from O₂ and H₂ in compressed CO₂. In order to keep reactant mix well, the stirring power in this study was kept at $\geq 70\%$. H₂ conversion, H₂O₂ selectivity and H₂O₂ yield all decreased with an increase in O₂/H₂ molar ratio. The optimal O₂/H₂ molar ratio was 1 in the range of this study. An increase in H₂ concentration led to an increase in H₂ conversion, H₂O₂ selectivity and yield. H₂O₂ yield was linearly proportional to H₂ concentration below 500 mM of H₂, implying that direct synthesis of H₂O₂ from O₂ and H₂ in compressed CO₂ was first order with respect to H₂ concentration. H₂ conversion increased, while H₂O₂ selectivity decreased, with the increase of catalyst mass, these in turn resulted in the almost no change in H₂O₂ yield in a broad range of catalyst mass. Experimental results also proved that H₂ conversion increased with an increase of Pd content in Pd/TS-1 catalyst, while H₂O₂ selectivity decreased. The combination of these effects led to the almost no change in H₂O₂ yield versus Pd content from 0.2%~0.6%. The addition of Pt to the Pd/TS-1 catalysts has a significant positive influence on H₂O₂ selectivity, while its effect on H₂ conversion is minor.

Since the support, TS-1, used in this study is an excellent catalyst for using H₂O₂ to conduct green oxidations, the direct synthesis of H₂O₂ from O₂ and H₂ in CO₂ with precious metal loaded TS-1 as the catalysts could be used as an *in situ* H₂O₂ source in carrying out selective oxidation. If the reaction of O₂ and H₂ in CO₂ was desired for generation of H₂O₂ as the final product, one should design the system such that the H₂O₂ is quickly removed from the vicinity of the Pd/Pt catalyst (to minimize degradation). It is likely in such case that a different support for the precious metals would be employed.

**6.0 ONE-POT GREEN SYNTHESIS OF PROPYLENE OXIDE USING *IN SITU*
GENERATED H₂O₂ IN CO₂**

The new green chemistry metric developed in this study was also used to evaluate the greenness of the following technologies for the synthesis of propylene oxide (PO): chlorohydrin, *t*-butyl hydroperoxide, ethylbenzene hydroperoxide, pre-manufactured H₂O₂ using methanol as the solvent and *in situ* generated H₂O₂ using compressed CO₂ as the solvent. The obtained greenness index GIR values for these technologies are shown in **Table 35**. The GIC values used in calculating GIR values are listed in **Table 36**. The GIR results indicated that among all these technologies, the process using *in situ* generated H₂O₂ as the oxidant and CO₂ as the solvent had the smallest GIR, thus it was the greenest technology by which PO can be synthesized among all these technologies.

Table 35 Greenness index GIR values of the chemical reactions in the synthesis of PO

Chemical reactions for the synthesis of PO	GIR	
$C_3H_6 + Cl_2 + Ca(OH)_2 \longrightarrow C_3H_6O + CaCl_2 + H_2O$	8.2	6- 1
$C_3H_6 + (CH_3)_3COOH \longrightarrow C_3H_6O + (CH_3)_3COH$	10.9	6- 2
$C_3H_6 + C_6H_5CH(OOH)CH_3 \longrightarrow C_3H_6O + C_6H_5CH(OH)CH_3$	10.4	6- 3
$C_3H_6 + H_2O_2 \xrightarrow{MeOH} C_3H_6O + H_2O$	7.5	6- 4
$C_3H_6 + H_2 + O_2 \xrightarrow{CO_2} C_3H_6O + H_2O$	6.3	6- 5

Table 36 GIC values of the substances used in the synthesis of PO by various processes

Substance	HR	FR	RR	ODP	GWP	<i>GIC</i>	MW
C ₃ H ₆	1	4	0	0	0	5	42
Cl ₂	4	0	0	0	0	16	70.9
H ₂ O	0	0	0	0	0	0	18
Ca(OH) ₂	2	0	0	0	0	4	74.1
C ₃ H ₆ O	3	4	2	0	0	15	58
CaCl ₂	2	0	1	0	0	5	111
(CH ₃) ₃ COOH	3	3	3	0	0	15	90.1
(CH ₃) ₃ COH	2	2	0	0	0	6	74.1
C ₆ H ₅ CH(OOH)CH ₃ *	3	2	3	0	0	14	138.2
C ₆ H ₅ CH(OH)CH ₃	2	2	0	0	0	6	122.2
3% H ₂ O ₂	1	0	1	0	0	1	34
MeOH	2	3	0	0	0	7	32
H ₂	0	4	3	0	0	7	2
O ₂	0	0	3	0	0	3	32
CO ₂	1	0	0	0	0.1	1.1	44

Note: *: Cumene hydroperoxide data were used since there were no available data for ethylbenzene hydroperoxide.

6.1 EXPERIMENTAL

6.1.1 Chemicals and catalysts

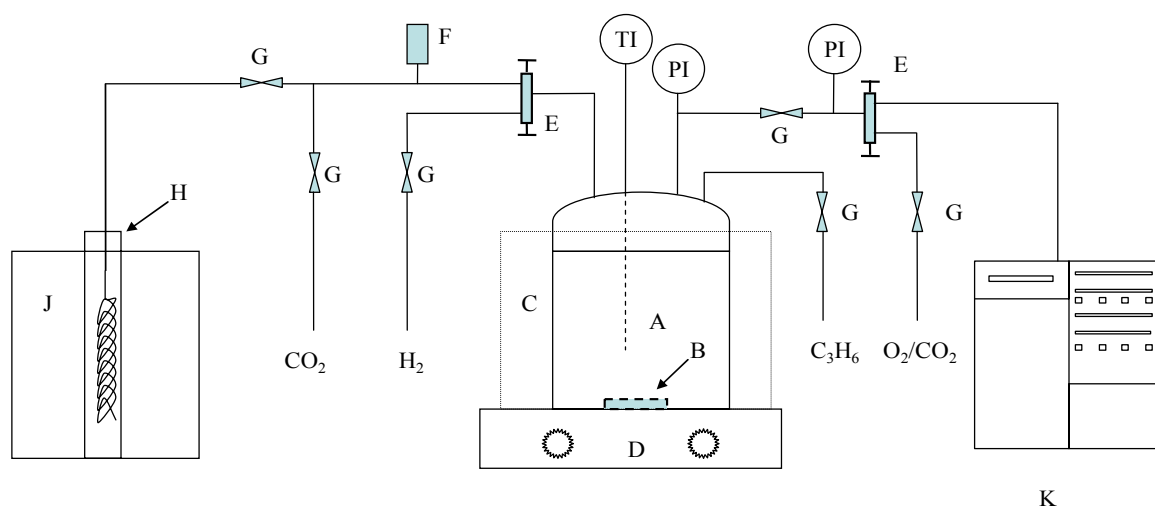
The purities of O₂, H₂, CO₂ (from Penn Oxygen, Jeannette, PA) and propylene (from Air Products Inc.) used in this study were all above 99.9%. Two special gas mixtures were used to obtain the calibration curve for GC analysis. The compositions of first gas mixture were 2.06% propylene, 2.09% propane and 2.16% propylene oxide with the balance CO₂ (Matheson Tri-Gas Inc., Montgomeryville, PA). The compositions of second were 0.101% acetone, 0.500% CO₂, 5.00% H₂, 3.99% O₂, 1.00% propane, 10.0% propylene and 0.315% propylene oxide with the balance N₂ (Scott Specialty Gases, Plumsteadville, PA).

Acetone ($\geq 99.5\%$, Aldrich), propylene oxide (99%, Aldrich), propylene glycol (1,2-propanediol, 99%, Acros Organics), 1-methoxy-2-propanol (98.5%, Acros Organics), propylene carbonate (99.5%, Acros Organics), ammonium carbonate (33.9% as NH₃, J. T. Baker), ammonium acetate (99%, J. T. Baker), ammonium trifluoroacetate (98%, Acros Organics), Amberlyst A-21 ion-exchange resin (Aldrich), sodium acetate (99+%, Aldrich) and sodium bicarbonate ($\geq 99.7\%$, EM Science) were all used as received without further purification.

The preparation of precious metal loaded catalyst (0.2%Pd+0.02%Pt)/TS-1 was the same as that given in **Section 5.1.1**.

6.1.2 General procedures for the direct synthesis of PO in CO₂

Similar to the direct synthesis of H₂O₂ from O₂ and H₂ in compressed CO₂, one-pot green synthesis of PO using *in situ* generated H₂O₂ from O₂ and H₂ in compressed CO₂ was also conducted in a 30ml stainless steel reactor manufactured by the University of Pittsburgh. A cylindrical glass liner was also used to prevent the decomposition of *in situ* generated H₂O₂ by the metal wall. The same passivation method was also used to passivate the reactor and glass liner to prevent the decomposition of generated H₂O₂. The experimental setup is shown in **Figure 24**. In a typical experiment, known amounts of inhibitor, methanol, water and catalyst were added to the reactor. A magnetic stirring bar was placed inside the reactor in order to keep the reactants mixing well. The reactor was first charged with known amounts of propylene, O₂, followed by CO₂, and then known amount of H₂. The reaction pressure was finally adjusted to desired pressure by adding more CO₂. The reaction temperature was controlled by a stirrer/hotplate. After the experiment, the amounts of un-reacted propylene, generated PO and propane in the reactor were analyzed by using an online HP 5890A gas chromatograph (GC) equipped with a TCD detector and a HayeSep D packed column (20ft×1/8") and controlled by a HP ChemStation. The reactor was then ice-cooled to 0~5°C. The gas mixture inside the reactor was vented into an acetone solution. This acetone solution was used to extract by-products [propylene glycol (PG), methoxypropanols (MP) etc] from the catalyst and analyzed by another 5890A GC equipped with a FID detector and a DB-1 capillary column (30m×0.253mm×0.50μm) to determine the quantities of by-products. A proportional relief valve was installed for safety.



A. High pressure reactor, **B.** Stirring bar, **C.** Vessel, **D.** Stirrer/hotplate, **E.** Three-way valves, **F.** Proportional relief valve, **G.** Two-way valves, **H.** Venting vessel, **J.** Glass vessel, **K.** Online gas chromatograph

Figure 24 Experimental setup for the green synthesis of PO using *in situ* generated H_2O_2 in CO_2

Propylene conversion, PO selectivity and PO yield were defined by the following equations, respectively.

$$\text{C}_3\text{H}_6 \text{ conversion (\%)} = \frac{\text{the amount of C}_3\text{H}_6 \text{ consumed during reaction (mmol)}}{\text{the amount of C}_3\text{H}_6 \text{ added to the reactor (mmol)}} \times 100 \quad \mathbf{6-6}$$

$$\text{PO selectivity (\%)} = \frac{\text{the amount of generated PO (mmol)}}{\text{the amount of C}_3\text{H}_6 \text{ consumed during reaction (mmol)}} \times 100 \quad \mathbf{6-7}$$

$$\text{PO yield (\%)} = \frac{\text{the amount of generated PO (mmol)}}{\text{the amount of C}_3\text{H}_6 \text{ added to the reactor (mmol)}} \times 100$$

6- 8

6.2 RESULTS AND DISCUSSION FOR THE GREEN SYNTHESIS OF PROPYLENE OXIDE

Compressed CO₂ has been previously proven to be an effective solvent for the direct synthesis of H₂O₂ from O₂ and H₂. In this study, *in situ* generated H₂O₂ in CO₂ was used as a green oxidant to oxidize propylene for a one-pot green synthesis of PO. Besides the advantages mentioned earlier, using compressed CO₂ as the solvent has special benefit over conventional solvents in that propylene is soluble in compressed CO₂. Therefore, O₂, H₂, propylene and CO₂ will form a homogeneous single phase under reaction conditions. This will significantly reduce or even eliminate mass transfer resistance during the epoxidation of propylene.

Similar to results obtained while using methanol as the solvent, Danciu et al^[19] found that attempts to increase propylene conversion also resulted in a substantial decrease in PO selectivity when CO₂ was used as a sole solvent. For example, when propylene conversion was increased from 7.5% to 9.5%, the PO selectivity decreased considerably from 94.3% to 77.1%. CO₂ is an environmentally benign solvent, but it is also a feeble one as can be seen from its low dielectric constant.^[17] Addition of small amounts of polar co-solvent can significantly enhance its solvent properties. On the other hand, Clerici et al^[67] reported the significant role played by methanol (a polar solvent) in the epoxidation of propylene using aqueous H₂O₂ solution over TS-1. In this study, we examined the effect of adding small amounts of polar co-solvent (methanol, water or their combination) to compressed CO₂ on the direct synthesis of PO using *in situ* generated

H₂O₂. The bifunctional catalyst used in the green synthesis of PO was (0.2%Pd+0.02%Pt)/TS-1 since it was proven to be an effective catalyst in the direct synthesis of H₂O₂ from O₂ and H₂ in compressed CO₂ in this study. The experimental results are listed as Entries 1-3 in **Table 37**: When methanol, water and their mixture were used as the co-solvent, the propylene conversion was high. But the hydrogenation of propylene to propane was the dominant reaction. Although the addition of methanol could enhance the formation of PO (in agreement with the observation of Clerici et al^[67]), it also led to side-reactions between generated PO and methanol to form methoxypropanols (MP). Further, the presence of water caused the hydrolysis of PO to form propylene glycols (PG). It is known^[71] that acidic conditions favor the hydrolysis of PO and also the reaction between PO and methanol. Considering the existence of surface acidity in TS-1,^[133, 134] it is hypothesized that this surface acidity contributed to promoting these side-reactions. In order to verify this hypothesis, ammonium acetate (the measured pH value of ammonium acetate, water and methanol in this study was 7.6 at room temperature) was added to the reactor as an inhibitor and the experimental results are given as Entries 4-6 in **Table 37**. It is observed that addition of ammonium acetate could significantly inhibit not only the hydrolysis of PO and the reaction between PO and methanol, but also the hydrogenation of propylene, especially when small amounts of methanol and water were used as the co-solvent in compressed CO₂. Comparing Entries 3 and 6, it can be seen that the addition of ammonium acetate led to the increase of PO yield from 9.4% to 23.5% and a significant increase in PO selectivity (from 21.7% to 81.8%); while, the propane, MP and PG selectivities all decreased considerably. The PO production rate for Entry 6 reached as high as 0.346 g h⁻¹ (g cat)⁻¹ due to the effective generation of H₂O₂ from O₂ and H₂ in CO₂^[24] and the likely decrease (or elimination) of mass transfer resistances.

Table 37 Green synthesis of PO using *in situ* generated H₂O₂ in CO₂

Entry	1	2	3	4	5	6	
Water, ml	0.25	-	0.25	0.25	-	0.25	
MeOH, ml	-	0.25	0.25	-	0.25	0.25	
NH ₄ COOCH ₃ , g	-	-	-	0.02	0.02	0.02	
C ₃ H ₆ conv., %	22.8	54.9	43.1	16.0	27.3	28.7	
PO yield, %	1.7	10.4	9.4	10.0	20.3	23.5	
Selectivity, %	PO	7.6	18.9	21.7	62.7	74.6	81.8
	C ₃ H ₈	75.3	75.2	54.5	26.3	13.5	10.4
	MP	0	3.7	9.2	0	6.3	2.5
	PG	15.3	0.4	13.1	4.6	3.7	2.9
	Others	1.8	1.8	1.6	6.4	1.8	2.4

Note: Other experimental conditions: (0.2%Pd+0.02%Pt)/TS-1=0.05g, C₃H₆=6.3mmol, H₂/C₃H₆=1, O₂/H₂=1; T=60°C, P=125bar, reaction time=5 hours

Since the surface acidity of TS-1 was relatively weak, we believed that the selected inhibitor (ammonium acetate) could effectively interact with TS-1 and neutralize its surface acidity, and therefore, suppress the side-reactions. In order to explore if this suppression effect was due to the neutralization of surface acidity of TS-1, the following experiments were run using two different inhibitors: Ammonium trifluoroacetate (the measured pH value was 6.4 in the mixture of methanol and water) and ammonium carbonate (the measured pH value was 9.7 in the

mixture of methanol and water). Experimental results and their comparison with ammonium acetate (pH=7.6) are given in **Figure 25**. The addition of ammonium trifluoroacetate provided an acidic environment for the catalyst and could not neutralize the surface acidity of TS-1, and therefore, led to a substantial decrease in PO selectivity (although the conversion of propylene increased due to the enhancement of the hydrogenation of propylene and the hydrolysis of generated PO). On the other hand, the addition of ammonium carbonate provided a stronger basic environment for the catalyst. As being expected, a strong suppression effect was observed for all side-reactions. However, due to the relatively higher pH value (stronger basic condition could also cause the hydrolysis of PO^[71]), the PO selectivity was lower than that when ammonium acetate (pH=7.6) was used.

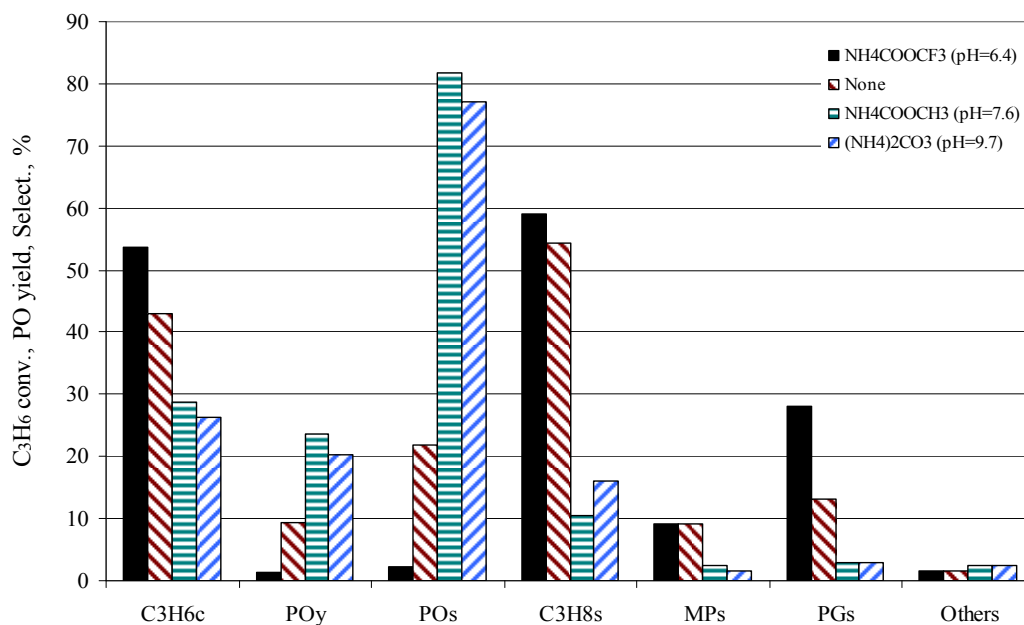


Figure 25 Effect of different inhibitors on green synthesis of PO in CO₂

Experimental conditions: (0.2%Pd+0.02%Pt)/TS-1=0.05g, water=0.25ml, methanol=0.25ml, inhibitor= 0.02g; C₃H₆=6.3mmol, H₂/C₃H₆=1, O₂/H₂=1; T=60°C, P=125bar, reaction time=5 hours (low case “c” stands for conversion, “y” for yield and “s” for selectivity)

In order to further verify that the suppression of side reactions was caused by the interaction between the inhibitor and TS-1, additional experiments were run using the following selected weak base inhibitors: Amberlyst A-21 (a weakly basic, macroreticular ion-exchange resin with alkyl amine functionality), sodium acetate and sodium bicarbonate. The experimental results are shown in **Table 38**. Although Amberlyst A-21 is a weak base, it is bonded to the macroreticular structure of ion exchange resin. In other words, it could not enter into the channels of TS-1 and interact with the surface acidity of TS-1. Therefore, no suppression effect was observed. Further increase the amounts of Amberlyst A-21 had no influence on the suppression of side reactions.

Surprisingly, when sodium acetate and sodium bicarbonate were used as the inhibitors, the PO yield and selectivity were low, possibly because sodium ions could be strongly adsorbed on the surface of channels of TS-1 and block the adsorption of methanol, thus leading to the decrease in PO yield and selectivity. When examining the role of sodium ions on adsorption sites in silicalite-1, Matsumura et al^[135] found the similar phenomenon in that the sodium ions located on the surface of the channels of silicalite-1 could block the adsorption of ethanol at its surface. Further increasing the amount of sodium ions led to a significant decrease in propylene conversion and PO yield possibly because more active sites of TS-1 were blocked. Literature results showed mixed conclusions when using sodium ions: Li et al^[136] reported that small amounts of sodium salt benefited the synthesis of PO using pre-manufactured H₂O₂, while Hancu^[137] found that the presence of sodium ions had negative impact on the direct synthesis of PO using a mixture of O₂ and H₂, which agreed with the observation of this study.

Therefore, in order to effectively suppress the side reactions occurred during the synthesis of PO using *in situ* generated H₂O₂ in compressed CO₂, the selected inhibitor should be able to interact with the surface acidity of TS-1, but this interaction should not be strong enough to block the adsorption of methanol.

Table 38 Experimental results using selected inhibitors with different interaction ability in the green synthesis of PO in CO₂

Inhibitor		Amberlyst A-21			NaCOOCH ₃		NaHCO ₃	
Amount, g		0.02	0.1	0.25	0.005	0.02	0.005	0.02
C ₃ H ₆ conversion, %		47.1	44.3	47.3	29.0	8.7	31.2	16.5
PO yield, %		10.2	11.6	8.2	8.2	4.6	6.7	4.0
Selectivity, %	PO	21.7	26.3	17.4	28.4	53.2	21.5	24.2
	C ₃ H ₈	68.9	67.5	78.9	67.4	35.1	75.4	69.2
	MP	5.3	3.9	2.0	2.2	0.0	1.7	3.1
	PG	3.6	1.9	1.2	1.5	9.3	0.8	2.3
	Others	0.5	0.4	0.4	0.3	2.4	0.7	1.2

Note: Other experimental conditions: (0.2%Pd+0.02%Pt)/TS-1=0.05g, water=0.25ml, methanol=0.25ml; C₃H₆=6.3mmol, H₂/C₃H₆=1, O₂/H₂=1; T=60°C, P=125bar, reaction time=5 hours

The effect of the amount of selected inhibitor (ammonium acetate) added to the reaction system was also examined in the range of 0.005g to 0.03g and the results are shown in **Figure 26**. We can conclude that, in the range of this study, although the effect of the amount of

inhibitor on the propylene conversion was minor, PO yield was increased with the increase of the amount of inhibitor until 0.02g. Accordingly, we observed the increase in PO selectivity and the decrease in propane selectivity. The influence of the amount of inhibitor on the selectivities of MP, PG and other by-products was not significant.

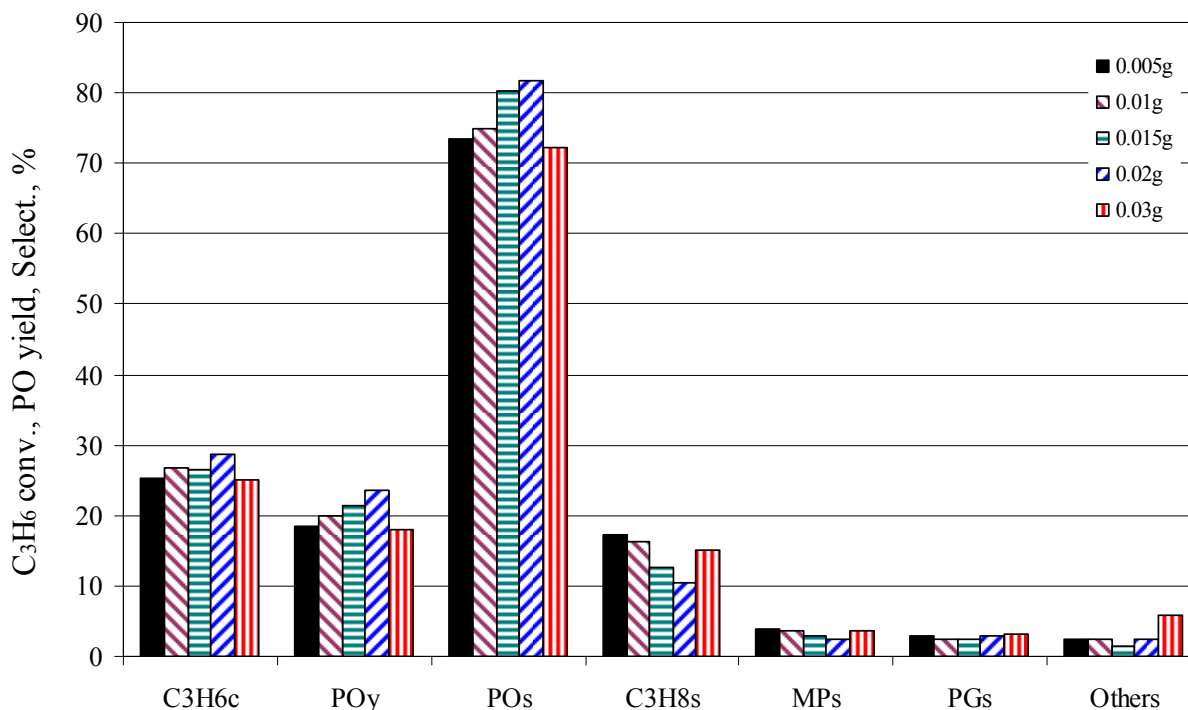


Figure 26 Effect of the amounts of selected inhibitor on the synthesis of PO

Experimental conditions: (0.2%Pd+0.02%Pt)/TS-1=0.05g, water=0.25ml, methanol=0.25ml, inhibitor=NH₄COOCH₃; C₃H₆=6.3mmol, H₂/C₃H₆=1, O₂/H₂=1; T=60°C, P=125bar, reaction time=5 hours (low case “c” stands for conversion, “y” for yield and “s” for selectivity)

The effect of reaction time on the epoxidation of propylene using *in situ* generated H₂O₂ in compressed CO₂ with methanol and water as the co-solvent is shown in **Figure 27**. It can be seen that propylene conversion, PO yield and PO selectivity were all increased with the increase

of reaction time, while propane selectivity was decreased along with the increase of reaction time. Experimental results also showed that when the reaction time was increased from 2 hours to 3 hours propane yield was increased from 1.9% to only 2.3%, while PO yield was increased from 7.5% to 16.4%.

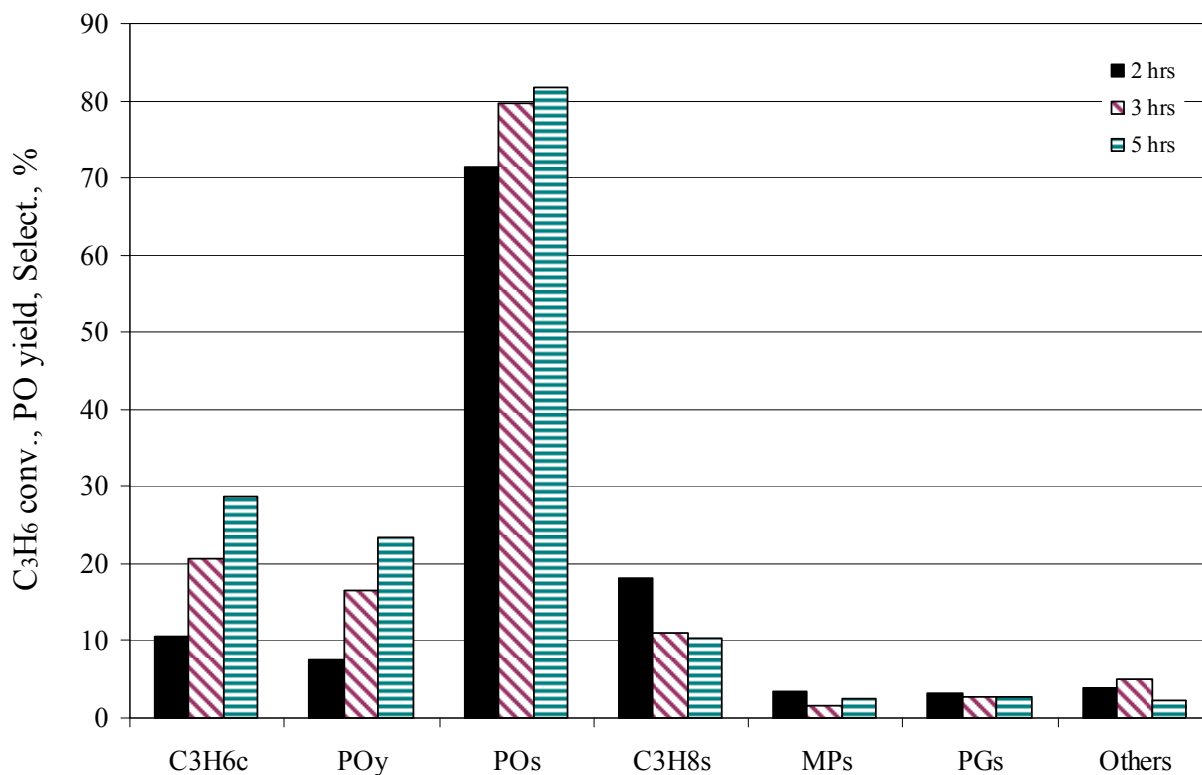


Figure 27 Effect of reaction time on green synthesis of PO in CO₂

Experimental conditions: (0.2%Pd+0.02%Pt)/TS-1=0.05g, water=0.25ml, methanol=0.25ml, NH₄COOCH₃= 0.02g; C₃H₆=6.3mmol, H₂/C₃H₆=1, O₂/H₂=1; T=60°C, P=125bar (low case “c” stands for conversion, “y” for yield and “s” for selectivity)

The effect of reaction temperature on the green synthesis of PO could be examined according to the following two conditions: (1) maintaining constant amounts of reactants and solvent while varying the reaction temperature; and (2) maintaining constant amounts of

reactants and constant reaction pressure while varying the reaction temperature. For the first condition, the change of reaction temperature has no effect on molar fractions of reactants and solvent, but the reaction pressure will change accordingly. For the second condition, the change of reaction temperature will result in the change of molar fractions of reactants and solvent since extra CO₂ is needed in order to keep constant reaction pressure. It is known that reaction rate changes along with the change of concentrations of reactants for non-zero order chemical reactions. Based on the experimental results, a power rate law developed by Taylor et al^[138] showed that the production rate of PO from the epoxidation of propylene using a mixture of O₂ and H₂ over Au/TS-1 was not zero order with respect to O₂, H₂ and propylene. Therefore, it is necessary to maintain constant reactants and solvents in order to examine the effect of reaction temperature. The corresponded pressures and experimental results under different reaction temperatures are given in **Table 39** in this study. As can be seen that an increase in reaction temperature resulted in a considerable increase in propylene conversion and PO yields. For example, when reaction temperature was increased from 50°C to 60°C, propylene conversion and PO yield were almost doubled. When conducting the gas phase epoxidation of propylene over Au/TS-1, Taylor et al^[138] also observed that temperature had strong effect on the production rate of PO. The PO selectivity in this study was also increased with the increase of reaction temperature, while the selectivity to the by-products PM and PG were all higher at lower temperature, implying that the hydrolysis of generated PO and the reaction between generated PO and methanol were easy to carry out under lower temperature compared with the synthesis of PO and the hydrogenation of propylene.

Table 39 Effect of reaction temperature on the green synthesis of PO in CO₂

Temperature, °C		40	50	60
Pressure, bar		100.5	113.1	125.0
C ₃ H ₆ conversion, %		14.1	16.0	28.7
PO yield, %		10.8	13.1	23.5
Selectivity, %	PO	77.0	81.5	81.8
	C ₃ H ₈	9.2	10.6	10.4
	MP	4.5	2.4	2.5
	PG	6.1	1.9	2.9
	Others	3.2	3.5	2.4

Note: Other experimental conditions: (0.2%Pd+0.02%Pt)/TS-1=0.05g, water=0.25ml, methanol =0.25ml, NH₄COOCH₃= 0.02g; C₃H₆=6.3mmol, H₂/C₃H₆=1, O₂/H₂=1; reaction time=5 hours

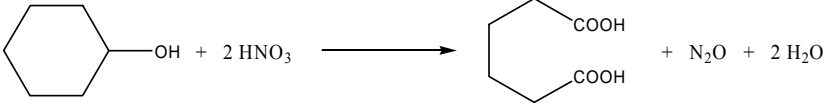
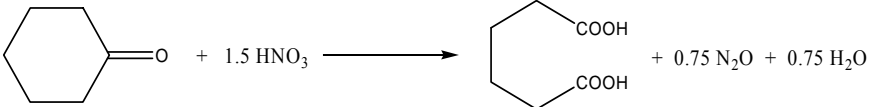
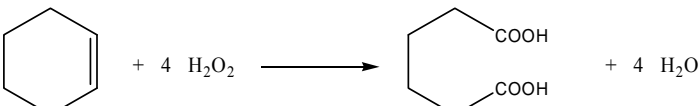
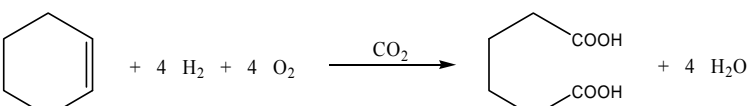
6.3 SUMMARY

From experimental results, it is concluded that supercritical CO₂ could be used as an environmentally benign solvent in one-pot green synthesis of PO using *in situ* generated H₂O₂ from O₂ and H₂ over (0.2%Pd+0.02%Pt)/TS-1. For the first time, the attempt to obtain over 20% of PO yield (while keeping vital PO selectivity) was achieved by using small amounts of polar co-solvents (methanol and water) and adding a selected weak base inhibitor (ammonium acetate) to suppress the following side-reactions: the hydrogenation of propylene, the hydrolysis of generated PO and the reaction between PO and methanol. The experimental results using different inhibitors with pH values ranging from 6.4 to 9.7 in a mixture of water and methanol (1:1 in volume) for the green synthesis of PO using *in situ* generated H₂O₂ in compressed CO₂ verified that this suppression effect was due to the interaction between the inhibitor and TS-1 leading to the neutralization of its surface acidity. The selected inhibitor should be able to interact with the surface acidity of TS-1, but this interaction should be strong enough to block the adsorption of methanol. The experimental results obtained in the temperature range of 40°C to 60°C also showed that the hydrolysis of generated PO and the reaction between the generated PO and methanol was easy to occur under lower temperature. Increasing reaction temperature resulted in an increase in propylene yield, PO yield and selectivity.

7.0 GREEN SYNTHESIS OF ADIPIC ACID USING *IN SITU* H₂O₂ IN CO₂

From literature review, we know that although cyclohexene could be used as an alternative raw material in the synthesis of adipic acid using pre-manufactured H₂O₂, one of the biggest obstacles in commercializing this process is that the current H₂O₂ price is high enough that this process can not be carried out economically. *In situ* generated H₂O₂ in compressed CO₂ may have the potential to replace pre-manufactured H₂O₂ since (1) it is proven previously that H₂O₂ could be effectively generated from O₂ and H₂ in compressed CO₂; (2) using *in situ* generated H₂O₂ to replace pre-manufactured H₂O₂ makes the synthesis of adipic acid greener. The green chemistry metric developed in this study was used to compare the greenness of various methods for the synthesis of adipic acid. The obtained GIR values are shown in **Table 40**. The GIC values for the involved chemicals are from **Table 23** and **Table 29**. Comparing with other methods, the method using *in situ* generated H₂O₂ from O₂ and H₂ in CO₂ has the lowest GIR value.

Table 40 GIR values for the synthesis of adipic acid by various methods

Chemical reactions for the synthesis of adipic acid	GIR	
 $\text{trans-1,2-cyclohexanediol} + 2 \text{HNO}_3 \longrightarrow \text{adipic acid} + \text{N}_2\text{O} + 2 \text{H}_2\text{O}$	5.76	7-1
 $\text{cyclohexanone} + 1.5 \text{HNO}_3 \longrightarrow \text{adipic acid} + 0.75 \text{N}_2\text{O} + 0.75 \text{H}_2\text{O}$	5.81	7-2
 $\text{cyclohexene} + 4 \text{H}_2\text{O}_2 \longrightarrow \text{adipic acid} + 4 \text{H}_2\text{O}$	5.21	7-3
 $\text{cyclohexene} + 4 \text{H}_2 + 4 \text{O}_2 \xrightarrow{\text{CO}_2} \text{adipic acid} + 4 \text{H}_2\text{O}$	2.92	7-4

7.1 EXPERIMENTAL

7.1.1 Chemicals and catalysts

The purities of O₂, H₂ and CO₂ (from Penn Oxygen, Jeannette, PA) used in this study were all above 99.9%. Cyclohexene (CHE, 99%, Aldrich), cyclohexene oxide (CHEO, 98%, Aldrich), cyclohexanone (CHAO, 99.9%, Fisher Scientific), *trans*-1,2-cyclohexanediol (*trans*-Diol, 98%, Aldrich), *cis*-1,2-cyclohexanediol (*cis*-Diol, 99%, Aldrich), 2-hydroxycyclohexanone dimer (HCHAO, Aldrich), 2-cyclohexen-1-one (CHENone, 95+%, Aldrich), 2-cyclohexen-1-ol (CHENol, 95%, Aldrich), adipic acid (AA, 99+%, Aldrich), glutaric acid (GA, 99%, Aldrich),

succinic acid (SA, $\geq 99\%$, Aldrich), $\text{Na}_2\text{SiO}_3 \cdot 9\text{H}_2\text{O}$ ($>99\%$, Fisher Scientific), hexadecyltrimethylammounium bromide (CTMABr, 99%, Sigma), $\text{Na}_2\text{WO}_4 \cdot 2\text{H}_2\text{O}$ (99%, Aldrich), ethyl acetate (99.5+%, Sigma-Aldrich) were all used as received without further purification.

The procedures for the synthesis of W-MCM-41 was similar to that given by Dai et al^[139]. The synthesis was carried out in a three-neck flask equipped with a condenser. 5.825g of $\text{Na}_2\text{SiO}_3 \cdot 9\text{H}_2\text{O}$ were added to 25ml of water at 85°C. This solution was stirred for 10 minutes. 2.45g of hexadecyltrimethylammounium bromide (CTMABr) was then added to obtain a solution. 3.2ml of $\text{Na}_2\text{WO}_4 \cdot 2\text{H}_2\text{O}$ (0.2mmol/ml) were added to this solution and stirred for another 10 minutes. Under vigorous stirring, 7.5ml of ethyl acetate were quickly added. The reaction mixture became clear at first and then turned white in minutes. The vigorous stirring was maintained for 20 minutes and then reduced to moderate for 24 hours. During this whole process, the temperature was kept at 85°C. The resulting mixture was allowed to cool to room temperature, and then filtered and washed with deionized water 3 times. The obtained white solid was dried at 80°C and then calcined at 600°C in air for 4 hours to remove the template. 1.305g of W-MCM-41 was obtained as a white powder.

This synthesis method is environmentally benign since it used Na_2SiO_3 to replace expensive organic silica and ethyl acetate (which can be hydrolyzed in water at certain temperature to form acetic acid and ethanol) to replace corrosive inorganic acid.

A wet impregnation method was used to load 1% palladium (Pd) and 0.1% platinum (Pt) on the W-MCM-41 molecular sieve. To 1g of W-MCM-41 in a 100ml flask, 10ml of deionized water was added. This slurry was stirred for several minutes. Known amount of 10% tetraamminepalladium(II) nitrate solution and 2% tetraammine-platinum chloride were added to

the slurry. The final mixture was allowed to stir for 24 hours and then filtered and washed with deionized water 3 times. The solid was dried at 100°C and calcined at 600°C for 4 hours and then cooled to room temperature. It was reduced with hydrogen under room temperature to obtain (1%Pd+0.1Pt)/W-MCM-41.

7.1.2 General procedures for the green synthesis of adipic acid in CO₂

The general procedures for the oxidation of cyclohexene to adipic acid using *in situ* generated H₂O₂ in compressed CO₂ as the oxidant are similar to that for the direct synthesis of H₂O₂ given in **Section 5.1.2** except that cyclohexene was used as the starting material. The tested catalysts were 0.35%Pd/TS-1 and (1.0%Pd+0.1%Pt)/W-MCM-41.

7.2 RESULTS AND DISCUSSION FOR THE GREEN SYNTHESIS OF ADIPIC ACID

7.2.1 Using precious metal loaded TS-1 as the catalyst

The experimental results for the oxidation of cyclohexene (CHE) and its derivatives [cyclohexene oxide (CHEO), *trans*-1,2-cyclohexanediol (*trans*-Diol) and *cis*-1,2-cyclohexanediol (*cis*-Diol)] over 0.35%Pd/TS-1 using *in situ* generated H₂O₂ from O₂ and H₂ in compressed CO₂ are shown in **Table 41**. Here 0.35%Pd/TS-1 was also a bifunctional catalyst: Pd was the active component for the *in situ* generation of H₂O₂ from O₂ and H₂ and TS-1 catalyzed the oxidation of cyclohexene by the *in situ* generated H₂O₂. It can be seen that the oxidation of cyclohexene by *in situ* generated H₂O₂ in compressed CO₂ generated only small amount of

adipic acid, intermediates (to adipic acid) and some cyclohexane (as mentioned earlier, Pd/TS-1 could also catalyze the hydrogenation of alkenes). The oxidation of cyclohexene oxide (CHEO) by the mixture of O₂ and H₂ in compressed CO₂ generated a large amount of diols implying that the hydrolysis of cyclohexene oxide was relatively easy under our reaction conditions. The amount of adipic acid generated from the oxidation of cyclohexene oxide in compressed CO₂ was an order of magnitude higher than that from cyclohexene. Considering the significant difference in adipic acid yields when *trans*-Diol and *cis*-Diol were used as the starting materials, it is concluded that the oxidation of *cis*-Diol by *in situ* generated H₂O₂ was relatively easy. This conclusion is consistent with the results obtained by Lee et al.^[92] when they used pre-manufactured H₂O₂ to oxidize cyclohexene over a TAPO-5 catalyst (titanium framework-substituted aluminophosphate number 5).

Control experiments run in this study showed that *cis*-Diol could not be oxidized by O₂ alone in compressed CO₂ under similar reaction conditions indicating that oxidation was due to the generation of H₂O₂ from O₂ and H₂ in compressed CO₂. Since the mechanistic pathway shown by **Scheme 3** disclosed that at least 3 moles of H₂O₂ were needed in order to oxidize one mole of Diol (either *trans*- or *cis*-), significant amounts of *in situ* H₂O₂ were likely generated in compressed CO₂ during the reaction process.

Table 41 Oxidation of cyclohexene and its derivatives by *in situ* H₂O₂ in CO₂

Substrate	CHE	CHEO	<i>trans</i> -Diol	<i>cis</i> -Diol	<i>cis</i> -Diol
Water, mmol	11.67	11.67	8.89	8.89	8.89
H ₂ :Substrate	8	6	6	6	
O ₂ :H ₂	4	4	4	4	
O ₂ :Diol					24
Products, mol%					
Adipic acid	0.24	2.46	6.16	13.20	0
CHENol/one ^a	0.15	0.58	0.93	0.64	0.18
CHAO	0.91	0.83	0.38	0.35	0.15
HCHAO	0.72	0.62	0.62	0.76	0.22
Diols	0.07	48.07			
Cyclohexane	0.89				

Note: Experimental conditions: substrate=1.18mmol, 0.35%Pd/TS-1=0.03g, T=90°C, P=145bar, reaction time=10 hours;

^a: a mixture of 2-cyclohexen-1-ol and 2-cyclohexen-1-one

7.2.2 Using precious metal loaded W-MCM-41 as the catalyst

Thermodynamically, the change of Gibbs free energy, ΔG_0^f for the oxidation of cyclohexene to cyclohexene oxide by H₂O₂ is -214.7kJ/mol at 298.15K meaning that this reaction could occur easily. This was also experimentally proven by Sato et al^[11] and Lee et al^[92] when they used pre-manufactured H₂O₂ to oxidize cyclohexene. But the experimental results listed in **Table 41** showed that the oxidation of cyclohexene to cyclohexene oxide by *in situ* generated H₂O₂ over

precious metal loaded TS-1 in compressed CO₂ was the slowest step in the direct synthesis of adipic acid from cyclohexene. These contradictory conclusions were caused by the relative small pore size of TS-1 which presents diffusional limitation to relatively bulky chemicals like cyclohexene. Although the critical dimensions of cyclohexene could not be found in literature, the critical dimensions of cyclohexane (4.7Å×6.2Å)^[140] could be used as a reference since they both have similar kinetic diameters (ca. 5.8Å).^[135] Because the pore size of TS-1 was only 5.6Å×5.3Å, cyclohexene could just fit into the pores of TS-1, but cyclohexene oxide could not be formed effectively since the epoxidation was a more sterically demanding reaction.^[73] The existence of this steric effect was observed by many researchers^[9, 73, 140, 141] when TS-1 was used to catalyze the oxidation of cyclohexene by pre-manufactured H₂O₂.

Therefore, many researchers tried to synthesize new molecular sieves with larger pore size in order to effectively carry out oxidation of bulky chemicals by H₂O₂. MCM-41 is one of the most important silicate mesoporous molecular sieves. First reported by researchers at Mobil^[142] (now ExxonMobil), MCM-41 features a hexagonally arranged pore system with pore diameter in the range of 20-100Å and an extremely large surface area of about 1000m²/g as shown in **Figure 28**.^[143] The discovery of MCM-41 provided new opportunities for creating highly dispersed and more accessible catalytic active sites by incorporating metal ions (such as W, Al, Ti, Fe and V etc) into its silica-based frameworks. The tungstate-incorporated MCM-41 (designated as W-MCM-41; its synthesis was reported by Zhang et al^[95] and Dai et al^[139]) presents special catalytic activity when using H₂O₂ aqueous solution to oxidize relatively bulky chemicals. For example, Zhang et al^[95, 144] proved that W-MCM-41 was an effective catalyst in the oxidation of cyclohexene by aqueous H₂O₂. When the molar ratio of cyclohexene/H₂O₂ was 1, the majority product was *trans*-1,2-cyclohexanediol, an intermediate in the synthesis of adipic

acid when cyclohexene was used as the starting material. The reaction proceeded because the mesoporous structure of W-MCM-41 presented no resistance for reactant and product to diffuse in and out the pore channels.

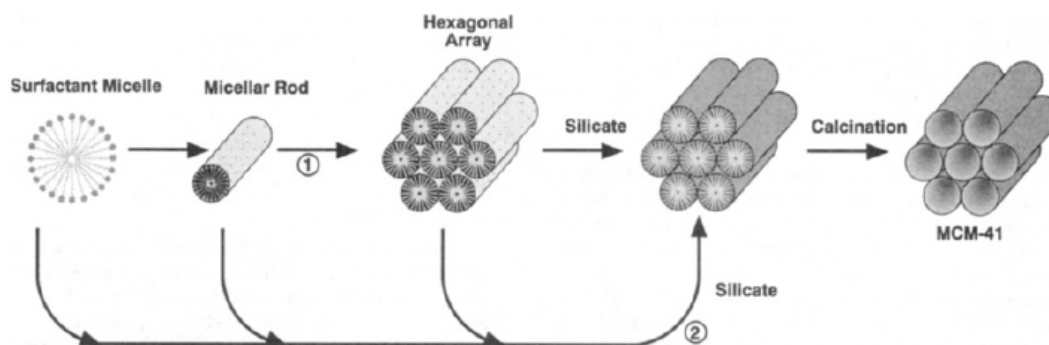
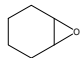
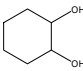
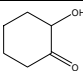
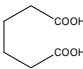


Figure 28 Possible mechanistic pathways for the synthesis of MCM-41: (1) liquid crystal phase initiated; (2) silicate anion initiated

In order to use H_2O_2 to effectively oxidize cyclohexene, molecular sieves with larger pore size should be adopted as the catalyst. According to the literature,^[95, 139, 144] W-MCM-41 is a mesoporous molecular sieve presenting high activity in the oxidation of cyclohexene to cyclohexene oxide using aqueous H_2O_2 . In this study, the as-synthesized W-MCM-41 was used as the catalyst in the oxidation of cyclohexene to adipic acid by pre-manufactured 30% H_2O_2 . The experimental results are listed in **Table 42** (here others include the intermediates to adipic acid, small amount of 2-cyclohexen-1-ol/one, 2-cyclohexan-1-ol/one, caprolactone and glutaric acid etc); the results using TAPO-5 (titanium framework-substituted aluminophosphate number 5) as the catalyst^[92] are also presented for comparison.

Table 42 Oxidation of cyclohexene by H₂O₂ with different catalysts

		This work		Lee et al ^[92]		
Catalyst		W-MCM41		TAPO-5		
Catalyst/CHE, g/ml		0.02/0.5		0.5/6.3		
H ₂ O ₂ :CHE (mol)		4:1		~3.6:1 (?)		
Solvent		5ml HOAc		-		
T, °C		75		80		
Time, hrs		10	24	12	24	72
Conversion, %		83.8	86.8	17.3	49.5	100
Yield, %		0.05	0.08	0	0	0
		32.0	20.9	10.1	32.9	30
		3.8	2.0	2.7	1.8	2.9
		14.2	29.9	0.5	6.5	30.3
	others	33.3	33.9	4.1	8.3	36.8

It can be seen from **Table 42** that the as-synthesized W-MCM-41 is an effective catalyst in carrying out the oxidation of cyclohexene to adipic acid using aqueous H₂O₂ in acidic condition. Even though the concentration of W-MCM-41 used in this study was lower than that of TAPO-5 used by Lee et al^[92] (the catalyst/CHE ratio in this study was 0.04, while for TAPO-5 system, it was 0.077), the oxidation reaction using W-MCM-41 was still faster than that using TAPO-5. For example, when the reaction time was 24 hours, for the W-MCM-41 system the cyclohexene conversion reached 86.8% with an adipic acid yield of 29.9%; while for TAPO-5

system, the conversion was 49.5% with an adipic acid yield of only 6.5%. Further, the amount of cyclohexene oxide was very low. The possible reasons are (1) the hydrolysis of cyclohexene oxide was relatively fast compared with other reactions shown in **Scheme 3**; (2) the radical mechanism to *cis*-Diol suggested by Lee et al^[92] may also play a significant role in this study. Furthermore, the similar distribution pattern of reaction intermediates and products also implied similar reaction pathways and control steps in this study (see **Scheme 3** for the mechanistic reaction pathways).

When compressed CO₂ was used as the solvent and different acids were used as the acidic medium, the experimental results and the comparison with that using TAPO-5 as the catalyst are shown in **Figure 29**. When acetic acid (HOAc) was used, the oxidation reaction was much slower compared with that using trifluoroacetic acid (TFA). This is because the fluorinated compound (trifluoroacetic acid) is more soluble in compressed CO₂ than that in its non-fluorinated counterpart (acetic acid). **Figure 29** also showed that the results in using TFA and W-MCM-41 in 10 hours were similar to that in using TAPO-5 in 24 hours. Therefore, it is concluded that although the oxidation of cyclohexene to adipic acid in compressed CO₂ over W-MCM-41 was slightly slower than that in acetic acid, it was still faster than that over TAPO. The distribution pattern of intermediates and products still implies the similar reaction pathways and control steps.

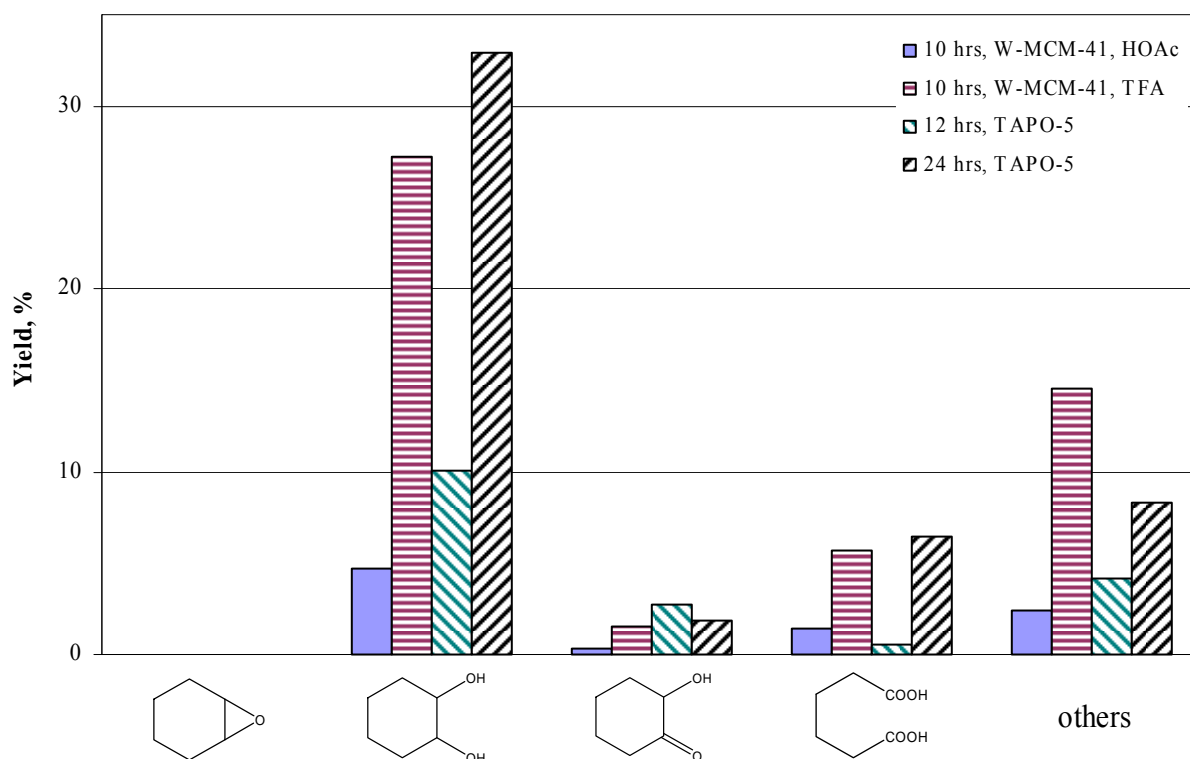


Figure 29 Oxidation of cyclohexene by 30% H₂O₂ in CO₂ with different acids

Experimental conditions: CHE=0.25ml, acid=0.25ml, H₂O₂:CHE=4:1, W-MCM-41=0.01g; T=75°C, P=138bar, reaction time=10 hours

When the mixture of O₂ and H₂ in compressed CO₂ was used to replace pre-manufactured H₂O₂ as the oxidant and (1%Pd+0.1%Pt)/W-MCM-41 was used to replace W-MCM-41 as the catalyst (this catalyst can catalyze both the *in situ* generation of H₂O₂ from O₂ and H₂ in compressed CO₂ and the oxidation of cyclohexene), the obtained results and comparison with the results of Lee et al^[92] are given in **Figure 30**. As can be seen that adipic acid yield in this study was still higher than that of Lee et al using pre-manufactured H₂O₂ as the oxidant and TAPO-5 as the catalyst under similar reaction temperature and time, but the yields of Diols and hydroxyketone were lower than that using TAPO-5. However, it should be pointed that during

the oxidation of cyclohexene by *in situ* generated H_2O_2 from O_2 and H_2 in compressed CO_2 using (1%Pd+0.1%Pt)/W-MCM-41 as the catalyst, hydrogenation of cyclohexene to cyclohexane (CHA) occurred because of the presence of precious metal and H_2 . This hydrogenation became the dominant reaction when TFA was used as the acidic medium provider, while for acetic acid, the hydrogenation reaction was mild.

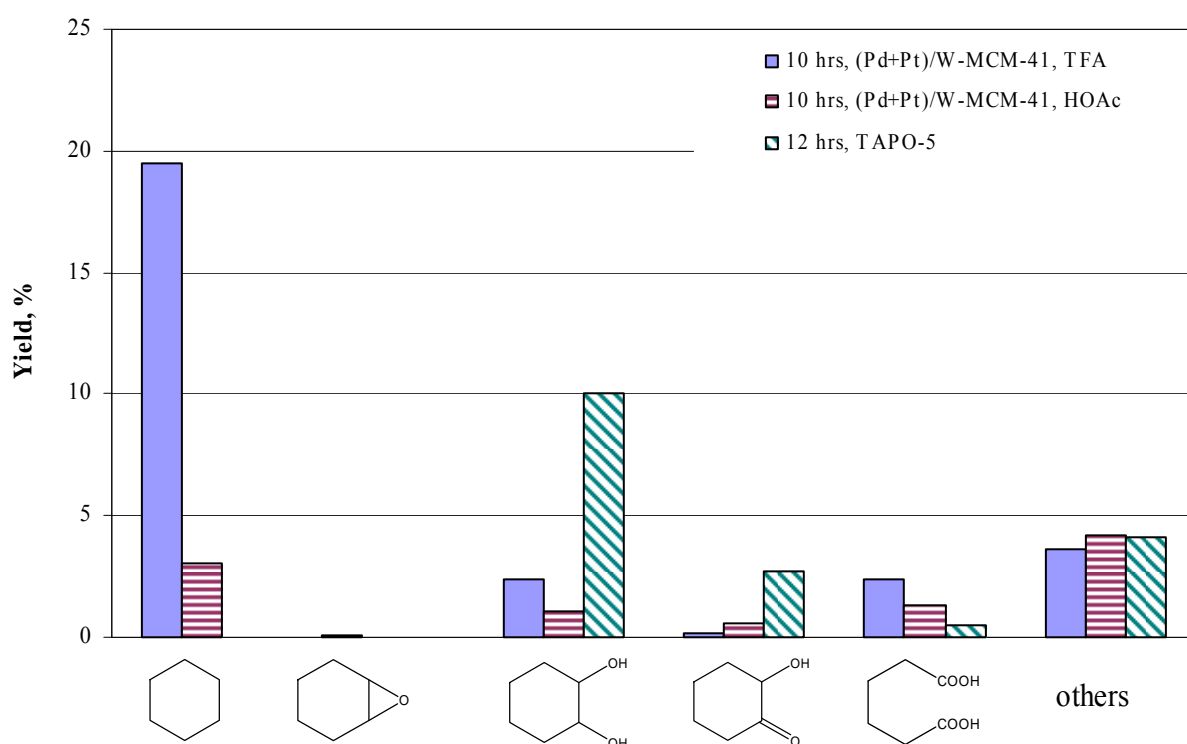


Figure 30 Oxidation of cyclohexene by *in situ* generated H_2O_2 in CO_2

Experimental conditions: CHE=0.25ml, acid=0.25ml, H_2 :CHE=4:1, O_2 : H_2 =4:1, (1%Pd+0.1%Pt)/W-MCM-41=0.01g; T=75°C, P=138bar, reaction time=10 hours

Due to the use of an acidic medium in the oxidation of cyclohexene and the generation of an acid (adipic acid) as the final product, the method developed in the green synthesis of propylene oxide using a weak base inhibitor to suppress the hydrogenation reaction could not be

used here. If we want to use *in situ* generated H_2O_2 as the oxidant to oxidize cyclohexene to synthesize adipic acid, a method would need to be developed to suppress the hydrogenation of cyclohexene.

7.3 SUMMARY

The experimental results in this study proved that the critical step in the oxidation of cyclohexene to adipic acid using *in situ* generated H_2O_2 over precious metal loaded TS-1 in compressed CO_2 was the epoxidation of cyclohexene, the oxidation of related intermediates (cyclohexene oxide, *trans*- and *cis*-Diols, 2-hydroxycyclohexanone) to adipic acid was relatively easy. However, the lower conversion of cyclohexene implied the existence of diffusion limitation for cyclohexene due to the small pore size of TS-1.

Mesoporous molecular sieve W-MCM-41 was synthesized by an environmentally benign method. Experimental results proved that this as-synthesized W-MCM-41 was an effective catalyst in catalyzing the oxidation of cyclohexene to adipic acid by pre-manufactured H_2O_2 under the condition of with and without using CO_2 as the solvent. Using *in situ* generated H_2O_2 from O_2 and H_2 over (1.0%Pd+0.1%Pt)/W-MCM-41 in compressed CO_2 , attractive results were also obtained in the oxidation of cyclohexene to adipic acid. But the hydrogenation of cyclohexene to cyclohexane was also occurred due to the presence of precious metal and H_2 . A method should be developed to suppress this un-desired side-reaction.

8.0 CONCLUSIONS

In this study, we first developed a new green chemistry metric with the consideration of both quantity and quality of involved chemicals. The defined greenness index for a chemical GIC could be used to calculate the greenness index for a chemical formula GIF, greenness index for an oxidant GIO, greenness index for a chemical reaction GIR and greenness index for a product GIP. This new metric was successfully used in searching for greener process for the synthesis of H₂O₂, PO and adipic acid.

Based on the criteria established in this study, pyridine was selected as an indicator compound to measure the amounts of directly synthesized H₂O₂ in compressed CO₂. The experimental results proved, for the first time, that H₂O₂ could be effectively synthesized from O₂ and H₂ in compressed CO₂. The effects of the following operational parameters on H₂ conversion, H₂O₂ yield and selectivity were examined: stirring speed, O₂/H₂ molar ratio, H₂ concentration, catalyst mass, Pd content and the addition of Pt. The optimal reaction conditions for the direct synthesis of H₂O₂ were as followings: stirring power was over 65%, O₂/H₂ molar ratio=1, Low Pd content (<0.6%) with the addition of small amount of Pt (Pt/Pd=0.1 in weight).

The attempts to achieve over 20% of propylene conversion while keep vital PO selectivity was achieved, for the first time, by using *in situ* generated H₂O₂ in compressed CO₂ over precious metal loaded TS-1. In order to enhance the propylene conversion, small amounts of polar co-solvent (methanol and water) was used to enhance the solvent properties of

compressed CO₂. A selected weak base inhibitor was used to suppress the commonly encountered side-reactions: the hydrogenation of propylene, the hydrolysis of generated PO and the reaction between methanol and the generated PO. This suppression was due to the interaction between the inhibitor and TS-1 leading to the neutralization of surface acidity of TS-1.

The oxidation of cyclohexene by *in situ* generated H₂O₂ in compressed CO₂ over precious metal loaded TS-1 generated only small amount of adipic acid due to the diffusion limitation of cyclohexene in small pore size of TS-1. A mesoporous molecular sieve W-MCM-41 was synthesized by an environmentally benign method. This W-MCM-41 was experimentally proved to be an effectively catalyst to oxidize cyclohexene to adipic acid using pre-manufactured H₂O₂ under the condition of with and without compressed CO₂. The precious metal loaded W-MCM-41 was also proved to be an effective catalyst to oxidize cyclohexene to adipic acid using *in situ* generated H₂O₂ from O₂ and H₂ in compressed CO₂. However, it is necessary to develop a method to suppress the hydrogenation of cyclohexene during the oxidation using *in situ* generated H₂O₂.

9.0 RECOMMENDED FUTURE WORK

This study raised some important questions which need to be considered in the future:

1. For the commonly used chemicals, the hazardous ratings used in calculating the GIC could be found from their MSDS. However, for some special chemicals, there are no hazardous ratings data available. Further research work is needed to develop a method to evaluate their hazardous data by using some principles like group contribution method^[145] (a method widely used to evaluate the physical properties of chemicals). This method had been used by some researchers^[146] to estimate the toxicities of organic compounds.
2. Due to the interaction between TS-1 and H₂O₂, some *in situ* generated H₂O₂ could be effectively used to oxidize the indicator. Therefore, the H₂O₂ yields obtained in this study were the minimum yields we could obtain. A method should be developed to probe the mechanism of this interaction and to evaluate the amount of un-reactive H₂O₂.
3. We verified that the suppression of common side reactions during the one-pot green synthesis of PO using *in situ* generated H₂O₂ in compressed CO₂ was due to the neutralization of surface acidity of TS-1. The interactive mechanism should be developed to understand this suppression effect.

4. A method should be developed to effectively suppress the hydrogenation of cyclohexene during the oxidation of cyclohexene to adipic acid using *in situ* generated H_2O_2 over precious metal loaded W-MCM-41 in compressed CO_2 .

APPENDIX

GC CONDITIONS USED IN THIS STUDY

The GC conditions for detecting H₂ and indicator in direct synthesis of H₂O₂ from O₂ and H₂ in compressed CO₂ are listed in **Table 43**. The GC conditions for detecting propane, propylene and PO in the green synthesis of PO using *in situ* generated H₂O₂ are listed in **Table 44**. The GC conditions for detecting cyclohexene, adipic acid and related intermediates and by-products in the green synthesis of adipic acid are the same as the detection of indicator listed in the right column of **Table 43**.

Table 43 GC conditions in the detection of H₂ and indicator in direct synthesis of H₂O₂ in compressed CO₂

Item	Detection of H ₂	Detection of Indicator
Detector	TCD	FID
Column	HayeSep D Packed column (20ft×1/8")	DB-1 capillary column (30m×0.253mm×0.50μm)
Sampling loop, μL	100	
Injection amount, μL		0.5

Table 43 (continued)

Carrier gas	N ₂	He
Carrier gas flowrate, ml/min	15	2.4
Carrier gas pressure, psi	70	60
Head pressure, psi	32	23
Reference gas flowrate, ml/min	22.5	
H ₂ flowrate, (<i>pressure</i>); ml/min, (<i>psi</i>)		30, (<i>18</i>)
Air flowrate, (<i>pressure</i>); ml/min, (<i>psi</i>)		402, (<i>42</i>)
Auxiliary gas flowrate, ml/min		45
Total flowrate, ml/min		480
Injection temperature, °C	100	250
Detector temperature, °C	120	275
Auxiliary temperature, °C	140	
Oven temperature, °C	35	40
Initial time, min	5.0	4.0
Rate, °C/min	10	15
Final temperature, °C	120	210
Final time, min	16.5	5.0

Table 44 GC conditions in the synthesis of PO using *in situ* generated H₂O₂ in CO₂

Item	Detection of C ₃ H ₆ and PO	Detection of by-products
Detector	TCD	FID
Column	HayeSep D Packed column (20ft×1/8")	DB-1 capillary column (30m×0.253mm×0.50μm)
Sample amount, μL	100	0.5
Carrier gas	He	He
Carrier gas flowrate, ml/min	30	2.4
Carrier gas pressure, psi	70	60
Head pressure, psi	52	23
Reference gas flowrate, ml/min	45	
H ₂ flowrate, (<i>pressure</i>); ml/min, (<i>psi</i>)		30, (18)
Air flowrate, (<i>pressure</i>); ml/min, (<i>psi</i>)		402, (42)
Auxiliary gas flowrate, ml/min		45
Total flowrate, ml/min		480
Injection temperature, °C	100	120
Detector temperature, °C	120	160
Auxiliary temperature, °C	140	
Oven temperature, °C	35	40
Initial time, min	5.0	4.0
Rate, °C/min	10	15
Final temperature, °C	120	160
Final time, min	16.5	5.0

BIBLIOGRAPHY

- [1] P. T. Anastas, M. M. Kirchhoff, *Accounts of Chemical Research* **2002**, 35, 686.
- [2] P. T. Anastas, J. C. Warner, *Green Chemistry: Theory and Practice*, Oxford University Press, New York, **1998**.
- [3] S. T. Oyama, A. N. Desikan, J. W. Hingtower, *Catalytic Selective Oxidation*, American Chemical Society, Washington DC, **1993**.
- [4] M. Hudlicky, *Oxidations in Organic Chemistry, Vol. 186*, American Chemical Society, Washington, DC, Washington, DC, **1990**.
- [5] G. Centi, F. Cavani, F. Trifiro, *Selective Oxidation by Heterogeneous Catalysis*, Kluwer Academic/Plenum Publishers, New York, **2001**.
- [6] D. D. Davis, D. R. Kemp, in *Kirk-Othmer Encyclopedia of Chemical Technology, Vol. 1*, 4th ed. (Eds.: J. I. Kroschwitz, M. Howe-Grant), John Wiley & Sons, Inc., New York, **1991**, pp. 466.
- [7] *Chem. Week* **2005**, 167(27), p36.
- [8] Q. Chen, *China Chemical Reporter* **2006**, 14(12), 19.
- [9] C. W. Jones, *Applications of Hydrogen Peroxide and Derivatives*, The Royal Society of Chemistry, Cambridge, **1999**.
- [10] R. Noyori, M. Aoki, K. Sato, *Chemical Communications (Cambridge, United Kingdom)* **2003**, 1977.
- [11] K. Sato, M. Aoki, R. Noyori, *Science* **1998**, 281, 1646.
- [12] H. Henkel, W. Weber, *US Patent* 1,108,752, **1914**.
- [13] M. Taramasso, G. Perego, B. Notari, *US Patent* 4,410,501, **1983**.
- [14] <http://www.iza-structure.org/databases/>.
- [15] B. K. Hodnett, *Heterogeneous Catalytic Oxidation*, John Wiley & Sons, Ltd, Chichester, **2000**.

- [16] C. A. Eckert, B. L. Knutson, P. G. Debenedetti, *Nature* **1996**, 383, 313.
- [17] E. J. Beckman, *Journal of Supercritical Fluids* **2004**, 28, 121.
- [18] P. Landon, P. J. Collier, A. F. Carley, D. Chadwick, A. J. Papworth, A. Burrows, C. J. Kiely, G. J. Hutchings, *Physical Chemistry Chemical Physics* **2003**, 5, 1917.
- [19] T. Danciu, E. J. Beckman, D. Hancu, R. N. Cochran, R. Grey, D. M. Hajnik, J. Jewson, *Angewandte Chemie International Edition* **2003**, 42, 1140.
- [20] Q. Chen, *Journal of Cleaner Production* **2006**, 14, 708.
- [21] Q. Chen, *Chemical Engineering and Processing* **2007**, Available online (doi:10.1016/j.cep.2006.12.012).
- [22] W. Eul, A. Moeller, N. Steiner, "Hydrogen Peroxide" in *Kirk-Othmer Encyclopedia of Chemical Technology*, Online ed. ed., John Wiley & Sons, Inc., Hoboken, NJ,, **2001**.
- [23] E. J. Beckman, *Green Chemistry* **2003**, 5, 332.
- [24] Q. Chen, E. J. Beckman, *Green Chemistry* **2007**, 9, 802.
- [25] R. E. Albers, M. Nystrom, M. Siverstrom, A. Sellin, A. C. Dellve, U. Andersson, W. Herrmann, T. Berglin, *Catalysis Today* **2001**, 69, 247.
- [26] A. Drelinkiewicz, *Journal of Molecular Catalysis A: Chemical* **1995**, 101, 61.
- [27] Q. Chen, *Inorganic Chemicals Industry* **2002**, 34(5), 15.
- [28] A. Drelinkiewicz, A. Waksmundzka-Gora, *Journal of Molecular Catalysis A: Chemical* **2006**, 246, 167.
- [29] A. P. Gelbein, *Chemtech* **1998**, 28(12), 1.
- [30] http://news.xinhuanet.com/photo/2006-07/28/content_4889656.htm.
- [31] H. Cui, *Dyestuff Industry* **1993**, 30(4), 27.
- [32] Y. Chen, G. Wang, J. Wu, *Jiangsu Chemical Industry* **1991**, 19(4), 27.
- [33] J. Henkelmann, T. Weber, T. Rohde, R. Busch, *US Patent* 7,053,244, **2006**.
- [34] D. Hancu, E. J. Beckman, *Green Chemistry* **2001**, 3, 80.
- [35] D. Hancu, H. Green, E. J. Beckman, *Industrial & Engineering Chemistry Research* **2002**, 41, 4466.
- [36] G. W. Hooper, *US Patent* 3,336,112, **1967**.

- [37] L. Kim, G. W. Schoenthal, *US Patent* 4,007,256, **1976**.
- [38] A. I. Dalton, Jr., R. W. Skinner, *US Patent* 4,336,239, **1982**.
- [39] L. W. Gosser, J. A. T. Schwartz, *US Patent* 4,832,938, **1989**.
- [40] S.-E. Park, J. W. Yoo, W. J. Lee, C. W. Lee, J.-S. Chang, Y. K. Park, *Bulletin of the Korean Chemical Society* **1999**, 20, 21.
- [41] R. Meiers, W. F. Holderich, *Catalysis Letters* **1999**, 59, 161.
- [42] S. E. Park, L. Huang, C. W. Lee, J. S. Chang, *Catalysis Today* **2000**, 61, 117.
- [43] J. S. Hwang, C. W. Lee, D. H. Ahn, H. S. Chai, S. E. Park, *Research on Chemical Intermediates* **2002**, 28, 527.
- [44] V. R. Choudhary, A. G. Gaikwad, S. D. Sansare, *Angewandte Chemie-International Edition* **2001**, 40, 1776.
- [45] P. Landon, P. J. Collier, A. J. Papworth, C. J. Kiely, G. J. Hutchings, *Chemical Communications (Cambridge, United Kingdom)* **2002**, 2058.
- [46] B. Bertsch-Frank, I. Hemme, L. Von Hoppel, S. Katusic, J. Rollmann, *US Patent* 6,387,346, **2002**.
- [47] M. Okumura, Y. Kitagawa, K. Yamaguchi, T. Akita, S. Tsubota, M. Haruta, *Chemistry Letters* **2003**, 32, 822.
- [48] R. Burch, P. R. Ellis, *Applied Catalysis B: Environmental* **2003**, 42, 203.
- [49] D. P. Dissanayake, J. H. Lunsford, *Journal of Catalysis* **2003**, 214, 113.
- [50] S. Chinta, J. H. Lunsford, *Journal of Catalysis* **2004**, 225, 249.
- [51] T. Haas, G. Stochiol, J. Rollmann, *US Patent* 6,764,671, **2004**.
- [52] G. Blanco-Brieva, E. Cano-Serrano, J. M. Campos-Martin, J. L. G. Fierro, *Chemical Communications (Cambridge, United Kingdom)* **2004**, 1184.
- [53] J. K. Edwards, B. Solsona, P. Landon, A. F. Carley, A. Herzing, M. Watanabe, C. J. Kiely, G. J. Hutchings, *Journal of Materials Chemistry* **2005**, 15, 4595.
- [54] J. K. Edwards, B. E. Solsona, P. Landon, A. F. Carley, A. Herzing, C. J. Kiely, G. J. Hutchings, *Journal of Catalysis* **2005**, 236, 69.
- [55] T. Ishihara, Y. Ohura, S. Yoshida, Y. Hata, H. Nishiguchi, Y. Takita, *Applied Catalysis, A: General* **2005**, 291, 215.
- [56] Y.-F. Han, J. H. Lunsford, *Catalysis Letters* **2005**, 99, 13.

- [57] Y.-F. Han, J. H. Lunsford, *Journal of Catalysis* **2005**, 230, 313.
- [58] M. Rueter, B. Zhou, S. Parasher, *US Patent* 7,144,565, **2006**.
- [59] T. Haas, G. Stochniol, J. Rollmann, *US Patent* 7,005,528, **2006**.
- [60] J. K. Edwards, B. E. Solsona, P. Landon, A. F. Carley, A. Herzing, C. J. Kiely, G. J. Hutchings, *Journal of Catalysis* **2005**, 236, 69.
- [61] P. A. Ramachandran, R. V. Chaudhari, *Three-Phase Catalytic Reactors*, Gordon and Breach Science Publishers, New York, **1983**.
- [62] L.-S. Fan, *Gas-Liquid-Solid Fluidization Engineering*, Butterworth-Heinemann, Boston, **1989**.
- [63] K. Akita, F. Yoshida, *Industrial & Engineering Chemistry Process Design and Development* **1973**, 12, 76.
- [64] B. G. Kelkar, S. P. Godbole, M. F. Honath, Y. T. Shah, N. L. Carr, W. D. Deckwer, *AIChE Journal* **1983**, 29, 361.
- [65] V. V. Krishnan, A. G. Dokoutchaev, M. E. Thompson, *Journal of Catalysis* **2000**, 196, 366.
- [66] www.htigrp.com/data/upfiles/news/Degussa.pdf.
- [67] M. G. Clerici, G. Bellussi, U. Romano, *Journal of Catalysis* **1991**, 129, 159.
- [68] G. Jenzer, T. Mallat, M. Maciejewski, F. Eigenmann, A. Baiker, *Applied Catalysis A: General* **2001**, 208, 125.
- [69] J. O. Pande, J. Tonheim, *Process Safety Progress* **2001**, 20, 37.
- [70] A. H. Tullo, P. L. Short, *Chemical & Engineering News* **2006**, 84(41), 22.
- [71] D. L. Trent, "Propylene oxide" in *Kirk-Othmer Encyclopedia of Chemical Technology*, Online ed., John Wiley & Sons, Inc., Hoboken, NJ, **2001**.
- [72] G. F. Thiele, E. Roland, *Journal of Molecular Catalysis A: Chemical* **1997**, 117, 351.
- [73] M. G. Clerici, P. Ingallina, *Journal of Catalysis* **1993**, 140, 71.
- [74] R. Meiers, U. Dingerdissen, W. F. Holderich, *Journal of Catalysis* **1998**, 176, 376.
- [75] B. Chowdhury, J. J. Bravo-Suarez, M. Date, S. Tsubota, M. Haruta, *Angewandte Chemie International Edition* **2006**, 45, 412.
- [76] W. Laufer, W. F. Hoelderich, *Applied Catalysis A: General* **2001**, 213, 163.

- [77] B. S. Uphade, M. Okumura, S. Tsubota, M. Haruta, *Applied Catalysis A: General* **2000**, *190*, 43.
- [78] B. S. Uphade, T. Akita, T. Nakamura, M. Haruta, *Journal of Catalysis* **2002**, *209*, 331.
- [79] B. Taylor, L. Cumararatunge, J. Lauterbach, W. N. Delgass, *Gold Bulletin* **2005**, *38*, 133.
- [80] *Chemical Week* **2005**, *167(15)*, p31.
- [81] *ICIS Chemical Business* **2007**, *2(59)*, p35.
- [82] H. A. Wittcoff, B. G. Reuben, J. S. Plotkin, *Industrial Organic Chemicals*, 2nd Edition ed., John Wiley & Sons, Inc., Hoboken, New Jersey, **2004**.
- [83] K. Weissermel, H.-J. Arpe, *Industrial Organic Chemistry*, Fourth, Completely Revised Edition ed., Wiley-VCH Verlag GmbH & Co. KGaA, Weinheim, **2003**.
- [84] M. T. Musser, in *Ullmann's Encyclopedia of Industrial Chemistry, Vol. 1*, 6th ed., Wiley-VCH, Weinheim, **2003**, pp. 453.
- [85] A. Shimizu, K. Tanaka, M. Fujimori, *Chemosphere: Global Change Science* **2000**, *2*, 425.
- [86] J. Perez-Ramirez, F. Kapteijn, K. Schoffel, J. A. Moulijn, *Applied Catalysis, B: Environmental* **2003**, *44*, 117.
- [87] A. Scott, *Chemical Week* **1998**, *160(6)*, 37.
- [88] www.rhodia.com.
- [89] S. Alini, A. Bologna, F. Basile, T. Montanari, A. Vaccari, *European Patent* 1,262,224 A1, **2002**.
- [90] Y. Deng, Z. Ma, K. Wang, J. Chen, *Green Chemistry* **1999**, *1*, 275.
- [91] H. Jiang, H. Gong, Z. Yang, X. Zhang, Z. Sun, *Reaction Kinetics and Catalysis Letters* **2002**, *75*, 315.
- [92] S. O. Lee, R. Raja, K. D. M. Harris, J. M. Thomas, B. F. G. Johnson, G. Sankar, *Angewandte Chemie-International Edition* **2003**, *42*, 1520.
- [93] S. Y. Jonsson, K. Farnegardh, J. E. Backvall, *Journal of the American Chemical Society* **2001**, *123*, 1365.
- [94] J. Y. Ryu, J. Kim, M. Costas, K. Chen, W. Nam, L. Que, *Chemical Communications (Cambridge, United Kingdom)* **2002**, 1288.
- [95] Z. R. Zhang, J. S. Sue, X. M. Zhang, S. B. Li, *Applied Catalysis A: General* **1999**, *179*, 11.

- [96] D. J. C. Constable, A. D. Curzons, V. L. Cunningham, *Green Chemistry* **2002**, 4, 521.
- [97] R. A. Sheldon, *Chemistry & Industry* **1992**, 903.
- [98] B. M. Trost, *Science* **1991**, 254, 1471.
- [99] Y. Usui, K. Sato, *Green Chemistry* **2003**, 5, 373.
- [100] A. Castellan, J. C. J. Bart, S. Cavallaro, *Catalysis Today* **1991**, 9, 237.
- [101] O. A. Sampson Jr., *US Patent* 3,359,308, **1967**.
- [102] J. C. Bare, G. A. Norris, D. W. Pennington, T. McKone, *Journal of Industrial Ecology* **2003**, 6, 49.
- [103] P. Saling, A. Kicherer, B. Dittrich-Kramer, R. Wittlinger, W. Zombik, I. Schmidt, W. Schrott, S. Schmidt, *International Journal of Life Cycle Assessment* **2002**, 7, 203.
- [104] <http://www.paint.org/hmis/index.cfm>.
- [105] <http://www.nfpa.org/>.
- [106] <http://www.mallbaker.com/Americas/catalog/features/safTlabel.asp>.
- [107] http://www.hc-sc.gc.ca/ewh-semt/occup-travail/whmis-simdut/index_e.html.
- [108] http://www.ilpi.com/msds/osha/1910_1200.html.
- [109] <http://www.ilpi.com/msds/ref/hmis.html>.
- [110] <http://ozone.unep.org/>.
- [111] <http://www.epa.gov/ozone/defns.html>.
- [112] <http://www.ipcc.ch/pub/syrgloss.pdf>.
- [113] <http://www.epa.gov/pbt/index.htm>.
- [114] <http://www.pbtprofiler.net/>.
- [115] R. Kresse, U. Baudis, P. Jager, H. H. Riechers, H. Wagner, J. Winkler, in *Ullmann's Encyclopedia of Industrial Chemistry*, 6th ed., Vol. 4, Wiley-VCH Verlag GmbH & Co. KGaA, Weinheim, Germany, **2003**, p. 432.
- [116] Y. Wang, X. Zhao, F. Li, S. Wang, J. Zhang, *Journal of Chemical Technology & Biotechnology* **2001**, 76, 857.
- [117] R. Ugo, R. Psaro, M. Pizzotti, P. Nardi, C. Dossi, A. Andreetta, G. Capparella, *Journal of Organometallic Chemistry* **1991**, 417, 211.

- [118] J. Dahlhaus, A. Hoehn, *Ger. Offen.* 19,635,723 (CA128: 206160), **1998**.
- [119] J. G. Acker, *Chemical & Engineering News* **2007**, 85 (32), 3.
- [120] D. Hancu, E. J. Beckman, T. Danciu, *US Patent* 6,710,192, **2004**.
- [121] J. W. Zubrick, *The Organic Chem Lab Survival Manual (5th Ed.)*, John Wiley & Sons, Inc., New York, **2001**.
- [122] R. Szostak, *Molecular Sieves Principles of Synthesis and Identification*, Van Nostrand Reinhold, New York, **1989**.
- [123] C. T. Wu, Y. Q. Wang, Z. T. Mi, L. Xue, W. Wei, E. Z. Min, S. Han, F. He, S. B. Fu, *Reaction Kinetics and Catalysis Letters* **2002**, 77, 73.
- [124] Q. F. Wang, L. Wang, Z. T. Mi, *Catalysis Letters* **2005**, 103, 161.
- [125] J. A. Dean, *Lange's Handbook of Chemistry (15th Ed.)*, 15th ed., McGraw-Hall, Inc., New York, **1999**.
- [126] L. Shaofeng, G. Pilcher, *The Journal of Chemical Thermodynamics* **1988**, 20, 463.
- [127] G. Varsanyi, S. Szoke, G. Keresztury, A. Gelleri, *Acta Chimica Academiae Scientiarum Hungaricae* **1970**, 65, 73.
- [128] M. R. Prasad, G. Kamalakar, G. Madhavi, S. J. Kulkarni, K. V. Raghavan, *Journal of Molecular Catalysis A: Chemical* **2002**, 186, 109.
- [129] Y. Izumi, H. Miyazaki, S. Kawahara, *US Patent* 4,009,252, **1977**.
- [130] G. Papparatto, R. D'Aloisio, G. De Alberti, R. Buzzoni, *European Patent* 1,160,196, **2001**.
- [131] K. L. Antcliff, D. M. Murphy, E. Griffiths, E. Giamello, *Physical Chemistry Chemical Physics* **2003**, 5, 4306.
- [132] F. Bonino, A. Damin, G. Ricchiardi, M. Ricci, G. Spano, R. D'Aloisio, A. Zecchina, C. Lamberti, C. Prestipino, S. Bordiga, *The Journal of Physical Chemistry B* **2004**, 108, 3573.
- [133] J. Q. Zhuang, Z. M. Yan, X. M. Liu, X. C. Liu, X. W. Han, X. H. Bao, U. Mueller, *Catalysis Letters* **2002**, 83, 87.
- [134] R. S. Drago, S. C. Dias, J. M. McGilvray, A. Mateus, *The Journal of Physical Chemistry B* **1998**, 102, 1508.
- [135] Y. Matsumura, K. Hashimoto, H. Kobayashi, S. Yoshida, *Journal of the Chemical Society, Faraday Transactions* **1990**, 86, 561.
- [136] G. Li, X. Wang, H. Yan, Y. Chen, Q. Su, *Applied Catalysis A: General* **2001**, 218, 31.

- [137] D. Hancu, *US Patent* 6,399,794 B1, **2002**.
- [138] B. Taylor, J. Lauterbach, G. E. Blau, W. N. Delgass, *Journal of Catalysis* **2006**, 242, 142.
- [139] W. L. Dai, H. Chen, Y. Cao, H. X. Li, S. H. Xie, K. N. Fan, *Chemical Communications (Cambridge, United Kingdom)* **2003**, 892.
- [140] J. C. van der Waal, M. S. Rigutto, H. van Bekkum, *Applied Catalysis, A: General* **1998**, 167, 331.
- [141] T. Tatsumi, M. Nakamura, K. Yuasa, H. Tominaga, *Chemistry Letters* **1990**, 297.
- [142] C. T. Kresge, M. E. Leonowicz, W. J. Roth, J. C. Vartuli, J. S. Beck, *Nature* **1992**, 359, 710.
- [143] J. S. Beck, J. C. Vartuli, W. J. Roth, M. E. Leonowicz, C. T. Kresge, K. D. Schmitt, C. T. W. Chu, D. H. Olson, E. W. Sheppard, S. B. McCullen, J. B. Higgins, J. L. Schlenker, *Journal of the American Chemical Society* **1992**, 114, 10834.
- [144] Z. R. Zhang, J. S. Sue, X. M. Zhang, S. B. Li, *Chemical Communications (Cambridge, United Kingdom)* **1998**, 241.
- [145] J. Marrero, R. Gani, *Fluid Phase Equilibria* **2001**, 183-184, 183.
- [146] T. M. Martin, D. M. Young, *Chemical Research in Toxicology* **2001**, 14, 1378.